



Universitat de Girona

RHODIUM(I) CATALYZED [2+2+2] CYCLOADDITION REACTIONS: EXPERIMENTAL AND THEORETICAL STUDIES

Anna DACHS SOLER

Dipòsit legal: GI-I 14-2011

<http://hdl.handle.net/10803/52981>

ADVERTIMENT. La consulta d'aquesta tesi queda condicionada a l'acceptació de les següents condicions d'ús: La difusió d'aquesta tesi per mitjà del servei [TDX](#) ha estat autoritzada pels titulars dels drets de propietat intel·lectual únicament per a usos privats emmarcats en activitats d'investigació i docència. No s'autoritza la seva reproducció amb finalitats de lucre ni la seva difusió i posada a disposició des d'un lloc aliè al servei TDX. No s'autoritza la presentació del seu contingut en una finestra o marc aliè a TDX (framing). Aquesta reserva de drets afecta tant al resum de presentació de la tesi com als seus continguts. En la utilització o cita de parts de la tesi és obligat indicar el nom de la persona autora.

ADVERTENCIA. La consulta de esta tesis queda condicionada a la aceptación de las siguientes condiciones de uso: La difusión de esta tesis por medio del servicio [TDR](#) ha sido autorizada por los titulares de los derechos de propiedad intelectual únicamente para usos privados enmarcados en actividades de investigación y docencia. No se autoriza su reproducción con finalidades de lucro ni su difusión y puesta a disposición desde un sitio ajeno al servicio TDR. No se autoriza la presentación de su contenido en una ventana o marco ajeno a TDR (framing). Esta reserva de derechos afecta tanto al resumen de presentación de la tesis como a sus contenidos. En la utilización o cita de partes de la tesis es obligado indicar el nombre de la persona autora.

WARNING. On having consulted this thesis you're accepting the following use conditions: Spreading this thesis by the [TDX](#) service has been authorized by the titular of the intellectual property rights only for private uses placed in investigation and teaching activities. Reproduction with lucrative aims is not authorized neither its spreading and availability from a site foreign to the TDX service. Introducing its content in a window or frame foreign to the TDX service is not authorized (framing). This rights affect to the presentation summary of the thesis as well as to its contents. In the using or citation of parts of the thesis it's obliged to indicate the name of the author.



Universitat de Girona

PhD thesis:

Rhodium(I) Catalyzed [2+2+2] Cycloaddition Reactions:
Experimental and Theoretical Studies

Anna Dachs Soler
2011

Doctorat Interuniversitari en Catàlisi Homogènia

PhD supervisors:
Prof. Miquel Solà i Puig
Prof. Anna Roglans i Ribas

Memòria presentada per a optar al títol de Doctora per la Universitat de Girona



Universitat de Girona

El professor Miquel Solà i Puig, catedràtic d'Universitat a l'Àrea de Química Física de la Universitat de Girona, i la professora Anna Roglans i Ribas, catedràtica d'Universitat a l'Àrea de Química Orgànica de la Universitat de Girona,

CERTIFIQUEM:

Que aquest treball titulat "Rhodium(I) Catalyzed [2+2+2] Cycloaddition Reactions: Experimental and Theoretic Studies", que presenta Anna Dachs Soler per a l'obtenció del títol de Doctora, ha estat realitzat sota la nostra direcció i que compleix els requeriments per a poder optar a Menció Europea.

Signatura

Prof. Miquel Solà Puig

Prof. Anna Roglans Ribas

Girona, 3 de Juny del 2011

Als meus pares, al meu germà,
a l'abuela,
a l'Isaac

“Tot està per fer i tot és possible”

Miquel Martí i Pol

*“La felicitat no s'aconsegueix amb grans cops de sort que apareixen en comptades ocasions,
sinó amb les petites coses que passen tots els dies”*

Benjamin Franklin

Acknowledgments

La realització d'una tesi doctoral és molt més que la obtenció d'un determinat títol, és una aventura personal, una experiència vital plena de moments durs i d'instants magnífics. És un viatge que, com tots els viatges, el més important no és el destí final, sinó tot allò que et trobes durant el camí. I en aquest camí, enmig de les provetes, els balons, les columnes i els càlculs, m'he trobat un conjunt de persones a les que vull agrair profundament el seu suport, la seva ajuda i la seva presència al meu costat, perquè m'han dut a concloure una etapa de la meva vida que mai podré oblidar.

Hi ha varies persones a les que els hi he d'agrair el fet que jo estigui avui aquí, davant de l'ordinador escrivint els últims fulls de la meva tesi... En primer lloc, vull agrair amb les meves més sinceres gràcies l'ajuda dels meus directors de tesi, Miquel i Anna, que m'han brindat de poder treballar aquests anys al seu laboratori i clusters, on he après com funciona realment el difícil món de la recerca. A tu Miquel, per tota l'ajuda i informació proporcionada d'aquest món "frikí" de la química computacional, i a tu Anna per l'ajuda que he rebut amb els problemes que han anat sorgint durant aquests darrers anys en el treball de laboratori. Ara ja se'm considera tota una "híbrid" de la química! En resum, moltes gràcies per totes les hores que m'heu dedicat, per totes les correccions i recomanacions que m'heu fet, per haver-me guiat durant tot el treball.

També agraeixo al *Ministerio de Educación i Ciencia* la concessió d'una beca predoctoral per la Formació de Personal Investigador (FPI) que ha permès finançar la realització d'aquesta tesi.

Per la determinació estructural dels compostos obtinguts durant la realització d'aquesta tesi doctoral ha estat necessària la utilització de diferents serveis d'anàlisis, als responsables dels quals agraeixo la seva ajuda: la Dra. Lluïsa Matas i al Dr. Teodor Parella en la resolució dels espectres de RMN i a l'Anna Costa per l'enregistrament dels espectres d'ESI-MS i els anàlisis elementals. A més a més,

també agrair a la Carme, de l'IQC, per tota l'ajuda amb la paperassa dels pagaments dels congressos i les petites xerrades que fèiem al seu despatx.

I ara et toca a tu Anna Pla. Tu ja saps que aquestes ganes d'iniciar-me en el món de la investigació ha estat en part gràcies a tu. Així que *només* et puc dir: gràcies per les discussions científiques, les xerrades, les abraçades, les *quedades*, i en definitiva, per ser part del meu dia a dia en tot moment, has sigut un pilar dels forts. Espero de debò, que després d'aquesta etapa, tot i la distància, podem continuar compartint molts moments!

També agrair a tots aquells amb qui he compartit hores de laboratori i hores de despatx. Als meus companys de grup "experimentals" que ja van marxar: Judit, Anna Torrent i Iván, amb els que seguim mantenint el contacte. A les que encara hi són: Sandra i Lídia amb les qui he compartit tantes hores de laboratori, dinars, sopars, cafès, *moments xocolata*, viatges, sortides de dia i de nit, moments d'alegria i de tristesa, de nervis i de tranquil·litat, de pessics i rialles, de *roba del mateix color!!!* Les tres juntes... *Visca les Kats!!!!* I sense oblidar-me de les noves incorporacions del grup: Magda i Mònica. A veure si fem més excursions!

I als meus companys de l'IQC...quin munt de gent amb qui s'han compartit varis moments divertits. Sobretot a la Sílvia Osuna, per tots els moments que ha hagut de dedicar a introduir-me al món dels càlculs...encara me'n recordo quan et deia: *se'm fusionen els àtoms...* moltíssimes gràcies Silvionso!!! I a tots els demés que tot i no estar al mateix despatx treballant, també hem passat bons moments junts: Ferran, Anna Díaz, Pata, Mireia, Hugas, Juanma, Pedro, Marcel, Cristina, Lluís, Eloy, Sergi, Laia, Dani, Carles, Quansong... en fi, tot l'IQC!

No em podria oblidar de la resta d'*excompanys* experimentals i els actuals, amb els que també hem compartit molts moments de feina i sobretot de diversió: l'Anna C, l'Arnau, la Laura, l'Isaac, en Buchanan, l'Isabel, la Montse R, en Rafael, la Vane, en Tiffa, la Gemma, l'Imma, l'Ana A., la Mònica F... i continua la llista de lipsians/es i inorgànics!

Als meus companys dels cursos de doctorat: Zanardi (el *italiano*), Andre *el mafioso* (el *portugués*), Stephan (el *alemán*), Isra, Isaac, Jordi, Elena, Maria Isabel, Laia, Sergi i Pilar, perquè vam aprendre moltes coses noves tant a Castelló com a Huelva, però sobretot, va ser una etapa increïble que segur que cap de nosaltres oblidarà! Pilar, tal y como dijimos mientras hacíamos el camino de Santiago, aunque un poco cansadas, "*algún día nos vamos a reír de esto*"... creo que ya ha llegado el momento de reírnos juntas!!!

I would like to thank Dr Anny Jutand to allow me to work in your research group. I spent there a very wonderful period of my thesis and I have happy memory of all the members of your group, and specially of Anna Serra, Pingping, Cong, Anne Mie and Pier Luca with I am very grateful for. A part de tots els companys de la residència, amb els quals, vam aprofitar d'allò més bé *notre vie à Paris. À retenir!*

Ha arribat el torn de la penya de l'espardenyà: Pilar, Marta, Díaz, Nikita, Mònica F, Alba, Naiara, Santi, Maira, Quim, Xevi, Olga, Carla i Ferran. Perquè tot el que vam arribar a viure junts durant la carrera ens faci mantenir junts per molts més anys, i així, poder continuar fent les nostres trobades anuals. Encara que cada any ens repetim que ens fem grans i que ja no aguantem com abans ... Doncs sí, però què millor que veure com ens fem grans i com les nostres vides van canviant??? A més, no ens podem queixar amb lo esportistes que ens estem tornant... que si trekking, curses de muntanya, vies ferrades, ... que continuem així i per molts més anys! Que també serà una manera de poder-nos veure més sovint!

Sortint del món químic... hi ha un munt de gent que m'ha acompanyat durant aquests anys a la meua vida i els quals m'han donat suport amb tot el que he anat fent, encara que en molts casos no sabessin ben bé què estava fent. Tan els d'Alpens com totes les de Vic, que no diré noms perquè són masses... però que gràcies a tots ells, els moments que han anat sorgint al llarg d'aquests anys, i tot el que hem arribat a fer junts, em donaven alegries per seguir endavant i energia per emprendre de nou amb la feina. Gràcies per preguntar com va la tesi! Però que pesats, no us en vull sentir a parlar més!!!

També volia agrair a les meves companyes de pis durant el Doctorat: la Díaz i la Nikita! Que tot i que ara ja estem separades, sempre em quedarà un bon record d'aquella època en la que intentàvem fer mil coses: que si cinema *V.O.*, excursions amb bicicleta, córrer per la devesa, sessions *LOST*, soparets, ...en fi, que gràcies per tot el temps compartit! A tu Nikita, gràcies per la gran paciència que vas tenir amb les dues *Annes* fent el doctorat... sempre parlant del mateix...que en som de pesades!!! I a tu Díaz, per totes les grans converses que vam arribar a tenir... sobretot pel tema doctorat! Ningú ens va dir que seria fàcil... però sembla que estem a punt d'acabar aquesta etapa i espero que el que ens espera ho podem continuar compartint!

Finalment, agrair sobretot a la meva família, per permetre que els hi hagi dedicat moltíssim menys temps del que realment es mereixien, i perquè tot i que encara es pregunten què és el que estic fent i perquè serveix... han fet un gran esforç perquè jo estudiés i sempre tingués lo millor que em podien donar.

I per acabar, moltíssimes gràcies a tu, Isaac. Per la teva paciència i comprensió. Pels ànims i per la llibertat que m'has donat. Per estar sempre quan et necessitava, tot i els moments més durs. Ho saps, oi?

A tots vosaltres, moltes gràcies.

Table of Contents

Table of Contents	13
Summary	17
Full List of Publications	29
Glossary of Abbreviations	33
CHAPTER 1. General Introduction	39
1.1. Transition-metal catalysts that have been more commonly used for the [2+2+2] cycloaddition reactions	41
1.1.1. <i>Chemoselective and Regioselective Features</i>	44
1.1.2. <i>Enantioselective Features</i>	50
1.1.3. <i>Participating unsaturated substrates</i>	53
1.1.4. <i>The postulated mechanism</i>	68
1.2. Computational Chemistry	79
1.2.1. <i>The Hartree-Fock approximation</i>	81
1.2.2. <i>The Density Functional Theory</i>	87
1.2.3. <i>Computational Details</i>	96
1.2.4. <i>Computational Chemistry in the lab</i>	98
CHAPTER 2. Objectives	109
CHAPTER 3. Density Functional Study of the [2+2+2] Cyclotrimerization of Acetylene Catalyzed by Wilkinson's Catalyst, RhCl(PPh₃)₃	119
CHAPTER 4. Rhodium(I)-Catalyzed Intramolecular [2+2+2] Cyclotrimerizations of 15-, 20-, and 25-Membered Azamacrocycles. Experimental and Theoretical Mechanistic Studies	129

CHAPTER 5. Rates and Mechanism of Rhodium-Catalyzed [2+2+2] Cycloaddition of Bisalkynes and a Monoalkyne	143
CHAPTER 6. RhCl(PPh ₃) ₃ -Catalyzed Intramolecular Cycloaddition of Eneidyne: the Nature of the Tether and Substituents Control the Reaction Mechanism	153
CHAPTER 7. Intramolecular [2+2+2] Cycloadditions of <i>Yne-yne-ene</i> and <i>Yne-ene-yne</i> enediynes Catalyzed by Rh(I): Experimental and Theoretical Mechanistic Studies	165
CHAPTER 8. Ene reactions between two alkynes? Doors open to thermally induced cycloisomerization of macrocyclic triynes and enediynes	203
CHAPTER 9. RESULTS and DISCUSSION	209
CHAPTER 10. CONCLUSIONS	245
Supplementary Data	253
Bibliography	255

Summary

The [2+2+2] cycloaddition reaction involves the formation of three carbon-carbon bonds in one single step using alkynes, alkenes, nitriles, carbonyls and other unsaturated reagents as reactants. This is one of the most elegant methods for the construction of polycyclic aromatic compounds and heteroaromatic, which have important academic and industrial uses.

Since Reppe et al. described the first nickel-catalyzed [2+2+2] cycloaddition to obtain substituted benzene derivatives in 1948, alkyne cycloaddition reactions catalyzed by transition-metals have become one of the most widely used methods to obtain polysubstituted benzenes.

Over the last decade, this reaction, which originally required stoichiometric amounts of transition metal and drastic reaction conditions, has become a highly efficient catalytic process. The applications of [2+2+2] cycloadditions range from the preparation of different organic compounds to the synthesis of natural products such as anticancer drugs and neuroprotective agents.

The thesis is divided into ten chapters including six related publications. The first study based on the Wilkinson's catalyst, $\text{RhCl}(\text{PPh}_3)_3$, compares the reaction mechanism of the [2+2+2] cycloaddition process of acetylene with the cycloaddition obtained for the model of the complex, $\text{RhCl}(\text{PH}_3)_3$. In an attempt to reduce computational costs in DFT studies, this research project aimed to substitute PPh_3 ligands for PH_3 , despite the electronic and steric effects produced by PPh_3 ligands being significantly different to those created by PH_3 ones. In this first study, detailed theoretical calculations were performed to determine the reaction mechanism of the two complexes. Despite some differences being detected, it was found that modelling PPh_3 by PH_3 in the catalyst helps to reduce the computational cost significantly while at the same time providing qualitatively acceptable results.

Taking into account the results obtained in this earlier study, the model of the Wilkinson's catalyst, $\text{RhCl}(\text{PH}_3)_3$, was applied to study different [2+2+2] cycloaddition reactions with unsaturated systems conducted in the laboratory. Our research group found that in the case of totally closed systems, specifically 15- and 25-membered azamacrocycles can afford benzenic compounds, except in the case of 20-membered azamacrocycle (20-MAA) which was inactive with the Wilkinson's catalyst. In this study, theoretical calculations allowed to determine the origin of the different reactivity of the 20-MAA, where it was found that the activation barrier of the oxidative addition of two alkynes is higher than those obtained for the 15- and 25-membered macrocycles. This barrier was attributed primarily to the interaction energy, which corresponds to the energy that is released when the two deformed reagents interact in the transition state. The main factor that helped to provide an explanation to the different reactivity observed was that the 20-MAA had a more stable and delocalized HOMO orbital in the oxidative addition step. Moreover, we observed that the formation of a strained ten-membered ring during the cycloaddition of 20-MAA presents significant steric hindrance.

Furthermore, in *Chapter 5*, an electrochemical study is presented in collaboration with Prof. Anny Jutand from Paris. This work allowed studying the main steps of the catalytic cycle of the [2+2+2] cycloaddition reaction between diynes with a monoalkyne. First kinetic data were obtained of the [2+2+2] cycloaddition process catalyzed by the Wilkinson's catalyst, where it was observed that the rate-determining step of the reaction can change depending on the structure of the starting reagents.

In the case of the [2+2+2] cycloaddition reaction involving two alkynes and one alkene in the same molecule (enediynes), it is well known that the oxidative coupling may occur between two alkynes giving the corresponding metallacyclopentadiene, or between one alkyne and the alkene affording the metallacyclopentene complex. Wilkinson's model was used in DFT calculations to analyze the different factors that may influence in the reaction mechanism. Here it was observed that the cyclic enediynes always prefer the oxidative coupling between two alkynes moieties, while

the acyclic cases have different preferences depending on the *linker* and the substituents used in the alkynes.

Moreover, the Wilkinson's model was used to explain the experimental results achieved in *Chapter 7* where the [2+2+2] cycloaddition reaction of enediynes is studied varying the position of the double bond in the starting reagent. It was observed that enediynes type *yne-ene-yne* preferred the standard [2+2+2] cycloaddition reaction, while enediynes type *yne-yne-ene* suffered β -hydride elimination followed a reductive elimination of Wilkinson's catalyst giving cyclohexadiene compounds, which are isomers from those that would be obtained through standard [2+2+2] cycloaddition reactions.

Finally, the last chapter of this thesis is based on the use of DFT calculations to determine the reaction mechanism when the macrocycles are treated with transition metals that are inactive to the [2+2+2] cycloaddition reaction, but which are thermally active leading to new polycyclic compounds. Thus, a domino process was described combining an *ene* reaction and a Diels-Alder cycloaddition.

Resum

La reacció de cicloaddició consisteix en la formació de tres enllaços carboni-carboni en un únic pas de reacció on poden estar involucrats alquins, alquens, nitrils, carbonils i altres compostos insaturats. És un dels mètodes més elegants per a la construcció de compostos aromàtics i heteroaromàtics policíclics amb importants usos acadèmics i industrials.

Després que Reppe et al. descrigués la primera versió catalitzada per níquel per a obtenir derivats benzènics substituïts en el 1948, les reaccions de cicloaddició d'alquins catalitzades per metalls de transició ha esdevingut en un dels mètodes més utilitzats per obtenir benzens polisubstituïts.

En l'última dècada, aquesta reacció, que en un principi requeria quantitats estequiomètriques de metalls de transició i condicions dràstiques de reacció, s'ha convertit en un procés catalític d'alta eficiència. Les seves aplicacions abasten un rang ampli de reaccions que van des de la preparació de diferents compostos orgànics, fins a la síntesi de productes naturals com medicaments contra el càncer i agents neuroprotectors.

La tesi es divideix en deu capítols que contenen sis publicacions relacionades. El primer estudi es basa en el catalitzador de Wilkinson, $\text{RhCl}(\text{PPh}_3)_3$, on es compara el mecanisme de reacció del procés de cicloaddició d'acetilè pel que s'obté amb el model del complex, $\text{RhCl}(\text{PH}_3)_3$. Aquest projecte de recerca va ser iniciat per estudiar la substitució de lligands PPh_3 per PH_3 en els estudis de DFT, que s'aplica habitualment per reduir el cost computacional, tot i que els efectes electrònics i estèrics produïts pels lligands PPh_3 són molt diferents dels creats per PH_3 . Malgrat algunes diferències observades, es va constatar que la substitució de PPh_3 per PH_3 en el catalitzador pot ser utilitzada per reduir el cost computacional de manera significativa i a l'hora obtenir resultats qualitativament acceptables.

Un cop obtinguts els resultats anteriors, es va utilitzar el model del catalitzador de Wilkinson, $\text{RhCl}(\text{PH}_3)_3$, per l'estudi teòric de diferents reaccions de cicloaddició amb sistemes insaturats duts a terme al laboratori. En el grup de recerca es va trobar que en el cas de sistemes totalment tancats, concretament els macrocicles de 15 i 25 baules, poden donar sistemes benzènics policíclics excepte en el cas del macrocicle de 20 baules, que va resultar inactiu vers el catalitzador de Wilkinson. En aquest estudi, la realització de càlculs teòrics va permetre determinar l'origen de la diferent reactivitat del macrocicle de 20 baules, on es va trobar que la barrera d'activació de l'addició oxidativa entre dos alquins és molt més alta que les que es van obtenir pel macrocicle de 15 i 25 baules. Aquesta barrera es va atribuir bàsicament a l'energia d'interacció, la qual correspon a l'energia que s'allibera quan els dos reactius deformats interaccionen en l'estat de transició. Concretament el principal factor que hi contribueix és que el macrocicle de 20 baules presenta més estabilitat i més deslocalització de l'orbital HOMO en el pas d'addició oxidativa. A més a més, es va observar que la formació d'anells de 10 baules durant la cicloaddició del macrocicle de 20 baules presenta impediments estèrics importants.

Per altra banda, en el *Capítol 5* es presenten estudis electroquímics realitzats en col·laboració amb la Prof. Anny Jutand de París, que van permetre estudiar el cicle catalític de la reacció de cicloaddició entre un dií i un monoalquí. Es van obtenir així les primeres dades cinètiques dels dos principals passos del cicle catalític amb el complex de Wilkinson, on es va observar que el pas determinant de la reacció pot variar en funció de l'estructura dels reactius de partida.

En el cas en què en la reacció de cicloaddició participin dos triples i un doble enllaç en la mateixa molècula (endiins), és conegut que l'addició oxidativa pot donar-se entre dos triples enllaços o un triple i un doble enllaç. El model del catalitzador de Wilkinson va ser utilitzat mitjançant càlculs DFT per analitzar els diferents factors que poden influir en el mecanisme de reacció. Aquí es va observar que els endiins cíclics sempre prefereixen l'addició oxidativa entre els dos triples enllaços, mentre que els acíclics tenen diferent preferència en funció del *linker* i dels substituents presents en els triples enllaços.

A més a més, el mateix model de Wilkinson es va utilitzar per explicar els resultats experimentals realitzats en el *Capítol 7* on s'estudia la reacció de cicloadició d'endiins variant la posició del doble enllaç en el reactiu de partida. Es va observar que els sistemes *in-en-in* preferien la cicloadició convencional donant el producte ciclohexadienic esperat, mentre que els sistemes *in-in-en* patien una β -eliminació seguida d'una eliminació reductiva del catalitzador de Wilkinson i donant, finalment, productes ciclohexadiènics els quals són isòmers dels que s'obtidrien mitjançant una cicloadició convencional.

Finalment, l'últim capítol d'aquesta tesi es basa en l'ús de càlculs DFT per determinar el mecanisme de reacció quan els macrocicles són tractats amb metalls de transició inactius per donar la reacció de cicloadició, però reaccionen tèrmicament obtenint nous compostos policíclics. Així es va descriure un procés dòmino on es combina una reacció *ene* seguida d'una cicloadició de Diels-Alder.

Resumen

La reacción de cicloadición consiste en la formación de tres enlaces carbono-carbono en un único paso de reacción a partir de alquinos, alquenos, nitrilos, carbonilos y otros compuestos insaturados. Es uno de los métodos más elegantes para la construcción de compuestos aromáticos y heteroaromáticos policíclicos con importantes usos académicos e industriales.

Después que Reppe et al. describiera la primera versión catalizada por níquel para obtener derivados bencénicos sustituidos en 1948, las reacciones de cicloadición catalizadas por metales de transición se ha convertido en uno de los métodos más utilizados para obtener bencenos polisustituidos.

En la última década, esta reacción que en un principio requería cantidades estequiométricas de metales de transición y condiciones drásticas de reacción, se ha convertido en un proceso catalítico de alta eficiencia. Sus aplicaciones abarcan un rango amplio para la preparación de diferentes compuestos orgánicos, además de la síntesis de productos naturales como medicamentos contra el cáncer y agentes neuroprotectores.

La tesis se divide en diez capítulos que contienen seis publicaciones relacionadas. El primer estudio se basa en el catalizador de Wilkinson, $\text{RhCl}(\text{PPh}_3)_3$, y en él se compara el mecanismo de reacción del proceso de cicloadición de acetileno con el que se obtiene con el modelo del complejo, $\text{RhCl}(\text{PH}_3)_3$. Este proyecto de investigación se realizó con el objetivo de averiguar el efecto de sustitución de los ligandos PPh_3 por PH_3 en los estudios teóricos DFT. Esta sustitución se aplica habitualmente para reducir el coste computacional aunque los efectos electrónicos y estéricos producidos por ligandos PPh_3 son muy diferentes de los creados por PH_3 . A pesar de algunas diferencias observadas, se constató que la sustitución de PPh_3 por PH_3 en el catalizador puede ser utilizada para reducir el coste computacional de manera significativa y además obtener resultados cualitativamente aceptables.

Una vez obtenidos los resultados anteriores, se aplicó el modelo de Wilkinson, $\text{RhCl}(\text{PH}_3)_3$, para el estudio teórico de diferentes reacciones de cicloadición de sistemas insaturados llevados a cabo en el laboratorio. En el grupo de investigación se encontró que en el caso de sistemas totalmente cerrados, concretamente los macrociclos de 15 y 25 eslabones, se pueden obtener sistemas bencénicos policíclicos excepto para el caso del macrociclo de 20 eslabones, que resultó inactivo con el catalizador de Wilkinson. En este estudio, la realización de cálculos teóricos permitió determinar el origen de la diferente reactividad del macrociclo de 20 eslabones, dado que se encontró que la barrera de activación de la adición oxidativa entre dos alquinos es mucho más alta que las que se obtienen por los macrociclos de 15 y 25 eslabones. Esta barrera se atribuyó básicamente a la energía de interacción, la que corresponde a la energía que se libera cuando los dos reactivos deformados interaccionan en el estado de transición. Concretamente el principal factor que contribuyó fue que el macrociclo de 20 eslabones presentaba más estabilidad y más deslocalización del orbital HOMO en la adición oxidativa. Además, se observó que la formación de anillos de 10 eslabones durante la cicloadición del macrociclo de 20 eslabones presenta impedimentos estéricos importantes.

Por otra parte, en el *Capítulo 5* se presentan estudios electroquímicos realizados en colaboración con la Prof. Anny Jutand de París, que permitieron estudiar el ciclo catalítico de la reacción de cicloadición entre un diíno y un monoalquino. Se obtuvieron así, los primeros datos cinéticos con el complejo de Wilkinson referente a los dos principales pasos del ciclo catalítico. Se observó que el paso determinante de la reacción puede variar en función de la estructura de los reactivos de partida.

En el caso en que participen dos triples y un doble enlace en la misma molécula (enediíno), es conocido que la adición oxidativa puede darse entre dos triples enlaces o un triple y un doble enlace. El modelo del catalizador de Wilkinson fue utilizado mediante cálculos DFT para analizar los diferentes factores que pueden influir en el mecanismo de reacción. Aquí se observa que los enediínos cíclicos siempre prefieren

la adición oxidativa entre los dos triples enlaces, mientras los acíclicos tienen diferente preferencia en función del *linker* y los sustituyentes presentes en los triples enlaces.

Además, el mismo modelo se utilizó para explicar los resultados experimentales obtenidos en el *Capítulo 7* donde se estudia la reacción de cicloadición de enediínos variando la posición del doble enlace en el reactivo de partida. Se observó que los sistemas *ino-eno-ino* prefieren la cicloadición convencional dando el producto ciclohexadiénico esperado, mientras que los sistemas *ino-ino-eno* sufren una β -eliminación seguida de una eliminación reductiva del catalizador de Wilkinson y dando, finalmente, productos ciclohexadiénicos los cuales son isómeros que se obtendrían mediante una cicloadición convencional.

Finalmente, el último capítulo de esta tesis se basa en el uso de cálculos DFT para determinar el mecanismo de reacción cuando los macrociclos son tratados con metales de transición que resultan inactivos para dar la reacción de cicloadición, pero son activos térmicamente obteniéndose nuevos compuestos policíclicos. Aquí se describió un proceso domino que combina una reacción *ene* seguida de una cicloadición de Diels-Alder.

Full List of Publications

The thesis is based on the following publications:

Chapter 3:

1. Dachs, A.; Osuna, S.; Roglans, A.; Solà, M.; Density Functional Study of the [2+2+2] Cyclotrimerization of Acetylene Catalyzed by Wilkinson's Catalyst, RhCl(PPh₃)₃. *Organometallics* **2010**, *29*, 562.

Chapter 4:

2. Dachs, A.; Torrent, A.; Roglans, A.; Parella, T.; Osuna, S.; Solà, M.; Rhodium(I)-Catalysed Intramolecular [2+2+2] Cyclotrimerisations of 15-, 20- and 25-Membered Azamacrocycles. Experimental and Theoretical Mechanistic Studies. *Chem. Eur. J.* **2009**, *15*, 5289.

Chapter 5:

3. Dachs, A.; Torrent, A.; Pla-Quintana, A.; Roglans, A.; Jutand, A.; Rates and Mechanism of Rhodium-Catalyzed [2+2+2] Cycloaddition of Bisalkynes and a Monoalkyne. *Organometallics* **2009**, *28*, 6036.

Chapter 6:

4. Dachs, A.; Roglans, A.; Solà, M.; RhCl(PPh₃)₃-Catalyzed Intramolecular Cycloaddition of Ene-diyne: The Nature of the Tether and Substituents Control the Reaction Mechanism. *Organometallics*, **2011**, *30*, 3151.

Chapter 7:

5. Dachs, A.; Pla-Quintana, A.; Parella, T.; Solà, M.; Roglans, A.; Intramolecular [2+2+2] cycloadditions of *yne-yne-ene* and *yne-ene-yne* enediyne catalyzed by Rh(I): experimental and theoretical mechanistic studies. *Chem. Eur. J.* submitted for publication.

Chapter 8:

6. González, I.; Pla-Quintana, A.; Roglans, A.; Dachs, A.; Solà, M.; Parella, T.; Farjas, J.; Roura, P.; Lloveras, V.; Vidal-Gancedo, J.; Ene reactions between two alkynes? Doors open to thermally induced cycloisomerization of macrocyclic triynes and enediyne. *Chem. Commun.* **2010**, *46*, 2944.

Publications not included in this thesis:

7. Pla-Quintana, A.; Torrent, A.; Dachs, A.; Pleixats, R.; Moreno-Mañas, M.; Parella, T.; Benet-Buchholz, B.; Roglans, A.; Chiral and Stable Palladium(0) Complexes of Polyunsaturated Aza-macrocyclic Ligands: Synthesis and Structural Analysis. *Organometallics* **2006**, *25*, 5612.
8. Brun, S.; Garcia, L.; González, I.; Torrent, A.; Dachs, A.; Pla-Quintana, A.; Parella, T.; Roglans, A.; Fused Tetracycles with a Benzene or Cyclohexadiene Core: [2+2+2] Cycloadditions on Macrocyclic Systems. *Chem. Commun.* **2008**, 4439.
9. Dachs, A.; Masllorens, J.; Pla-Quintana, A.; Farjas, J.; Parella, T.; Roglans, A.; Structural Differences between Open-Chain and Macrocyclic Triene Ligands: Influence on the Stability and Catalytic Properties. *Organometallics* **2008**, *27*, 5768.
10. Dachs, A.; Guerra-Fontseca, C.; Bickelhaupt, F.M.; Is the S_N2 reaction possible for the complex $Ni(CO)_4$? (in preparation).

Glossary of Abbreviations

ν (en IR)	Frequency (units: cm^{-1})
1,4-CHD	1,4-cyclohexadiene
APT	Attached Proton Test
Ar	Aryl
ATR	Attenuated Total Reflectance
BINAP	2,2'-bis(diphenylphosphino)-1,1'-binaphthyl
BOC	<i>tert</i> -Butyloxycarbonyl
Bu	Butyl
Bn	Benzyl
BPin	Boryl Pinacolate
Cp	Cyclopentadiene
cod	1,5-Cyclooctadiene
Cat.	Catalyst
DCE	1,2-dichloroethylene
DMSO	Dimethyl sulfoxide
DSC	Differential Scanning Calorimetry
DUPHOS	Diphosphine ligand
EA	Elemental Analysis
Et	Ethyl
Et ₂ O	Diethyl ether
EtOAc	Ethyl acetate
et al.	Collaborators
eq.	Equation
equiv.	Equivalent
ee	Enantiomeric excess
ESI-MS	ElectroSpray Ionization Mass Spectrometry
GC-MS	Gas Chromatography with Mass Spectrometry detection

h	hours
HRMS	High Resolution Mass Spectrometry
HSQC	Heteronuclear Single-Quantum Correlation
<i>i</i> Pr	<i>iso</i> -propyl
IR	Infrared Spectroscopy
L*	Chiral ligand
MALDI-TOF	Matrix Assisted Laser Desorption Ionization- Time of Flight
MeOH	Methanol
Me	Methyl
Ms	Messyl
m.p.	melting point
MW	Molecular Weight
NOE	Nuclear Overhauser Effect
NOESY	Nuclear Overhauser Spectroscopy
ORTEP	Oak Ridge Thermal Ellipsoid Plot Program for Crystal Structure Illustrations
Ph	Phenyl
r.t.	room temperature
T	Temperature
^t Bu	<i>tert</i> -Butyl
TFA	Trifluoroacetic Acid
THF	Tetrahydrofuran
TLC	Thin Layer Chromatography
TM	Transition Metal
UV	Ultraviolet Spectroscopy

Abbreviations used in Nuclear Magnetic Resonance (NMR).

δ	Chemical shift (units: ppm)
$^{13}\text{C-NMR}$	Nuclear Magnetic Resonance of carbon (13)
$^1\text{H-NMR}$	Nuclear Magnetic Resonance of proton
$^{31}\text{P-NMR}$	Nuclear Magnetic Resonance of phosphorous (31)
ID	Monodimensional
2D	Bidimensional
abs.	Absorption
ap.	apparent
COSY	Correlation Spectroscopy
d	Doublet
dd	Double doublet
dt	Double triplet
HMBC	Heteronuclear Multiple Bond Correlation
J	Coupling constant
m	Multiplet
s	Singlet
sept	Septuplet
t	Triplet
tt	Triple triplet

Abbreviations used in theoretical studies.

B3LYP	Becke, three parameter, Lee-Yang-Parr
BO	Born-Oppenheimer
deg.	degree
DFT	Density Functional Theory
ECP	Effective Core Potential
GGA	Generalized Gradient Approximation
GTO	Gaussian Type Orbitals
HF	Hartree-Fock
HK	Hohenberg and Kohn
IRC	Intrinsic Reaction Coordinates
K	Kelvin
KS	Kohn-Sham
LCAO-MO	Linear Combination of Atomic Orbitals
LDA	Local Density Approximation
LST	Linear Synchronous Transit
MO	Molecular Orbitals
PES	Potential Energy Surface
QST	Quadratic Synchronous Transit
SCF	Self-Consistent Field
STO	Slater Type Orbitals
TS	Transition State

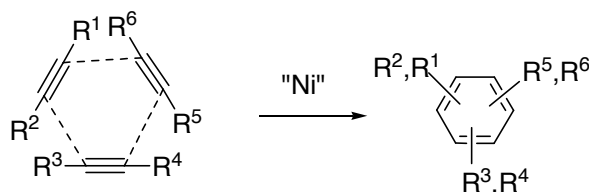
Chapter 1. **GENERAL**
INTRODUCTION

This chapter explains the rationale behind the research presented in this thesis and aims to orientate the reader with regards to mechanistic aspects of [2+2+2] cycloaddition reactions. Both general aspects and recent advances in this kind of reaction are discussed. [2+2+2] Cycloaddition reactions find their applications in organic chemistry as a key step in the synthesis of many natural products. Given this, their relevance as an efficient reaction to obtain polysubstituted benzenes or cyclohexadienes is described.

1.1. Transition-metal catalysts that have been more commonly used for the [2+2+2] cycloaddition reactions

The development of novel reactions, useful reagents, and efficient catalysts to enable the formation of carbon-carbon bonds is an area of considerable interest in organic chemistry. Reactions forming multiple bonds, rings and/or stereocentres are particularly important tools for the efficient assembly of complex molecular structures. In this respect, cycloaddition reactions are considered to be particularly useful when more than one carbon-carbon or carbon-heteroatom bond is formed.

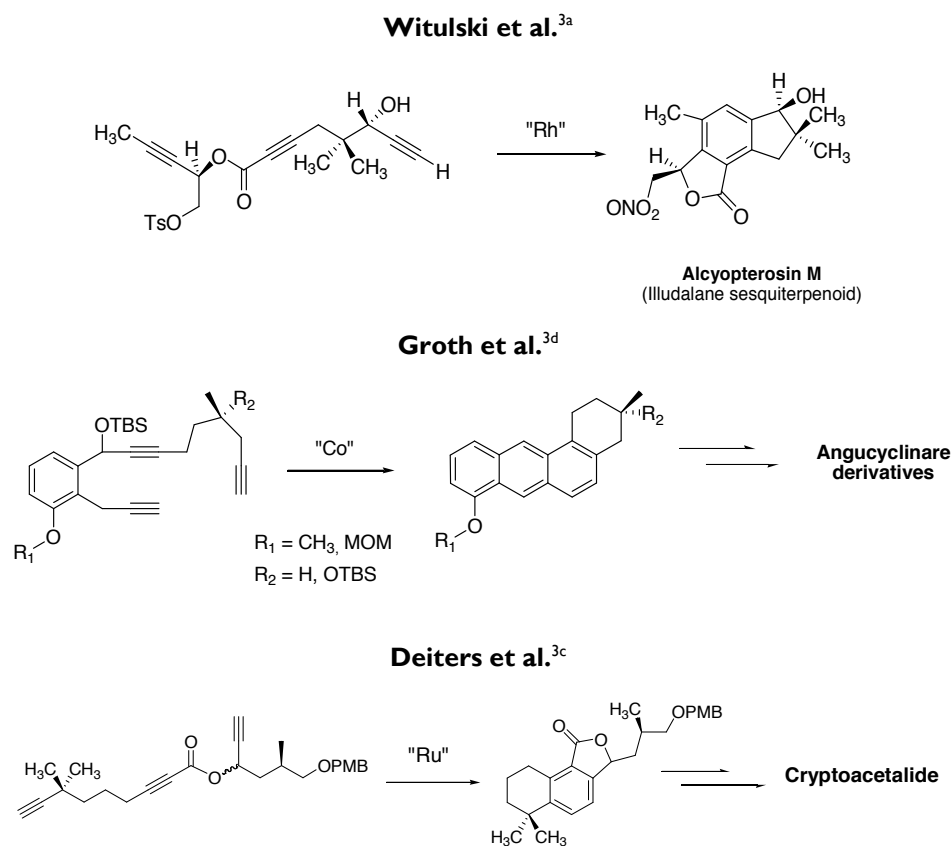
[2+2+2] Cycloaddition reactions involving alkynes, in which three carbon-carbon bonds are formed in one step, is one of the most elegant methods for the construction of polycyclic aromatics, which have important academic and industrial uses. In 1948, Reppe et al.¹ described the first transition metal catalyzed version of this transformation under nickel catalysis to obtain substituted benzene derivatives (Scheme 1.1).



Scheme 1.1. [2+2+2] alkyne cycloaddition reaction catalyzed by Ni

After this discovery, the alkyne cycloaddition reaction catalyzed by transition-metals became one of the most used methods to obtain substituted benzenes.² Over the last decade, this reaction, which originally required stoichiometric amounts of transition metal and drastic reaction conditions, has become a highly efficient catalytic process. Examples of its applications are the synthesis of natural products such as anticancer

drugs, and the development of neuroprotective agents.³ The key step of the synthesis of these molecules is a transition metal-catalyzed intramolecular [2+2+2] cycloaddition from the corresponding triyne (Scheme 1.2).



Scheme 1.2. Synthesis of different natural products by [2+2+2] cycloaddition reaction

These applications continue to grow with the development of new catalytic systems. A significant number of reports have recently focused on the application of cycloaddition for the construction of new carbo- and heterocyclic frameworks where numerous transition metals (Figure 1.1) have been found to promote these processes.

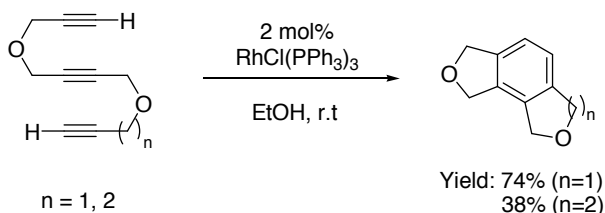
<table border="1"> <tr><td>hydrogen</td><td>H</td><td>1.0079</td></tr> <tr><td>lithium</td><td>Li</td><td>6.941</td></tr> <tr><td>sodium</td><td>Na</td><td>22.990</td></tr> <tr><td>potassium</td><td>K</td><td>39.098</td></tr> <tr><td>rubidium</td><td>Rb</td><td>85.468</td></tr> <tr><td>cesium</td><td>Cs</td><td>132.91</td></tr> <tr><td>francium</td><td>Fr</td><td>[223]</td></tr> </table>																		hydrogen	H	1.0079	lithium	Li	6.941	sodium	Na	22.990	potassium	K	39.098	rubidium	Rb	85.468	cesium	Cs	132.91	francium	Fr	[223]	<table border="1"> <tr><td>beryllium</td><td>Be</td><td>9.0122</td></tr> <tr><td>magnesium</td><td>Mg</td><td>24.304</td></tr> <tr><td>calcium</td><td>Ca</td><td>40.078</td></tr> <tr><td>strontium</td><td>Sr</td><td>87.62</td></tr> <tr><td>barium</td><td>Ba</td><td>137.33</td></tr> <tr><td>radium</td><td>Ra</td><td>[226]</td></tr> </table>																		beryllium	Be	9.0122	magnesium	Mg	24.304	calcium	Ca	40.078	strontium	Sr	87.62	barium	Ba	137.33	radium	Ra	[226]	<table border="1"> <tr><td>boron</td><td>B</td><td>10.811</td></tr> <tr><td>aluminum</td><td>Al</td><td>26.982</td></tr> <tr><td>gallium</td><td>Ga</td><td>69.723</td></tr> <tr><td>indium</td><td>In</td><td>114.82</td></tr> <tr><td>thallium</td><td>Tl</td><td>204.38</td></tr> <tr><td>unununium</td><td>Uun</td><td>[271]</td></tr> <tr><td>unununium</td><td>Uub</td><td>[277]</td></tr> </table>																		boron	B	10.811	aluminum	Al	26.982	gallium	Ga	69.723	indium	In	114.82	thallium	Tl	204.38	unununium	Uun	[271]	unununium	Uub	[277]	<table border="1"> <tr><td>carbon</td><td>C</td><td>12.011</td></tr> <tr><td>silicon</td><td>Si</td><td>28.086</td></tr> <tr><td>germanium</td><td>Ge</td><td>72.64</td></tr> <tr><td>tin</td><td>Sn</td><td>118.71</td></tr> <tr><td>lead</td><td>Pb</td><td>207.2</td></tr> <tr><td>unununium</td><td>Uun</td><td>[271]</td></tr> <tr><td>unununium</td><td>Uub</td><td>[277]</td></tr> </table>																		carbon	C	12.011	silicon	Si	28.086	germanium	Ge	72.64	tin	Sn	118.71	lead	Pb	207.2	unununium	Uun	[271]	unununium	Uub	[277]	<table border="1"> <tr><td>nitrogen</td><td>N</td><td>14.007</td></tr> <tr><td>phosphorus</td><td>P</td><td>30.974</td></tr> <tr><td>arsenic</td><td>As</td><td>74.922</td></tr> <tr><td>selenium</td><td>Se</td><td>78.96</td></tr> <tr><td>tellurium</td><td>Te</td><td>127.6</td></tr> <tr><td>polonium</td><td>Po</td><td>[209]</td></tr> <tr><td>unununium</td><td>Uun</td><td>[271]</td></tr> <tr><td>unununium</td><td>Uub</td><td>[277]</td></tr> </table>																		nitrogen	N	14.007	phosphorus	P	30.974	arsenic	As	74.922	selenium	Se	78.96	tellurium	Te	127.6	polonium	Po	[209]	unununium	Uun	[271]	unununium	Uub	[277]	<table border="1"> <tr><td>oxygen</td><td>O</td><td>15.999</td></tr> <tr><td>sulfur</td><td>S</td><td>32.065</td></tr> <tr><td>chromium</td><td>Cr</td><td>51.996</td></tr> <tr><td>manganese</td><td>Mn</td><td>54.938</td></tr> <tr><td>iron</td><td>Fe</td><td>55.845</td></tr> <tr><td>cobalt</td><td>Co</td><td>58.933</td></tr> <tr><td>nickel</td><td>Ni</td><td>58.693</td></tr> <tr><td>copper</td><td>Cu</td><td>63.546</td></tr> <tr><td>zinc</td><td>Zn</td><td>65.39</td></tr> <tr><td>cadmium</td><td>Cd</td><td>112.41</td></tr> <tr><td>mercury</td><td>Hg</td><td>200.59</td></tr> <tr><td>unununium</td><td>Uun</td><td>[271]</td></tr> <tr><td>unununium</td><td>Uub</td><td>[277]</td></tr> </table>																		oxygen	O	15.999	sulfur	S	32.065	chromium	Cr	51.996	manganese	Mn	54.938	iron	Fe	55.845	cobalt	Co	58.933	nickel	Ni	58.693	copper	Cu	63.546	zinc	Zn	65.39	cadmium	Cd	112.41	mercury	Hg	200.59	unununium	Uun	[271]	unununium	Uub	[277]	<table border="1"> <tr><td>fluorine</td><td>F</td><td>18.998</td></tr> <tr><td>chlorine</td><td>Cl</td><td>35.453</td></tr> <tr><td>bromine</td><td>Br</td><td>79.904</td></tr> <tr><td>iodine</td><td>I</td><td>126.90</td></tr> <tr><td>astatine</td><td>At</td><td>[210]</td></tr> <tr><td>unununium</td><td>Uun</td><td>[271]</td></tr> <tr><td>unununium</td><td>Uub</td><td>[277]</td></tr> </table>																		fluorine	F	18.998	chlorine	Cl	35.453	bromine	Br	79.904	iodine	I	126.90	astatine	At	[210]	unununium	Uun	[271]	unununium	Uub	[277]	<table border="1"> <tr><td>helium</td><td>He</td><td>4.0026</td></tr> <tr><td>neon</td><td>Ne</td><td>20.180</td></tr> <tr><td>argon</td><td>Ar</td><td>39.948</td></tr> <tr><td>krypton</td><td>Kr</td><td>83.80</td></tr> <tr><td>xenon</td><td>Xe</td><td>131.29</td></tr> <tr><td>radon</td><td>Rn</td><td>[222]</td></tr> </table>																		helium	He	4.0026	neon	Ne	20.180	argon	Ar	39.948	krypton	Kr	83.80	xenon	Xe	131.29	radon	Rn	[222]
hydrogen	H	1.0079																																																																																																																																																																																																																																																																																																																																				
lithium	Li	6.941																																																																																																																																																																																																																																																																																																																																				
sodium	Na	22.990																																																																																																																																																																																																																																																																																																																																				
potassium	K	39.098																																																																																																																																																																																																																																																																																																																																				
rubidium	Rb	85.468																																																																																																																																																																																																																																																																																																																																				
cesium	Cs	132.91																																																																																																																																																																																																																																																																																																																																				
francium	Fr	[223]																																																																																																																																																																																																																																																																																																																																				
beryllium	Be	9.0122																																																																																																																																																																																																																																																																																																																																				
magnesium	Mg	24.304																																																																																																																																																																																																																																																																																																																																				
calcium	Ca	40.078																																																																																																																																																																																																																																																																																																																																				
strontium	Sr	87.62																																																																																																																																																																																																																																																																																																																																				
barium	Ba	137.33																																																																																																																																																																																																																																																																																																																																				
radium	Ra	[226]																																																																																																																																																																																																																																																																																																																																				
boron	B	10.811																																																																																																																																																																																																																																																																																																																																				
aluminum	Al	26.982																																																																																																																																																																																																																																																																																																																																				
gallium	Ga	69.723																																																																																																																																																																																																																																																																																																																																				
indium	In	114.82																																																																																																																																																																																																																																																																																																																																				
thallium	Tl	204.38																																																																																																																																																																																																																																																																																																																																				
unununium	Uun	[271]																																																																																																																																																																																																																																																																																																																																				
unununium	Uub	[277]																																																																																																																																																																																																																																																																																																																																				
carbon	C	12.011																																																																																																																																																																																																																																																																																																																																				
silicon	Si	28.086																																																																																																																																																																																																																																																																																																																																				
germanium	Ge	72.64																																																																																																																																																																																																																																																																																																																																				
tin	Sn	118.71																																																																																																																																																																																																																																																																																																																																				
lead	Pb	207.2																																																																																																																																																																																																																																																																																																																																				
unununium	Uun	[271]																																																																																																																																																																																																																																																																																																																																				
unununium	Uub	[277]																																																																																																																																																																																																																																																																																																																																				
nitrogen	N	14.007																																																																																																																																																																																																																																																																																																																																				
phosphorus	P	30.974																																																																																																																																																																																																																																																																																																																																				
arsenic	As	74.922																																																																																																																																																																																																																																																																																																																																				
selenium	Se	78.96																																																																																																																																																																																																																																																																																																																																				
tellurium	Te	127.6																																																																																																																																																																																																																																																																																																																																				
polonium	Po	[209]																																																																																																																																																																																																																																																																																																																																				
unununium	Uun	[271]																																																																																																																																																																																																																																																																																																																																				
unununium	Uub	[277]																																																																																																																																																																																																																																																																																																																																				
oxygen	O	15.999																																																																																																																																																																																																																																																																																																																																				
sulfur	S	32.065																																																																																																																																																																																																																																																																																																																																				
chromium	Cr	51.996																																																																																																																																																																																																																																																																																																																																				
manganese	Mn	54.938																																																																																																																																																																																																																																																																																																																																				
iron	Fe	55.845																																																																																																																																																																																																																																																																																																																																				
cobalt	Co	58.933																																																																																																																																																																																																																																																																																																																																				
nickel	Ni	58.693																																																																																																																																																																																																																																																																																																																																				
copper	Cu	63.546																																																																																																																																																																																																																																																																																																																																				
zinc	Zn	65.39																																																																																																																																																																																																																																																																																																																																				
cadmium	Cd	112.41																																																																																																																																																																																																																																																																																																																																				
mercury	Hg	200.59																																																																																																																																																																																																																																																																																																																																				
unununium	Uun	[271]																																																																																																																																																																																																																																																																																																																																				
unununium	Uub	[277]																																																																																																																																																																																																																																																																																																																																				
fluorine	F	18.998																																																																																																																																																																																																																																																																																																																																				
chlorine	Cl	35.453																																																																																																																																																																																																																																																																																																																																				
bromine	Br	79.904																																																																																																																																																																																																																																																																																																																																				
iodine	I	126.90																																																																																																																																																																																																																																																																																																																																				
astatine	At	[210]																																																																																																																																																																																																																																																																																																																																				
unununium	Uun	[271]																																																																																																																																																																																																																																																																																																																																				
unununium	Uub	[277]																																																																																																																																																																																																																																																																																																																																				
helium	He	4.0026																																																																																																																																																																																																																																																																																																																																				
neon	Ne	20.180																																																																																																																																																																																																																																																																																																																																				
argon	Ar	39.948																																																																																																																																																																																																																																																																																																																																				
krypton	Kr	83.80																																																																																																																																																																																																																																																																																																																																				
xenon	Xe	131.29																																																																																																																																																																																																																																																																																																																																				
radon	Rn	[222]																																																																																																																																																																																																																																																																																																																																				
<table border="1"> <tr><td>scandium</td><td>Sc</td><td>44.956</td></tr> <tr><td>titanium</td><td>Ti</td><td>47.887</td></tr> <tr><td>vanadium</td><td>V</td><td>50.942</td></tr> <tr><td>chromium</td><td>Cr</td><td>51.996</td></tr> <tr><td>manganese</td><td>Mn</td><td>54.938</td></tr> <tr><td>iron</td><td>Fe</td><td>55.845</td></tr> <tr><td>cobalt</td><td>Co</td><td>58.933</td></tr> <tr><td>nickel</td><td>Ni</td><td>58.693</td></tr> <tr><td>copper</td><td>Cu</td><td>63.546</td></tr> <tr><td>zinc</td><td>Zn</td><td>65.39</td></tr> <tr><td>cadmium</td><td>Cd</td><td>112.41</td></tr> <tr><td>mercury</td><td>Hg</td><td>200.59</td></tr> <tr><td>unununium</td><td>Uun</td><td>[271]</td></tr> <tr><td>unununium</td><td>Uub</td><td>[277]</td></tr> </table>																		scandium	Sc	44.956	titanium	Ti	47.887	vanadium	V	50.942	chromium	Cr	51.996	manganese	Mn	54.938	iron	Fe	55.845	cobalt	Co	58.933	nickel	Ni	58.693	copper	Cu	63.546	zinc	Zn	65.39	cadmium	Cd	112.41	mercury	Hg	200.59	unununium	Uun	[271]	unununium	Uub	[277]	<table border="1"> <tr><td>yttrium</td><td>Y</td><td>88.906</td></tr> <tr><td>zirconium</td><td>Zr</td><td>91.224</td></tr> <tr><td>niobium</td><td>Nb</td><td>92.906</td></tr> <tr><td>molybdenum</td><td>Mo</td><td>95.94</td></tr> <tr><td>technetium</td><td>Tc</td><td>[98]</td></tr> <tr><td>ruthenium</td><td>Ru</td><td>101.07</td></tr> <tr><td>rhodium</td><td>Rh</td><td>102.91</td></tr> <tr><td>silver</td><td>Ag</td><td>107.87</td></tr> <tr><td>cadmium</td><td>Cd</td><td>112.41</td></tr> <tr><td>indium</td><td>In</td><td>114.82</td></tr> <tr><td>tin</td><td>Sn</td><td>118.71</td></tr> <tr><td>antimony</td><td>Sb</td><td>121.76</td></tr> <tr><td>tellurium</td><td>Te</td><td>127.6</td></tr> <tr><td>iodine</td><td>I</td><td>126.90</td></tr> <tr><td>xenon</td><td>Xe</td><td>131.29</td></tr> <tr><td>radon</td><td>Rn</td><td>[222]</td></tr> </table>																		yttrium	Y	88.906	zirconium	Zr	91.224	niobium	Nb	92.906	molybdenum	Mo	95.94	technetium	Tc	[98]	ruthenium	Ru	101.07	rhodium	Rh	102.91	silver	Ag	107.87	cadmium	Cd	112.41	indium	In	114.82	tin	Sn	118.71	antimony	Sb	121.76	tellurium	Te	127.6	iodine	I	126.90	xenon	Xe	131.29	radon	Rn	[222]	<table border="1"> <tr><td>lanthanum</td><td>La</td><td>138.91</td></tr> <tr><td>cerium</td><td>Ce</td><td>140.12</td></tr> <tr><td>praseodymium</td><td>Pr</td><td>140.91</td></tr> <tr><td>neodymium</td><td>Nd</td><td>144.24</td></tr> <tr><td>promethium</td><td>Pm</td><td>[145]</td></tr> <tr><td>samarium</td><td>Sm</td><td>150.36</td></tr> <tr><td>europium</td><td>Eu</td><td>151.96</td></tr> <tr><td>gadolinium</td><td>Gd</td><td>157.25</td></tr> <tr><td>terbium</td><td>Tb</td><td>158.93</td></tr> <tr><td>dysprosium</td><td>Dy</td><td>162.50</td></tr> <tr><td>holmium</td><td>Ho</td><td>164.93</td></tr> <tr><td>erbium</td><td>Er</td><td>167.26</td></tr> <tr><td>thulium</td><td>Tm</td><td>168.93</td></tr> <tr><td>ytterbium</td><td>Yb</td><td>173.04</td></tr> </table>																		lanthanum	La	138.91	cerium	Ce	140.12	praseodymium	Pr	140.91	neodymium	Nd	144.24	promethium	Pm	[145]	samarium	Sm	150.36	europium	Eu	151.96	gadolinium	Gd	157.25	terbium	Tb	158.93	dysprosium	Dy	162.50	holmium	Ho	164.93	erbium	Er	167.26	thulium	Tm	168.93	ytterbium	Yb	173.04	<table border="1"> <tr><td>actinium</td><td>Ac</td><td>[227]</td></tr> <tr><td>thorium</td><td>Th</td><td>232.04</td></tr> <tr><td>protactinium</td><td>Pa</td><td>231.04</td></tr> <tr><td>uranium</td><td>U</td><td>238.03</td></tr> <tr><td>neptunium</td><td>Np</td><td>[237]</td></tr> <tr><td>plutonium</td><td>Pu</td><td>[244]</td></tr> <tr><td>americium</td><td>Am</td><td>[243]</td></tr> <tr><td>curium</td><td>Cm</td><td>[247]</td></tr> <tr><td>berkelium</td><td>Bk</td><td>[247]</td></tr> <tr><td>californium</td><td>Cf</td><td>[251]</td></tr> <tr><td>einsteinium</td><td>Es</td><td>[252]</td></tr> <tr><td>fermium</td><td>Fm</td><td>[257]</td></tr> <tr><td>mendelevium</td><td>Md</td><td>[258]</td></tr> <tr><td>nobelium</td><td>No</td><td>[259]</td></tr> </table>																		actinium	Ac	[227]	thorium	Th	232.04	protactinium	Pa	231.04	uranium	U	238.03	neptunium	Np	[237]	plutonium	Pu	[244]	americium	Am	[243]	curium	Cm	[247]	berkelium	Bk	[247]	californium	Cf	[251]	einsteinium	Es	[252]	fermium	Fm	[257]	mendelevium	Md	[258]	nobelium	No	[259]																																																																																	
scandium	Sc	44.956																																																																																																																																																																																																																																																																																																																																				
titanium	Ti	47.887																																																																																																																																																																																																																																																																																																																																				
vanadium	V	50.942																																																																																																																																																																																																																																																																																																																																				
chromium	Cr	51.996																																																																																																																																																																																																																																																																																																																																				
manganese	Mn	54.938																																																																																																																																																																																																																																																																																																																																				
iron	Fe	55.845																																																																																																																																																																																																																																																																																																																																				
cobalt	Co	58.933																																																																																																																																																																																																																																																																																																																																				
nickel	Ni	58.693																																																																																																																																																																																																																																																																																																																																				
copper	Cu	63.546																																																																																																																																																																																																																																																																																																																																				
zinc	Zn	65.39																																																																																																																																																																																																																																																																																																																																				
cadmium	Cd	112.41																																																																																																																																																																																																																																																																																																																																				
mercury	Hg	200.59																																																																																																																																																																																																																																																																																																																																				
unununium	Uun	[271]																																																																																																																																																																																																																																																																																																																																				
unununium	Uub	[277]																																																																																																																																																																																																																																																																																																																																				
yttrium	Y	88.906																																																																																																																																																																																																																																																																																																																																				
zirconium	Zr	91.224																																																																																																																																																																																																																																																																																																																																				
niobium	Nb	92.906																																																																																																																																																																																																																																																																																																																																				
molybdenum	Mo	95.94																																																																																																																																																																																																																																																																																																																																				
technetium	Tc	[98]																																																																																																																																																																																																																																																																																																																																				
ruthenium	Ru	101.07																																																																																																																																																																																																																																																																																																																																				
rhodium	Rh	102.91																																																																																																																																																																																																																																																																																																																																				
silver	Ag	107.87																																																																																																																																																																																																																																																																																																																																				
cadmium	Cd	112.41																																																																																																																																																																																																																																																																																																																																				
indium	In	114.82																																																																																																																																																																																																																																																																																																																																				
tin	Sn	118.71																																																																																																																																																																																																																																																																																																																																				
antimony	Sb	121.76																																																																																																																																																																																																																																																																																																																																				
tellurium	Te	127.6																																																																																																																																																																																																																																																																																																																																				
iodine	I	126.90																																																																																																																																																																																																																																																																																																																																				
xenon	Xe	131.29																																																																																																																																																																																																																																																																																																																																				
radon	Rn	[222]																																																																																																																																																																																																																																																																																																																																				
lanthanum	La	138.91																																																																																																																																																																																																																																																																																																																																				
cerium	Ce	140.12																																																																																																																																																																																																																																																																																																																																				
praseodymium	Pr	140.91																																																																																																																																																																																																																																																																																																																																				
neodymium	Nd	144.24																																																																																																																																																																																																																																																																																																																																				
promethium	Pm	[145]																																																																																																																																																																																																																																																																																																																																				
samarium	Sm	150.36																																																																																																																																																																																																																																																																																																																																				
europium	Eu	151.96																																																																																																																																																																																																																																																																																																																																				
gadolinium	Gd	157.25																																																																																																																																																																																																																																																																																																																																				
terbium	Tb	158.93																																																																																																																																																																																																																																																																																																																																				
dysprosium	Dy	162.50																																																																																																																																																																																																																																																																																																																																				
holmium	Ho	164.93																																																																																																																																																																																																																																																																																																																																				
erbium	Er	167.26																																																																																																																																																																																																																																																																																																																																				
thulium	Tm	168.93																																																																																																																																																																																																																																																																																																																																				
ytterbium	Yb	173.04																																																																																																																																																																																																																																																																																																																																				
actinium	Ac	[227]																																																																																																																																																																																																																																																																																																																																				
thorium	Th	232.04																																																																																																																																																																																																																																																																																																																																				
protactinium	Pa	231.04																																																																																																																																																																																																																																																																																																																																				
uranium	U	238.03																																																																																																																																																																																																																																																																																																																																				
neptunium	Np	[237]																																																																																																																																																																																																																																																																																																																																				
plutonium	Pu	[244]																																																																																																																																																																																																																																																																																																																																				
americium	Am	[243]																																																																																																																																																																																																																																																																																																																																				
curium	Cm	[247]																																																																																																																																																																																																																																																																																																																																				
berkelium	Bk	[247]																																																																																																																																																																																																																																																																																																																																				
californium	Cf	[251]																																																																																																																																																																																																																																																																																																																																				
einsteinium	Es	[252]																																																																																																																																																																																																																																																																																																																																				
fermium	Fm	[257]																																																																																																																																																																																																																																																																																																																																				
mendelevium	Md	[258]																																																																																																																																																																																																																																																																																																																																				
nobelium	No	[259]																																																																																																																																																																																																																																																																																																																																				

Figure 1.1. Transition-metal catalyst more common

There are many different aspects of this type of processes that are studied where unsaturated substrates are involved, as the high activity catalytic systems, chemo- and regioselectivity, enantioselectivity when possible, and also mechanistic studies governing these transformations.

Since this thesis will focus on the particular case of Rh-catalyzed [2+2+2] cycloaddition reactions, the precedents described will mainly concentrate on this kind of catalytic systems.

Grigg et al.⁴ were the first to describe the intramolecular cycloaddition of a series of triynes catalyzed by rhodium, in particular by the Wilkinson's catalyst (RhCl(PPh₃)₃) (Scheme 1.3). They observed that the cyclization of 1,6-triynes (when n=1) is much faster and cleaner compared to triynes when n=2, which requires harder reaction conditions to effect de cyclization.



Scheme 1.3. Intramolecular [2+2+2] cycloaddition reaction of triynes

The Wilkinson's complex, $\text{RhCl}(\text{PPh}_3)_3$, has been extensively employed until nowadays, and also combinations of cationic complexes of Rh (as example, $\text{Rh}(\text{cod})_2\text{BF}_4$) with bisphosphine ligands or with phosphoramidite ligands as we will see in the next sections.

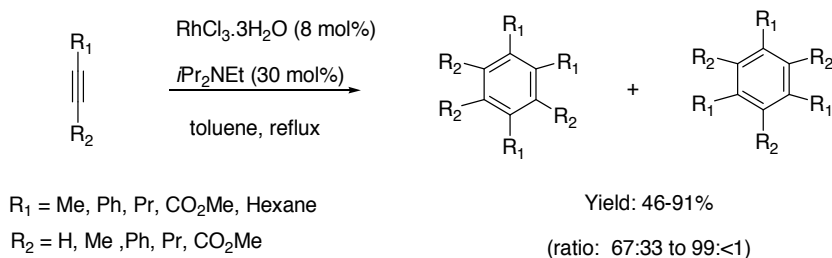
1.1.1. Chemoselective and Regioselective Features

Depending on the starting pattern, reactions can be categorized as intermolecular, partially intramolecular or intramolecular.

Due to the atom efficient and convergent nature of the cycloaddition approach, this process is considered to have advantages in the construction of highly substituted benzene rings over conventional strategies based on electrophilic aromatic substitutions or *ortho*-metalation reactions.

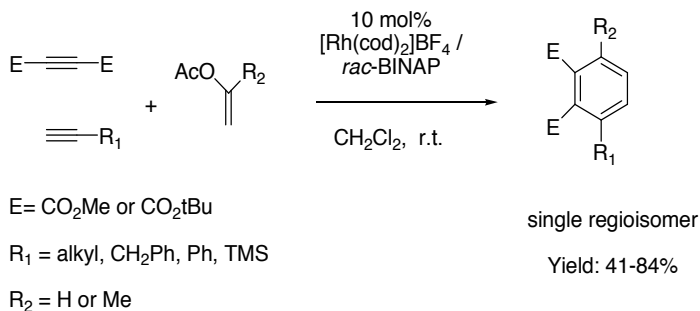
In the intermolecular approach, despite such synthetic potential, the difficulty in controlling chemo- and regioselectivity diminishes its utility in organic synthesis.

Over the last few years, promising new approaches to substituted arenes from three alkynes have been reported using stoichiometric amounts of transition-metal complexes.^{2r,5,6} However, recently, Hiroshi Tanaka et al.^{7a,b} performed a $\text{RhCl}_3 \cdot 3\text{H}_2\text{O}$ /amine-catalyzed cyclization of alkynes, which can be used for various mono- and disubstituted acetylenes and provides tri- or hexa substituted benzenes regioselectivity in high yields (Scheme 1.4).



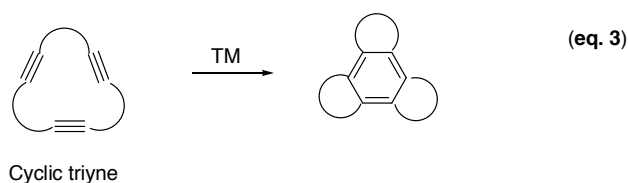
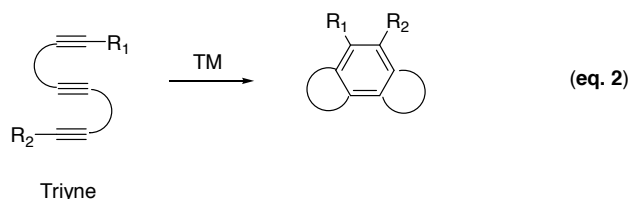
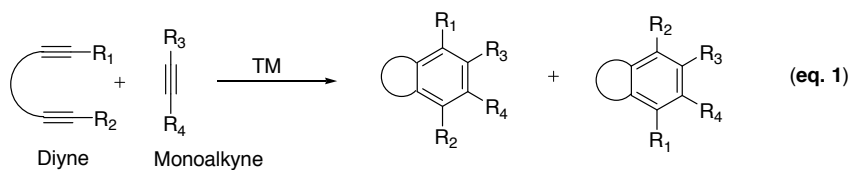
Scheme 1.4. Cyclootrimerization of various alkynes

Ken Tanaka et al.⁸ reported selective trimerizations of three different alkyne components attempting to solve the lingering problem of chemo- and regioselectivity in the intermolecular [2+2+2] cycloaddition reaction in the synthesis of arenes. The use of alkynes surrogates leads to more advances in [2+2+2] cycloadditions to polysubstituted benzenoid systems (Scheme 1.5). Thus, significant challenges still remain.



Scheme 1.5. Rh-catalyzed cycloaddition using enol acetates as alkyne surrogates

On the other hand, the intramolecular reaction is highly attractive as it gives multicyclic compounds from acyclic substrates in one pot. The intramolecular cycloaddition falls into two distinct categories as shown in Scheme 1.6. The partially intramolecular approach via the cycloaddition of a diyne with a monoalkyne (eq. 1) and the completely intramolecular cyclization of a tryne (eq. 2 and 3).



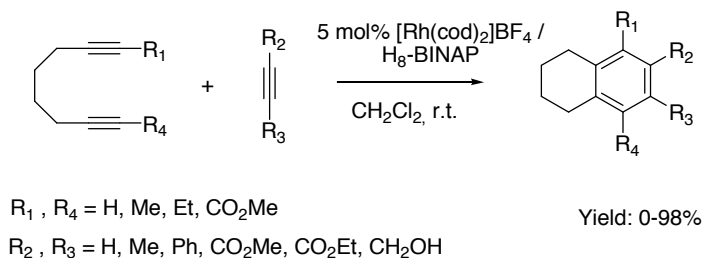
TM = Transition Metal

Scheme 1.6. Partially intramolecular cycloaddition reactions (eq.1) and intramolecular cycloaddition reactions (eq.2 and 3)

While the partially intramolecular methods have the advantage of using readily accessible diynes and monoalkynes, the dimerization of the diyne component is a serious drawback. Thus, a considerable excess of monoalkyne is generally required to prevent such a side reaction. On the other hand, the cyclization of triynes affords the desired products with complete selectivity, but the preparation of a triyne substrate possessing the necessary substituents or functional groups at the desired positions often needs lengthy synthetic operations.

Several examples of partially intramolecular [2+2+2] cycloaddition between diynes and monoynes for the synthesis of substituted benzenes have been studied using different transition metal complexes as catalyst.^{2,9}

K.Tanaka et al. described the cationic rhodium(I)/H₈-BINAP complex-catalyzed [2+2+2] cycloaddition of 1,7-octadiyne derivatives with monoynes for the synthesis of functionalized tetrahydronaphthalenes, which are found in several pharmaceutical ingredients (Scheme 1.7).^{9b}



Scheme 1.7. Rhodium-catalyzed [2+2+2] cycloaddition of 1,7-octadiyne derivatives with monoynes

As have been referred to earlier, completely intramolecular reactions are particularly interesting as they provide complex polycyclic systems in a single synthetic operation (eq. 2, Scheme 1.6).¹⁰ Furthermore, if the three alkynes form part of a closed system, *i.e.* a macrocycle, fused tetracycles may easily be obtained (eq. 3, Scheme 1.6).

Despite this strategy being synthetically attractive, hardly any cycloaddition reactions of macrocyclic systems containing triple bonds have been reported. Vollhardt, in a paper published in 1976,¹¹ prepared 1,5,9-cyclododecatriyne (Figure 1.2), which proved to be inert in the presence of light, high pressure and temperature, acidic conditions, and the CpCo(CO)₂ catalyst due to strain in the three four-membered rings formed.

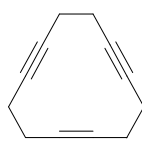
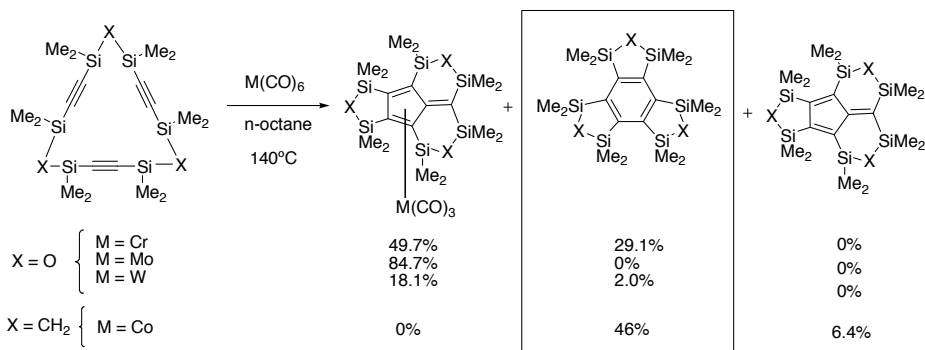


Figure 1.2. Structure of 1,5,9-cyclododecatriyne

The cycloaddition of cyclotrienes into tricyclic benzene derivatives has only been reported in two silicon-tethered macrocycles by Sakurai et al.¹² in low yields and in the presence of other π electron systems (Scheme 1.8).



Scheme 1.8. Intramolecular cyclization of macrocyclic polyacetylenes tethered by disiloxane and disilmethylene bridges

In recent years our group has been interested in the synthesis and applications of polyalkyne azamacrocyclic systems (Figure 1.3).^{13,14} Early on we observed that the [2+2+2] cycloaddition of the closed derivatives could easily result in highly functionalized tetracyclic fused structures in a one-pot atom-economical process. In addition, since our macrocyclic systems contain nitrogen atoms in the tethers between unsaturations, their [2+2+2] cycloaddition reaction opens the door to the construction of polycyclic azaheterocycles.

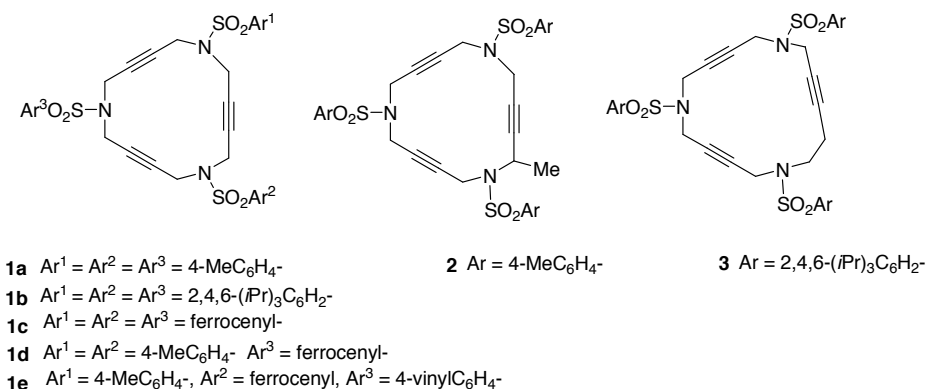
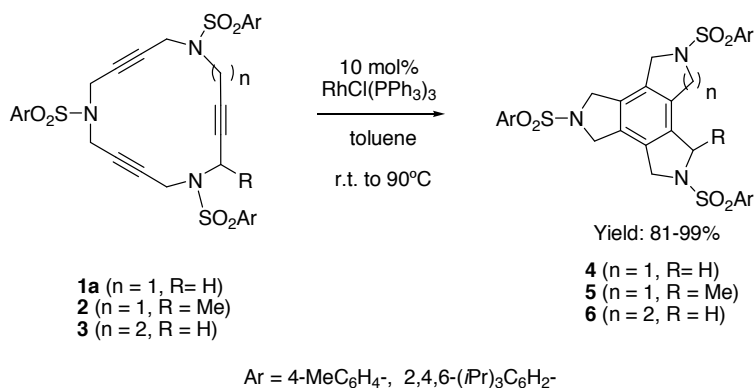


Figure 1.3. Triacetylenic azamacrocycles

All of these macrocycles can be synthesized stepwise from easily available arenesulfonamides and the corresponding 1,4-dihalobutynes compounds. Optimization of the preparation of key intermediates has made it possible to synthesize a wide variety of polyunsaturated azamacrocycles efficiently. For a recent review see reference [15].

Our group started investigating different TM complexes such as $\text{Pd}(\text{PPh}_3)_4$, $\text{CpCo}(\text{CO})_2$, $(\text{PCy}_3)_2\text{Cl}_2\text{Ru}=\text{CHPh}$ and $\text{RhCl}(\text{PPh}_3)_3$, to test their suitability for the cycloaddition of macrocyclic systems. As a result of these earlier studies it was concluded that rhodium gave the best results. (Scheme 1.9).^{14b}

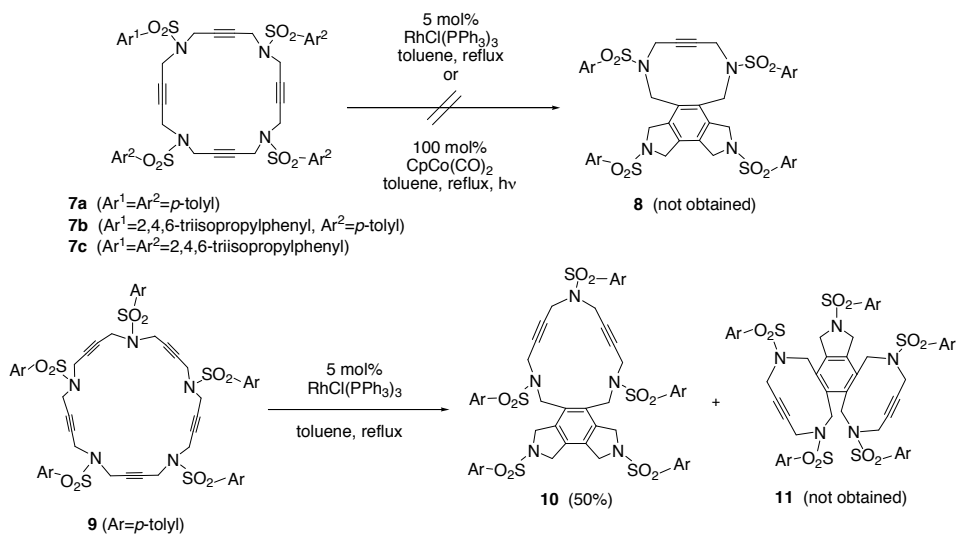


Scheme 1.9. Cycloaddition reactions of macrocycles **1a**, **2** and **3**

Wilkinson's catalyst was also used for the cycloaddition of 20- and 25-membered azamacrocycles (Scheme 1.10). When 20-membered macrocycles **7a-c** were treated with $\text{RhCl}(\text{PPh}_3)_3$ in refluxing toluene, no reaction took place. In all three cases, starting materials together with decomposition products were obtained. A stoichiometric amount of $\text{CpCo}(\text{CO})_2$ was also tested. The macrocycle was refluxed in toluene and the solution was heated by light irradiation. However, this reaction also failed and the starting macrocycle was recovered (Scheme 1.10).

In the case of the 25-membered ring **9**, there are two possible ways of cyclization, namely cycloaddition between three consecutive triple bonds to afford compound **10**

and cycloaddition between non-consecutive triple bonds to afford compound **11**. When 25-membered macrocycle **9** was treated with a catalytic amount of rhodium complex, the cyclotrimerized compound **10** resulting from the reaction of three contiguous alkynes was obtained as the only product of the process (Scheme 1.10).



Scheme 1.10. Cycloaddition reactions of 20- and 25-membered azamacrocycles

The lack of the reactivity of the 20-membered azamacrocycle is studied by DFT calculations in this thesis, as well as the chemoselectivity in the cycloaddition of the 25-membered azamacrocycle to obtain the product **10** in front of **11** (Chapter 4).

1.1.2. Enantioselective Features

Active molecules of many drugs are single enantiomers of chiral compounds and, in some cases, the opposite enantiomer may behave antagonistically and cause undesired side effects. As a result of this, the development of synthetic methods for the production of single enantiomers of chiral compounds is highly valuable. Several techniques are now used to obtain enantiopure materials: optical resolution¹⁶ and asymmetric synthesis.^{16,17} Optical resolution strategies have the disadvantage of half of

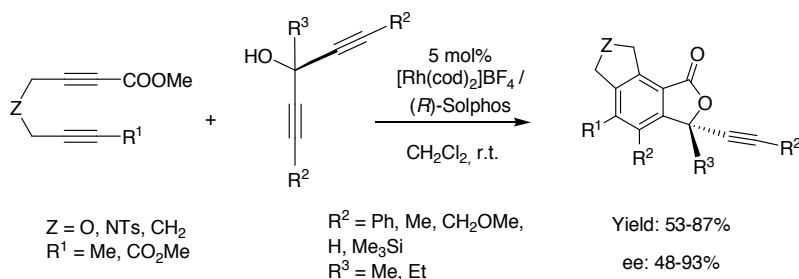
the product being the undesired enantiomer. Due to this drawback, asymmetric synthesis, defined as the conversion of an achiral starting material to a chiral product in a chiral environment, is currently the most powerful and commonly used method for chiral molecule preparation. In the last few years, asymmetric catalysis has become one of the most important areas of research and major breakthroughs have been achieved.^{17b}

Most asymmetric catalysts developed to date are metal complexes with chiral organic ligands. The chiral ligand modifies the reactivity and selectivity of the metal centre leading to the formation of one of the two possible enantiomeric products being favoured. However, of the thousands of chiral ligands available, only a few can be applied to a broad range of reactions and substrates.

In the particular case of the [2+2+2] cycloaddition reaction catalyzed by rhodium (I), the groups of Tanaka^{2n,s,18,19} and Shibata^{2q,20} are those that have most contributed to this goal. The developed methodology involves the use of the catalytic system formed by a cationic Rhodium complex ($[\text{Rh}(\text{cod})_2]\text{BF}_4$) and chiral diphosphines BINAP-type, which have enabled the preparation of enantioselective compounds with axial, planar and central chirality with excellent enantiomeric excesses.

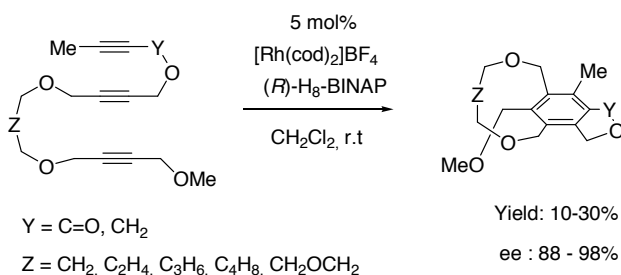
Rhodium is one of the most efficient catalysts to allow the asymmetric synthesis due to the ability to produce *in situ* different complexes with chiral phosphine ligands. As a result of this, some enantioselective studies using Rh-chiral-catalyst can be found in the literature.^{2n,q,18-20}

One of the first studies reported by Tanaka et al.^{18a} was the asymmetric assembly of enantioenriched 3,3-disubstituted phthalides (Scheme 1.11).



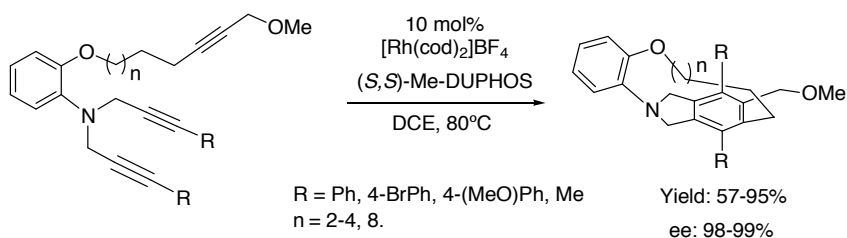
Scheme 1.11. Rh/(*R*)-Solphos-catalyzed enantioselective [2+2+2] cycloaddition of symmetrical 1,6-diynes with monoalkynes

Tanaka et al.^{19a,b} also described the enantioselective synthesis of planar-chiral metacyclophanes through cationic Rh(I)/H₈-BINAP-catalyzed intramolecular alkyne cycloaddition (Scheme 1.12).



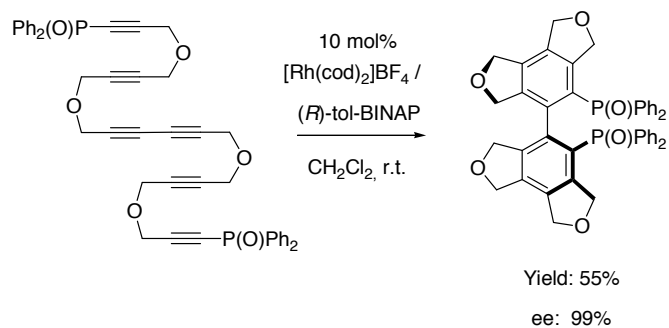
Scheme 1.12. Enantioselective synthesis of planar-chiral metacyclophanes

Shibata et al.²⁰ developed a highly enantioselective intramolecular reaction of nitrogen-branched triynes. A cationic Rh-Me-DUPHOS complex efficiently catalyzed the reaction to yield tripodal cage compounds with different length tethers (Scheme 1.13).



Scheme 1.13. Intramolecular [2+2+2] cycloaddition of branched triynes

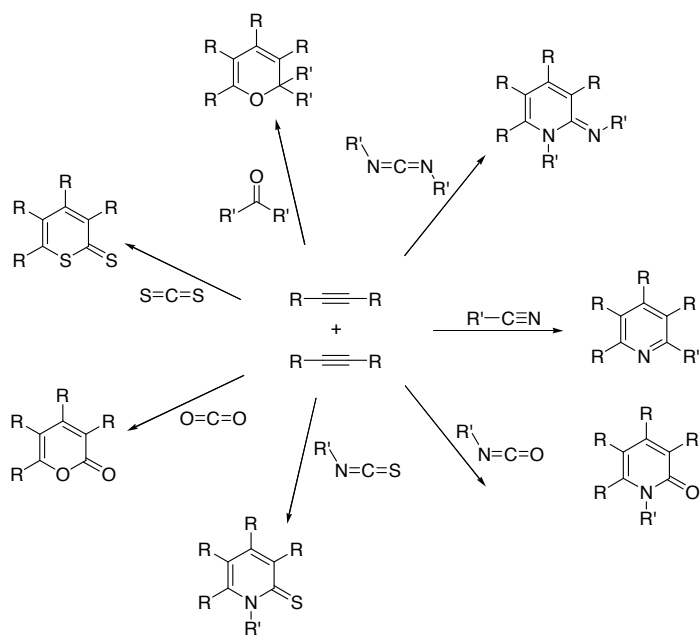
Tanaka et al.^{19c} have recently reported an asymmetric synthesis of axially chiral biaryl diphosphine ligands by rhodium-catalyzed enantioselective intramolecular double [2+2+2] cycloaddition (Scheme I.14).



Scheme I.14. Synthesis of the axially chiral biaryl diphosphine ligands

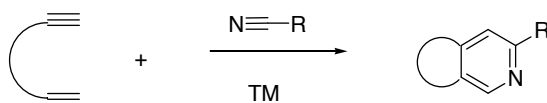
I.1.3. Participating unsaturated substrates

In recent years cycloaddition reactions have been modified to incorporate unsaturations such as olefins,^{2e,m,l} isocyanates,^{21,22a,b} nitriles,^{2i,o,p,22c,d} and carbonyls,^{22e,f} to deliver useful end products (Scheme I.15).^{2m}



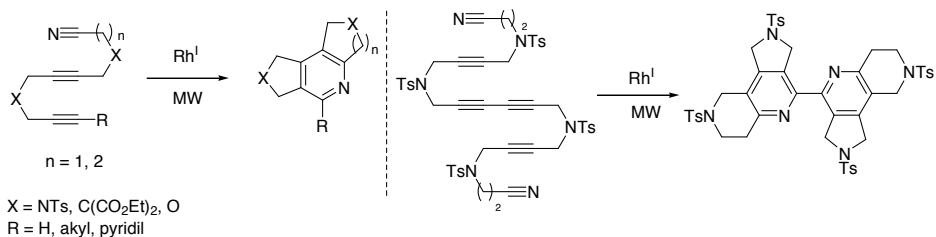
Scheme 1.15. [2+2+2] Cycloaddition between two alkynes and one unsaturated moiety which contains a heteroatom

When a nitrile molecule is used, pyridinic products can be easily obtained (Scheme 1.16).^{2i,p} These compounds are attractive since they are found in many natural products, whilst also constituting the core of many currently available pharmaceutical drugs. From the point of view of coordination chemistry, they are particularly useful as ligands, especially the bipyridine derivatives.



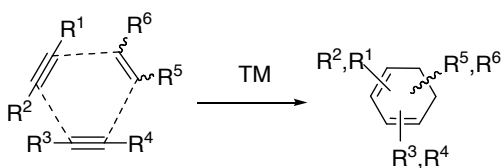
Scheme 1.16. [2+2+2] cycloaddition reaction with a nitrile group

Our research group has contributed to this investigation in studying the synthesis of pyridines and bipyridines with high functionality from cyanodiyne and under rhodium catalysis using microwave heating (Scheme 1.17).²³



Scheme 1.17. Synthesis of pyridines and bipyridines from cyanodiynes

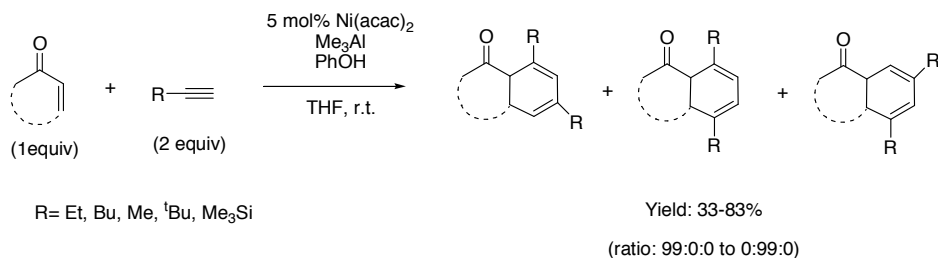
Other interesting unsaturated substrates which can participate in [2+2+2] cycloadditions are olefins. In this case, polysubstituted 1,3-cyclohexadienes can be obtained (Scheme 1.18),^{2e,m,l} which are attractive compounds for their use as reagents in Diels-Alder reactions.



Scheme 1.18. [2+2+2] cycloaddition reaction with an olefin molecule

There are several cases in the literature investigating the chemo- and regioselectivities of the formation of 1,3-cyclohexadienes from two alkynes and one olefin molecule.²⁴ Itoh et al,²⁵ reported the first palladium cycloaddition of two acetylenes with an olefin. Electron-donating olefins were found to suppress the competing cycloaddition reaction of three molecules of acetylene to obtain a catalytic stereoselective production of cyclohexadienes.

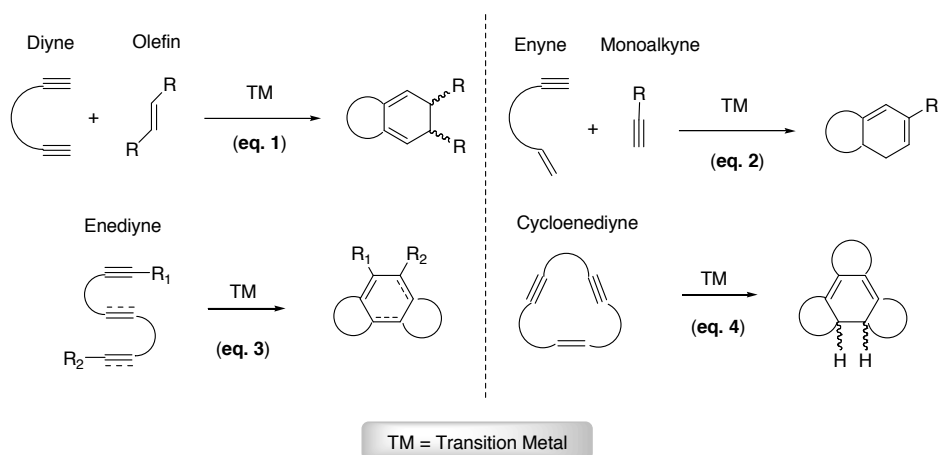
Ikeda et al.^{24b} published the first regioselective catalytic cycloaddition of three different unsaturated molecules by reacting one olefin and alkynes with different substituents by a nickel-aluminium catalyst system (Scheme I.19).



Scheme I.19. Catalytic selective cycloaddition of three different unsaturated molecules

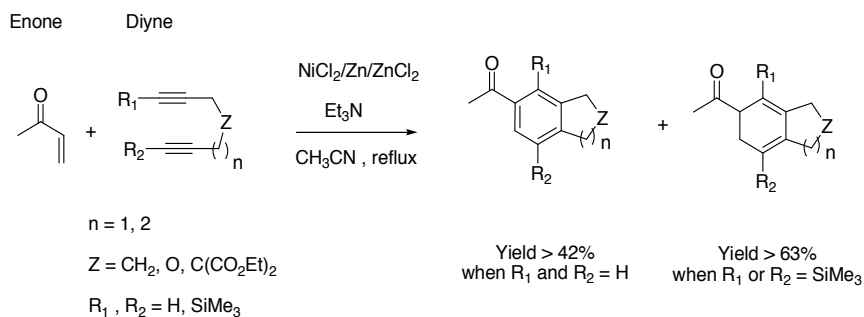
Despite these results, the chemo- and regioselectivity of the formation of 1,3-cyclohexadiene from two alkynes and one alkene molecule is too specific as they depend on the substrates and the catalytic system used. The catalytic control of both chemo- and regioselectivity is therefore still a formidable challenge.

The intramolecular approximations of two alkynes and one alkene manage to reduce the chemo- and regioselectivity aspects. The partially intramolecular approach may proceed via the cycloaddition of a diyne with a monoalkyne (eq. 1) or via the cycloaddition of an enyne with a monoalkyne (eq. 2) and the completely intramolecular cyclization of a enediyne or cycloenediyne (eq. 3 and 4, respectively) (Scheme I.20).



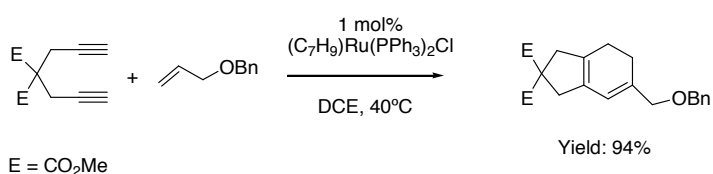
Scheme 1.20. Different intramolecular approximations with two alkynes and one alkene

One of the first examples of a completely regiochemically controlled cycloaddition of diynes and alkenes was reported by Ikeda et al.²⁶ They found that a terminally unsubstituted diyne reacted with enones to give an aromatized compound, rather than a 1,3-cyclohexadiene, with the concomitant incorporation of two hydrogen atoms into another molecule of the starting enone. On the other hand, the reaction of a trimethylsilyl-substituted diyne with an equimolar amount of enone regioselectively gave a cyclohexadiene product (Scheme 1.21).



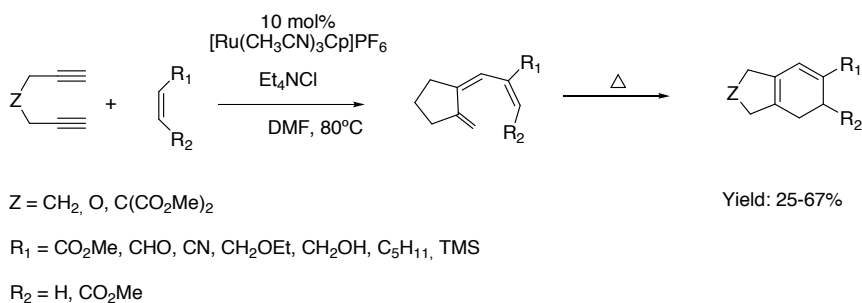
Scheme 1.21. Cycloaddition of an enone with non-terminal diynes

Itoh et al.²⁷ were the first to observe that the cycloaddition reaction between a diyne with an olefin molecule produces a regioisomer of the expected cyclohexadiene, where the position of a proton has changed causing a reorganization of the double bonds at the end product. They explained the formation of this regioisomer by a concomitant 1,5-H shift (Scheme 1.22) and the final product structure was deduced by NMR spectrum where only one vinyl proton absorption was observed together with the absorption of the two vicinal methylene protons on the 1,3-cyclohexadiene ring.



Scheme 1.22. [2+2+2] cycloaddition of a diyne with an allyl benzyl ether

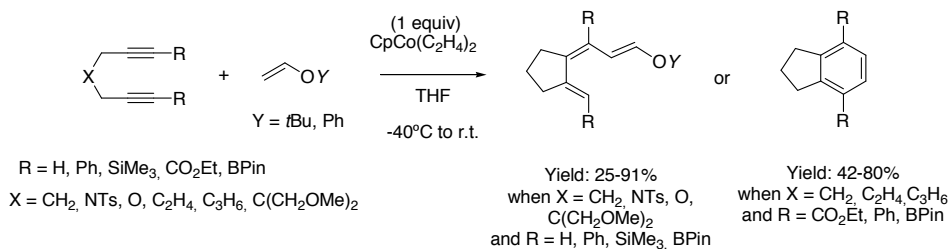
This process was synthetically exploited by Saá et al. in 2006. This group used a Ru-catalyst to couple diynes with alkenes to give cyclohexadienic products (Scheme 1.23).²⁸



Scheme 1.23. Ru-catalyzed [2+2+2] cycloaddition of terminal 1,6-diynes with acyclic alkenes

A 1,5-H shift was discarded suggesting a β -elimination, followed by a reductive elimination, affording hexatrienes as intermediates, which undergo a thermal disrotatory $6e^- \pi$ electrocyclicization to give regioisomeric cyclohexadienes. The mechanism proposed will be shown in the next section (1.1.4).

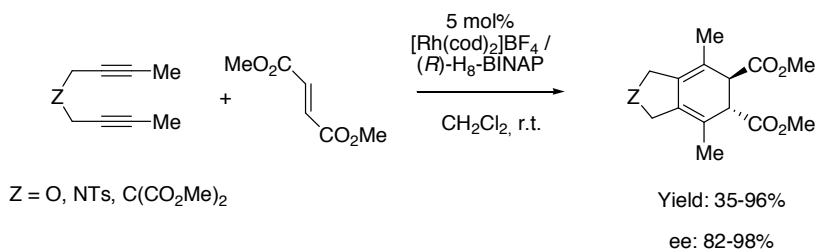
Aubert, Gandon et al.²⁹ reported this new type of reactivity exhibited by $[\text{CpCoL}_2]$ on the cobalt-mediated $[2+2+2]$ cycloaddition of diynes with alkenes (Scheme 1.24).



Scheme 1.24. Co-oligomerization of diynes with enol ethers

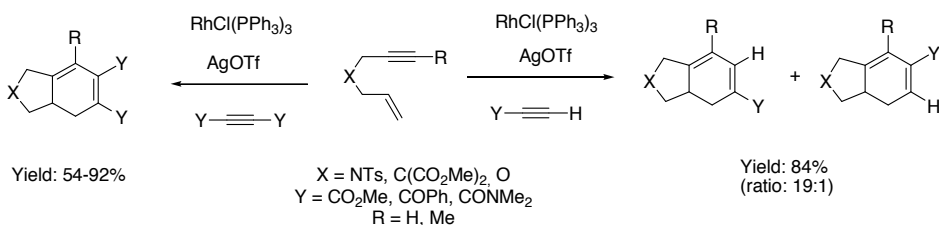
They observed that the trienic compounds undergo 6π -electrocyclization followed by dehydroalkoxylation giving rise to benzene derivatives, which arise from $[2+2+2]$ cycloaddition of alkynes.

On the other hand, K.Tanaka et al.³⁰ reported cationic Rh(I)/H₈-BINAP-catalyzed enantioselective partially intramolecular $[2+2+2]$ cycloadditions of diynes with *trans* alkenes. This represents a versatile new method for the synthesis of enantioenriched C₂-symmetric cyclohexadiene derivatives (Scheme 1.25).



Scheme 1.25. Cationic Rh(I)/(R)-H₈-BINAP-catalyzed enantioselective $[2+2+2]$ cycloaddition of 1,6-diynes with dimethyl fumarate

In the case of the reaction of an enyne with a monoalkyne (eq. 2 in Scheme 1.20),³¹ Evans et al.^{31d} explored the Wilkinson's complex catalyzed reactions of 1,6-enynes with symmetrical and unsymmetrical alkynes (Scheme 1.26).

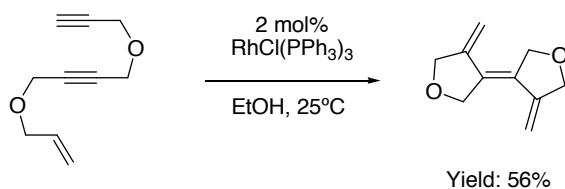


Scheme 1.26. Partially intramolecular metal-catalyzed [2+2+2] cycloadditions of 1,6-enynes with symmetrical and unsymmetrical alkynes

They concluded that a terminal alkyne is crucial for controlling the regioselectivity of the process and that the nature of the 1,2-substituted alkyne has an impact on the overall efficiency of this transformation.

Completely intramolecular cycloaddition reactions (eq. 3 in Scheme 1.20) afford cyclohexadienic compounds from enediynes. Volhardt et al.^{2e} employed stoichiometric amounts of CpCo(CO)₂ to permit the cycloaddition of several enediynes for the synthesis of polycyclic natural products.

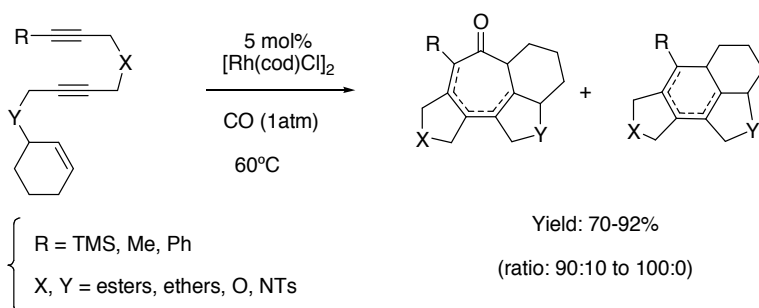
In the case of yne-ene-ynes and yne-yne-enes, few cases have been reported. Grigg et al.^{4b} investigated the first Wilkinson's complex catalyzed intramolecular [2+2+2] cycloadditions reactions of enediynes. They observed that enediynes (*yne-ene-yne*), although the attempts to carry out the reaction at elevated temperatures, failed to cyclise or to give linear dimers. In contrast, the enediyne (*yne-yne-ene*) gave the unusual bicyclic triene shown in Scheme 1.27.



Scheme 1.27. [2+2+2] Cycloaddition reaction of enediyne (*yne-yne-ene*) catalyzed by the Wilkinson's catalyst

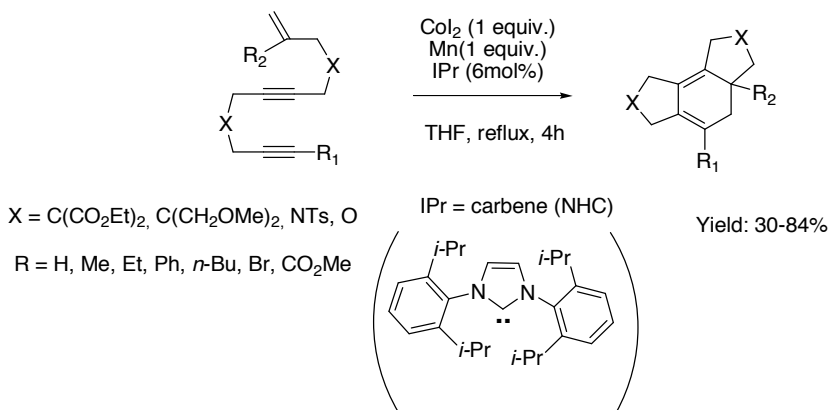
Yamamoto et al. reported the Pd-catalyzed reaction of an oxygen-tethered *yne-ene-yne*, which gave a mixture of cyclohexa-1,3- and 1,4-dienes.^{31b} Pd-catalyst could also be used in the cycloaddition of *yne-yne-enes*.

Ojima et al.^{32a,b} described the first example of a Rh-catalyzed totally intramolecular [2+2+2+1] cycloaddition process of enediynes, including CO as the single carbon component. Next, this group^{32c} published the formation of fused tetracyclic compounds where a 1:1 mixture of regioisomers of the expected product and its diene-shifted regioisomers were achieved (Scheme 1.28).



Scheme 1.28. [2+2+2+1] cycloaddition of enediyne type *yne-yne-ene* with CO

Aubert, Gandon et al. have been pioneers in studying cobalt complexes as efficient catalysts in this kind of processes.³³ In one of their last studies they analyzed the replacement of phosphines or cyclopentadienyl ligands by N-heterocyclic carbenes (NHC) for the Co metal (Scheme 1.29).^{33g}



Scheme 1.29. Cyclization of enediyne using Co₂/Mn/IPr

The use of NHCs with cobalt salts is easier to implement than CpCo(CO)₂ and more efficient. Moreover, when using carbene ligands the Co complex can be used catalytically and the chemoselectivity of the reaction is improved compared to the corresponding PPh₃-based system.

In the ongoing project of our group about the synthesis of polyunsaturated azamacrocycles (see for instance, Figure 1.3), 15-, 16- and 17-membered enediyne macrocycles were efficiently prepared (Figure 1.4).^{14b,d,15,34}

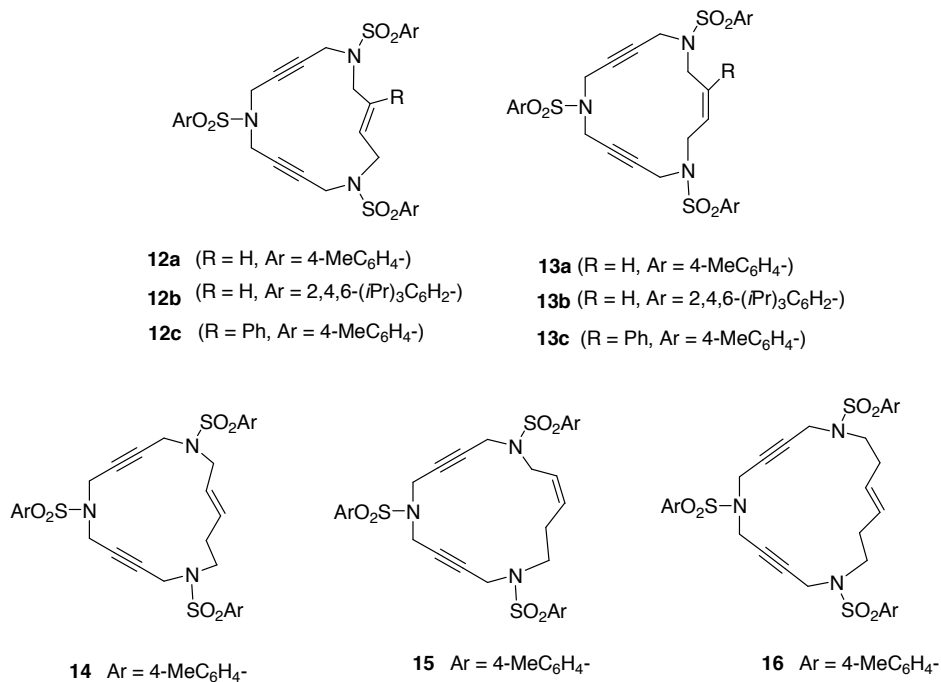
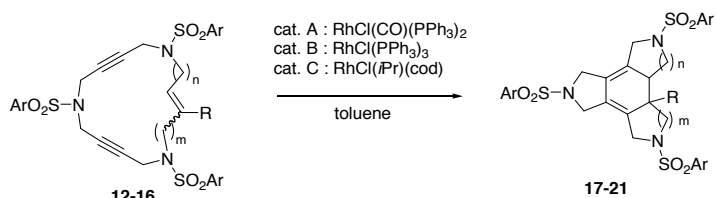


Figure I.4. Enediyne azamacrocycles

Consecutively, we decided to study the cycloaddition process of this series of azamacrocyclic enediynes (Table I.1). The first cases tested were 15-membered macrocycles **12a,b** and **13a,b** having a *trans* and a *cis* olefin respectively. Using a 5% molar of RhCl(CO)(PPh₃)₃ in toluene at 90 °C gave high yields of the cycloisomerized compounds **17a,b** and **18a,b** (Entries 1-4, Table I.1). No side reactions of the cyclohexadiene system such as aromatization or further cycloadditions took place.

The reaction proceeded with total stereoselectivity and initial stereochemistry of the macrocyclic double bond was maintained during the cycloaddition process. This experimental finding is consistent with the common mechanism proposed for this kind of cycloadditions in which two alkyne groups undergo initial coupling and subsequent incorporation of the olefin may then occur either by an insertion process or a Diels-Alder reaction.



Entry	MCC	Reaction conditions	Product	Yield (%)
1	12a	cat. A (5% molar), 90°C, 24h	 17a (Ar = 4-MeC ₆ H ₄ -)	98
2	12b	cat. A (5% molar), 90°C, 24h	17b (Ar = 2,4,6-(<i>i</i> Pr) ₃ C ₆ H ₂ -)	80
3	13a	cat. A (5% molar), 90 °C, 24 h	 18a (Ar = 4-MeC ₆ H ₄ -)	79
4	13b	cat. A (5% molar), 90 °C, 24 h	18b (Ar = 2,4,6-(<i>i</i> Pr) ₃ C ₆ H ₂ -)	68
5	12b	cat. B (5% molar), 90 °C, 24 h	17b (Ar = 2,4,6-(<i>i</i> Pr) ₃ C ₆ H ₂ -)	80
6	12b	cat. C (5% molar), 50 °C, 3 d	17b (Ar = 2,4,6-(<i>i</i> Pr) ₃ C ₆ H ₂ -)	98
7	12c	cat. B (5% molar), reflux, 24 h	 17c	95
8	13c	cat. B (5% molar), reflux, 24 h	 18c	71
9	14	cat. B (10% molar), 80 °C, 5 h	 19	90
10	15	cat. B (10% molar), 80 °C, 5 h	 20	87
11	16	cat. B (10% molar), 60 °C, 4 h	 21	98

Table I.I. Cycloaddition of azamacrocyclic enediynes 12-16

In order to see whether the Wilkinson's catalyst also promotes the cycloaddition process, macrocycle **12b** was treated with 5% molar of $\text{RhCl}(\text{PPh}_3)_3$ in toluene at 90°C . Compound **17b** was obtained in an 80% yield, demonstrating that Wilkinson's catalyst exhibits a similar efficiency with respect to $\text{RhCl}(\text{CO})(\text{PPh}_3)_2$ (Entry 5, Table I.1). Macrocycle **12b** was also cycloisomerized using the rhodium-N-heterocyclic carbene complex $[\text{RhCl}(\text{IPr})(\text{cod})]$ which after 3 days at 50°C in toluene gave a 98% yield of **17b** (Entry 6, Table I.1).^{34b}

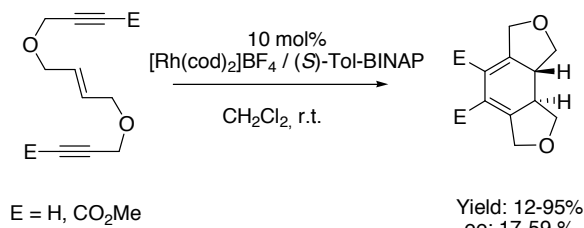
The effect of variations on the macrocycle scaffold, either substituents on the double bond or larger cavities, was then tested on the [2+2+2] cycloaddition of enediyne macrocycles. Harsher reaction conditions were required to cycloisomerize macrocyclic enediynes containing a phenyl substituent on the double bond (**12c** and **13c**). Refluxing toluene was necessary whereas 90°C was sufficient for the non-substituted macrocycles **12a,b** and **13a,b** (Entries 7 and 8, Table I.1).

In order to study the scope of the methodology, we chose different macrocycles (**14**, **15** and **16**) whose later cycloisomerization³⁵ led to various fused tetracycles such as 5,5,6- and 5,6,6-ring systems. As a general trend we observed that for enediyne macrocycles, the formation of 5,6,6-membered rings fused to the cyclohexadienic core (product **21**) was much faster than the formation of 5,5,6-ring system (products **19** and **20**), which in turn was faster than the formation of the 5,5,5-tetra fused structures (products **17** and **18**) (Entries 9-11, Table I.1).^{14d} Although there was a certain tendency to the formation of larger rings, which gave faster reactions, all the macrocycles afforded fused tetracycles unlike in other methods of synthesis, where the failure to construct 5,5,5- has been attributed to ring constraint.³⁶

The enantioselective cycloaddition of enediynes using chiral catalysts which would lead to enantioenriched cycloadducts is the next aspect that appears in the literature. There are only two reported studies of enantioselective cycloaddition of open-chain enediynes using chiral catalysts to afford enantioenriched cyclohexadienes. The two studies used chiral rhodium complexes and the choice of chiral ligands, as well as the

nature of the tether between unsaturations, was very important to obtain good yields and high enantiomeric excesses.^{30,37}

K.Tanaka et al.³⁰ employed a cationic rhodium (I)/(*S*)-Tol-BINAP complex to catalyze an enantioselective intramolecular [2+2+2] cycloaddition of a *trans* enediyne (Scheme I.30).



Scheme I.30. Cationic Rh(I)/(*S*)-Tol-BINAP-catalyzed enantioselective [2+2+2] cycloaddition of *trans* enediynes

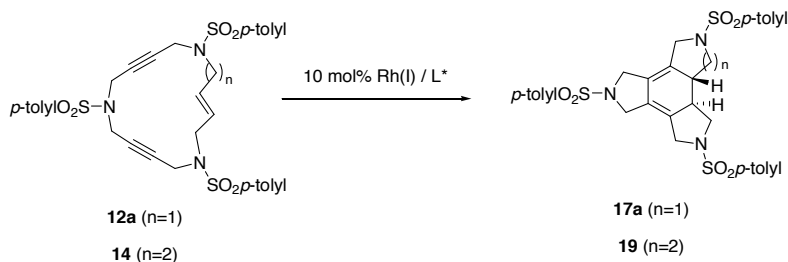
Shibata et al.³⁷ reported that Rh-*H*₈-BINAP complex catalyzes an enantioselective [2+2+2] cycloaddition of symmetrical and unsymmetrical (*E*)-enediynes (Scheme I.31), where they conclude that the choice of substituents on the alkyne termini is very important for high enantioselectivity.



Scheme I.31. [2+2+2] Cycloaddition of carbon-tethered symmetrical enediynes

In our group, the enantioselective cycloaddition of enediynes **12a**, **13c-16** (Figure 1.4) using a chiral rhodium complex which would lead to chiral cycloadducts was the next aspect to be evaluated. The first chiral rhodium complex tested was the commercially available (bicyclo [2.2.1] hepta-2,5-diene) [2*S*,3*S*]-bis(diphenylphosphino)butane rhodium(I) perchlorate. The best reaction conditions found to obtain a high ratio yield/enantiomeric excess was toluene as a solvent at 65°C for one day for the two macrocycles **12a** (Entry 1, Table 1.2) and **14** (Entry 2, Table 1.2). In the two cases, only moderate enantiomeric excesses were obtained.

In order to improve these results, a chiral bidentate ligand, *N*-phosphino *tert*-butylsulfonamide (PNSO) prepared by Prof. Riera's group was tested in the macrocyclic enediynes **12a** and **14** (Entry 3, 4 and 5, Table 1.2). Macrocyclic enediyne **12a** was treated with *N*-phosphino *tert*-butylsulfonamide rhodium complex in CH₂Cl₂ at room temperature. After 28 h of reaction the yield of **17a** was 77% and the ee was 48% (Entry 3, Table 1.2). When the dichloromethane was substituted for toluene the reaction time was reduced considerably from 28 h to 5.5 h and a 79% yield of **17a** with slightly improved 50% of ee was obtained (Entry 4, Table 1.2). The latter reaction conditions were applied for macrocycle **14**. In this case an excellent yield of 94% of **19** was obtained although the ee dropped to 7% (Entry 5, Table 1.2). The enantiomer formed with the PNSO/Rh complex was the opposite of that obtained in entries 1 and 2. Other experiments using [RhCl(cod)]₂ and several chiral phosphines did not lead to better chirality induction than that described in Table 1.2.



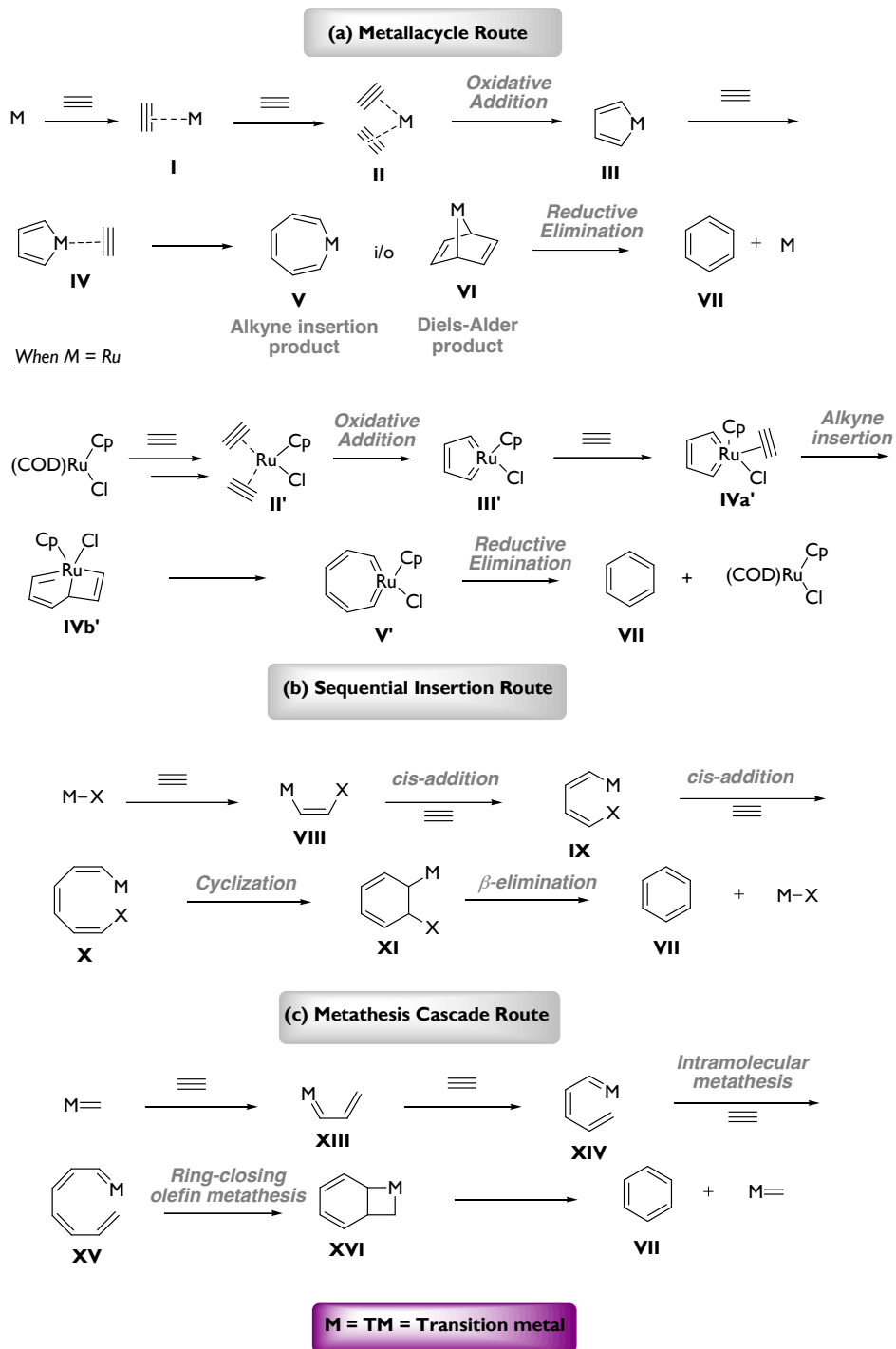
Entry	MCC	Catalyst (10%mol)	Reaction conditions	Product	Yield (%)	e.e (%)
1	12a		toluene, 65°C, 24h	17a	95	44
2	14		toluene, 65°C, 24h	19	46	41
3 ^a	12a		CH ₂ Cl ₂ , r.t., 28h	17a	77	48
4 ^a	12a		toluene, r.t., 5.5h	17a	79	50
5 ^a	14		toluene, r.t., 5.5h	19	94	7

^a The enantiomer obtained in these cases was the opposite of that obtained in entries 1 and 2.

Table I.2. Enantioselective [2+2+2] cycloaddition reaction of macrocyclic enediynes **12a** and **14**

1.1.4. The postulated mechanism

Transition-metal catalyzed alkyne cycloadditions can be broadly divided into the following three categories on the basis of their postulated reaction mechanisms (Scheme 1.32): a) metallacycle route; b) sequential insertion route; c) metathesis cascade route. β



Scheme 1.32. Possible mechanisms of alkyne cycloaddition

The most widely accepted mechanism is the metallacycle route, shown in the general Scheme 1.32.^{2f,h,i} Initially, one alkyne moiety displaces a ligand on the metal to form alkyne complex **I**, followed by a second alkyne coordination to form compound **II**. Oxidative coupling may occur to give the coordinative unsaturated metallacyclopentadiene **III**, in which the metal adopts a formal oxidation state two units higher than in its precursor **II**. Complex **III** may then coordinate a third molecule of alkyne to give **IV**, which proceeds to generate either an alkyne-insertion to form the metallacycloheptatriene **V**, or a Diels-Alder type addition to furnish bicyclic complex **VI**. Finally, the benzene ring **VII** is formed by the reductive elimination of the metal, and the catalyst (M) is recovered. A myriad of metallacyclopentadiene complexes relevant to cycloaddition have been isolated to date, and some of them actually give aromatic products upon treatment with alkynes.³⁸ On the basis of DFT calculations performed by Yamamoto et al.,^{10c} and Kirchner et al.³⁹ a novel mechanism was proposed for CpRuCl-catalyzed alkyne cycloaddition. The rate-determining step is the oxidative cyclization, which produces a ruthenacycle intermediate (type **III'**, Scheme 1.32). The key feature of this mechanism is the isomerization from ruthenacyclopentadiene(alkyne) complex (type **IVa'**) to ruthenabicyclo[3.2.0]heptatriene (**IVb'**), which gives rise to a seven-membered type **V'** ruthenacycle.

On the other hand, a sequential carbometallation mechanism operates in cycloadditions catalyzed by transition-metal hydrides or halides M-X, shown in Scheme 1.32b.^{10a,40} Initially, there is a *cis*-addition of the M-X to the alkyne to form the intermediate **VIII**, followed by consecutive *cis*-addition of this intermediate to another two alkynes to form species **X**. Intermediate **XI** is formed after cyclization of compound **X**. Benzene derivative **VII** is obtained after β -elimination of M-X and the catalyst is recovered.

In addition to these well-known precedents, a metathesis cascade using Grubbs' ruthenium carbene complex proved to be effective for the cyclization of triynes (Scheme 1.32c).⁴¹ The mechanism postulated consists of an initial intermolecular reaction, ruthenium carbene complex adds to the triple bond to obtain compound

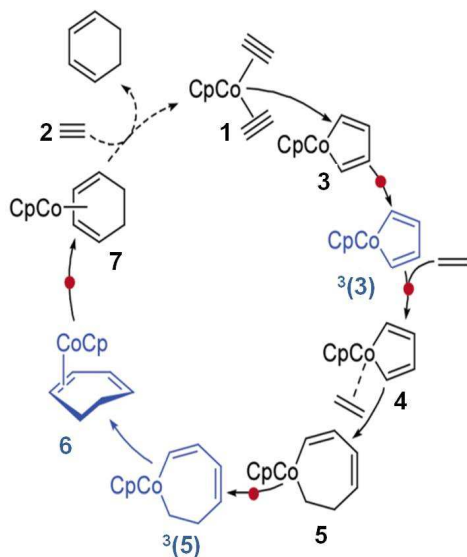
XIII. This intermediate undergoes an intramolecular metathesis reaction *via* **XIV** to produce a conjugated carbene complex **XV**. The final ring-closing olefin metathesis step leads to the formation of the bicyclic system **XVI** which evolves to the aromatic system **VII**, this should provide a strong driving force for the overall reaction cascade.

The elucidation of the mechanistic aspects of homogeneous catalysis has been an ambitious scientific goal since the early days of organometallic chemistry. Due to the enormous progress in computational chemistry over the last few years, theoretical methods are playing an increasingly important role in identifying possible elementary reactions. Ultimately, the aim is to understand these fundamental transformations in order to monitor and tune changes in reactivity toward a given synthetic purpose. It is therefore useful to combine experimental work with theoretical studies based on density functional theory (DFT) calculations.

Recent progress in computational chemistry has shown that many important chemical and physical properties of the species involved in these reactions can be predicted from first principles by various computational techniques. This ability is especially important in those cases where experimental results are difficult to obtain.

Cobalt complexes have been used extensively for mediating cocyclizations of alkynes, often with high levels of chemo-, regio-, and stereoselectivity. Although the mechanism of this reaction has been the subject of many experimental and computational studies, it has yet to be fully elucidated. After pioneering semiempirical⁴² efforts, a more detailed DFT analysis was reported by Albright et al. in 1999 who first provided a rigorous and detailed computational description of the whole mechanism of acetylene trimerization catalyzed by the CpCo fragment.⁴³ Using a larger basis set, Koga et al. theoretically explored the regioselectivity of the first step of the CpCo-catalyzed acetylene trimerization and reexamined the work by Albright, addressing different mechanistic schemes in both the singlet and triplet state⁴⁴ where they concluded that there is a change in spin state along the reaction coordinate. The work took explicit account of the fact that 18-electron cobalt species usually exist as singlet states, whereas their 16-electron congeners have triplet ground states.⁴⁵

Gandon, Vollhardt et al.^{46a} extended the approach to the cobalt-mediated synthesis of cyclohexadiene from acetylene and ethylene, finding that alkene incorporation proceeds via insertion into a Co-C σ -bond since as the resulting seven-membered metallacycle is a key intermediate (**5** of the Scheme 1.33).

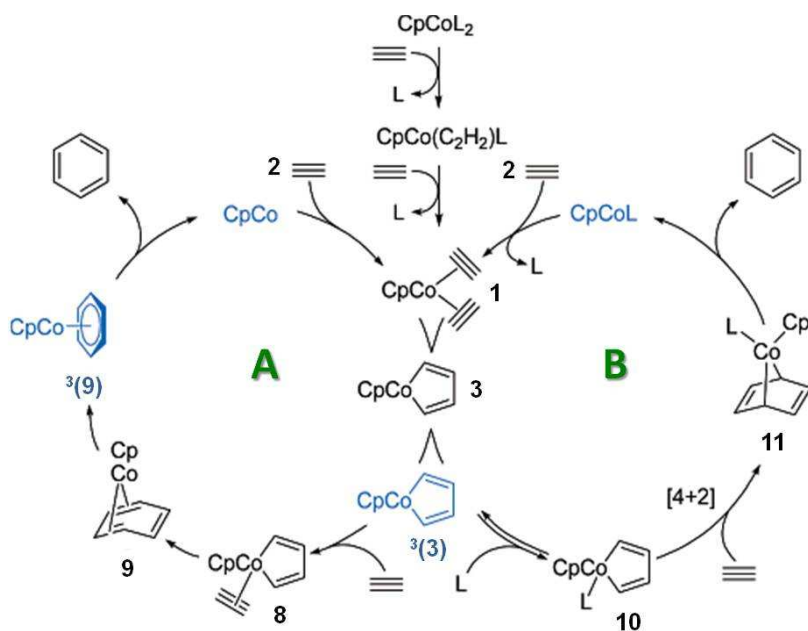


Scheme 1.33. Two-state reactivity mechanism for the cobalt-catalyzed cycloaddition to cyclohexadiene where triplet species appear in blue and singlet species in black

Interestingly, the formation of the free arene and the release of CpCoL involves several spin state changes (Scheme 1.33).

Gandon, Vollhardt et al.^{46b} reported a new study where parallel mechanisms for the [2+2+2] cycloaddition of alkynes were achieved (Scheme 1.34). After the oxidative coupling step from a bisalkyne complex (**1** in Scheme 1.34) to a cobaltacyclopentadiene (**3** in Scheme 1.34), which spontaneously relaxes to the triplet ground state (³**3**) in Scheme 1.34) two mechanisms are involved. In the absence of strong σ -donors ligands (PR_3 , CO, THF) and electron-poor alkynes, the catalytic cycle followed is **A**, while **B** is preferred in the presence of σ -donor ligands. As a result,

reactions in strong σ -donor solvents or employing $\text{CpCo}(\text{PR}_3)_2$ or $\text{CpCo}(\text{CO})_2$, for the specie **10** (Scheme I.34) is a likely relay point.

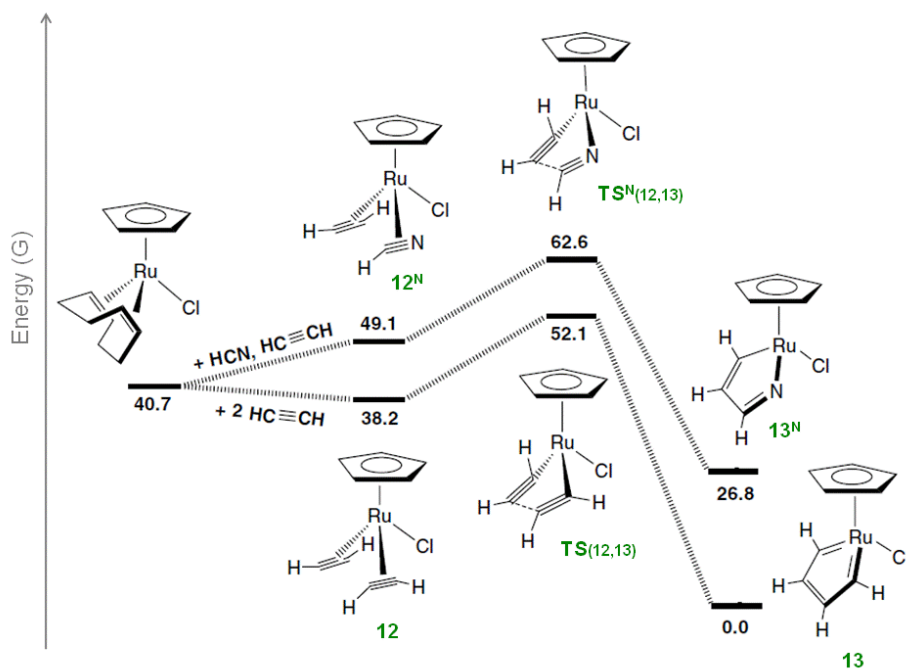


Scheme I.34. Two-state mechanisms for the cobalt-catalyzed alkyne cycloaddition to benzene (triplet species are depicted in blue)

Accurate computational studies for the same reactions and the cocyclization of acetylene and CS_2 have been carried out by Kirchner et al. with CpRuCl as the catalyst.⁴⁷ They conclude that the differences between the two systems (Co- and Ru-system), namely the larger variety of intermediates envisaged for the ruthenium system as compared to cobalt, may be partly related to the atomic radii. The smaller radius of Co (1.25 vs 1.33 Å for Ru) may control interligand interactions in a different way.

Kirchner et al.⁴⁸ proposed a mechanism of the CpRuCl -catalyzed synthesis of pyridine from acetylene and HCN on reexamining the previous work by Yamamoto et al.^{10c,49}

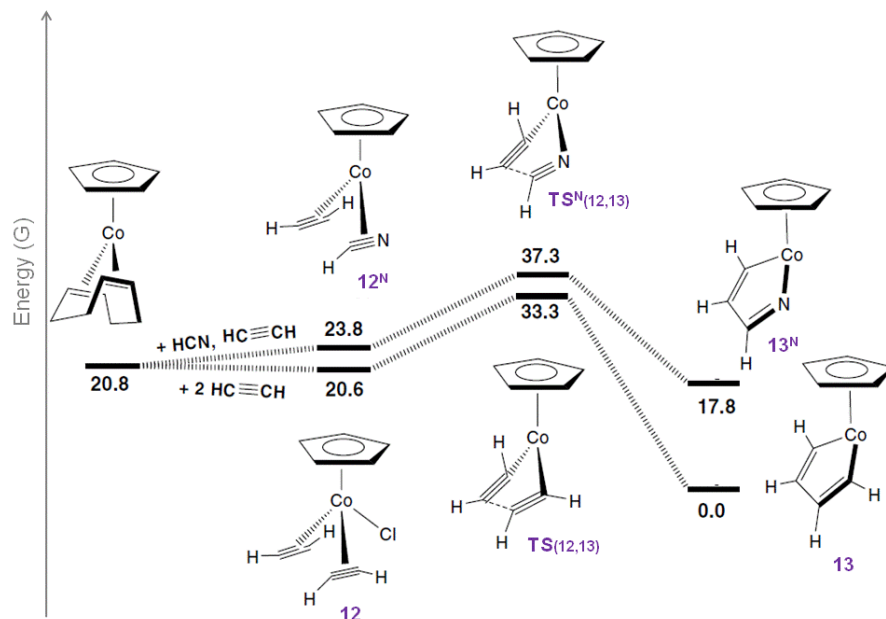
In their discussion, part of the mechanism of the same reaction catalyzed by CpCo and CpRh fragments is studied. They found that the key reaction step is the oxidative coupling of two alkyne ligands (route **12** → **13**) to give the metallacyclopentatriene **13** (Ru) (Scheme 1.35) and the metallacyclopentadiene **13** (Co and Rh) intermediates (Scheme 1.36).



Scheme 1.35. Gibbs energy profile (in kcal/mol) for the conversion of Ru-catalyst into the respective metallacycles **13** and **13^N**

In the case of the Ru, the Gibbs activation energies for two acetylenes oxidatively coupled is 13.9 kcal/mol while the same process with one acetylene and one nitrile has an energy barrier of 21.9 kcal/mol. Thus, the acetylenes coupling is favoured kinetically and also the formation of **13** is thermodynamically preferred. Moreover, after exploring successive pathways, Kirchner et al. observed that the benzene formation was thermodynamically preferred to the pyridinic product, depending on the

substituents on the alkynes. Despite these observations, from a kinetic point of view and starting from the metallacyclopentatriene (**13**), the addition of nitriles to afford pyridines is easier than the addition of acetylenes to give benzenes.



Scheme 1.36. Gibbs energy profile (in kcal/mol) for the conversion of Co-catalyst into the respective metallacycles **13** and **13^N**

The results on the CpCo and CpRh systems were found to be similar to those of the CpRuCl fragment, where the processes alkyne-alkyne or one alkyne and one nitrile coupling were by and large the same in both cases (range of 12.7-16.5 kcal/mol), independent of the metal fragment (Scheme 1.36). Despite these results, few differences were found between the Co and Rh systems and CpRuCl in the subsequent steps, traced partly to the absence of the Cl coligand and the structure of the metallacycloheptatriene, (Figure 1.5), which was only detected in the RhCp System.

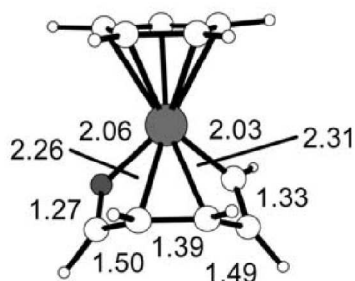


Figure I.5. Optimized structure at B3LYP level of the rhodacycloheptatriene detected only for RhCp complex (distances in Å)

On the other hand, an important conclusion that can be obtained by Kirchner (Scheme I.35 and Scheme I.36) was that the oxidative coupling of two alkyne moieties is thermodynamically and kinetic more favourable than the coupling of one alkyne and one nitrile molecule.

Bickelhaupt et al.⁵⁰ presented in 2007 the results of a theoretical investigation on the mechanism of $[(\eta^5\text{-C}_5\text{H}_5)\text{Rh}]$ -catalyzed cycloaddition of acetylene to benzene and cocycloaddition of acetylene and acetonitrile to 2-methylpyridine. They were interested in the chemical reactivity of rhodium complexes, especially in terms of their suitability for catalytic systems. It was the first one that addresses the mechanism of cycloaddition reactions catalyzed by indenyl-rhodium complex. They found that the mechanism of acetylene self-trimerization catalyzed by the CpRh fragment was essentially analogous to that described with CpCo as catalyst, but it was slightly energetically disfavoured. The release of benzene occurs by stepwise addition of two acetylene molecules, which regenerates the catalyst. In the presence of acetonitrile, a nitrile molecule competes with acetylene to coordinate to the rhodacycle, to generate an intermediate that subsequently evolves to a peculiar bicyclic intermediate (Figure I.6) which allows establishing an analogy with the mechanisms catalyzed by CpRuCl (see intermediate **IVb'** in Scheme I.32a).

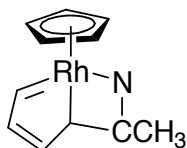
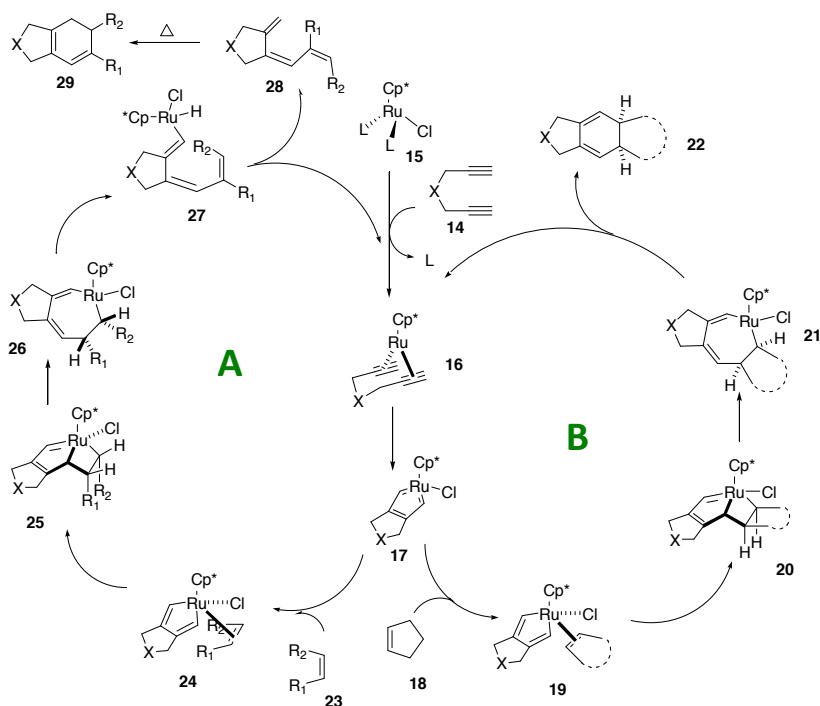


Figure I.6. Bicyclic intermediate isolated with Rh-catalyst

The seven-membered-ring species, which were located on the PES (Potential Energy Surface) of CpRh are energetically disfavoured intermediates and were thus excluded from the mechanisms; in contrast these seven-membered-ring intermediates play a crucial role in CpRuCl-catalyzed trimerizations. Therefore, Bickelhaupt et al. concluded that the electronic structure of the metal core is more important than its size (covalent atomic radius) in controlling the mechanistic stages of the CpM-catalyzed processes.

Saá et al.⁵¹ analyzed the changes of the reaction mechanism of the Ru(II)-catalyzed [2+2+2] cycloaddition between 1,6-diyne and alkenes to afford 1,3-cyclohexadienes with the nature of the starting alkene. Starting from cyclic alkenes (**18**), standard 1,3-cyclohexadienes (**22**, Scheme I.37) were obtained (from the reductive elimination of intermediate **21**), while if the reactants were linear alkenes (**23**), a tandem process was observed which involved a linear coupling of 1,6-diyne and alkenes to 1,3,5-hexatrienes (**27**) (from a β -elimination of intermediate **26** followed by a reductive elimination) followed by a pure electrocyclization of **28** to give 1,3-cyclohexadienes, **29**.

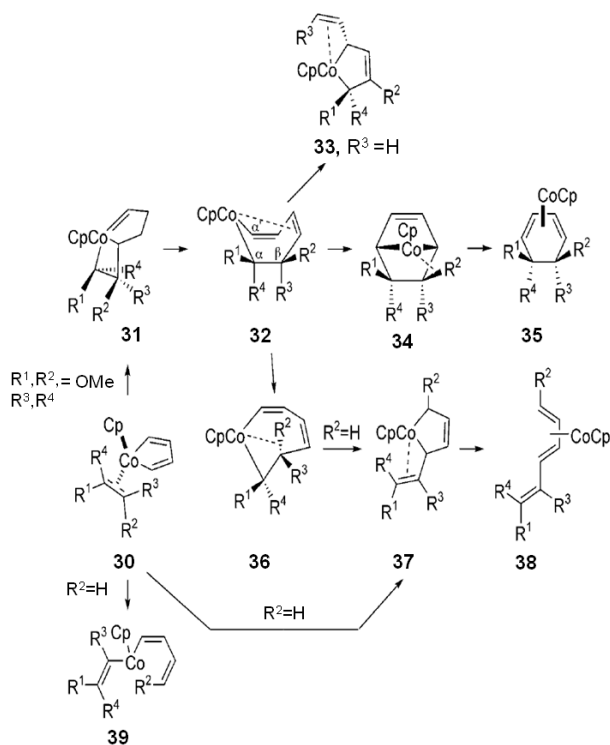


Scheme 1.37. Proposed mechanisms for the formal and standard Ru-catalyzed [2+2+2] cycloadditions of terminal 1,6-diyne with acyclic and cyclic alkenes

These new intermediates (trienes like **27** in Scheme 1.37) identified by Saá with Ru-catalyst were recently observed by Aubert, Gandon et al.²⁹ in the cobalt-mediated co-oligomerization of alkynes with enol ethers (Scheme 1.24). The DFT studies gave the possible isomerization of species **30** (Scheme 1.38) to obtain the cyclohexadiene derivatives (**35**) or the triene complexes (**38**).

The insertion of the alkene molecule into a Co-C bond to give seven-membered complexes **32**, was the preferred route for this bound alkene in **30**, regardless of the presence of the alkoxy group (OMe). Next, the energies connected to the isomerization of **32** to **35** via **34**, and of **32** to **38** via **36** and **37** were relatively low-lying, and no pronounced energetic predilection for either pathway could be discerned. Therefore, they noticed that the structural factors influence this outcome strongly and the calculations also suggested that the trienes and cyclohexadienes shared a common intermediate, and that the formation of trienes follows the β -

hydride elimination pathway $32 \rightarrow 36 \rightarrow 37 \rightarrow 38$ (Scheme 1.38), while the formation of the cyclohexadiene follows ($32 \rightarrow 34 \rightarrow 35$). This result is in consonance with those obtained for the CpRu systems by Saá.⁵¹



Scheme 1.38. Computed possible isomerizations of **30**

1.2. Computational Chemistry

Computational Chemistry is a branch of chemistry that uses computers to assist in solving chemical problems. Recent years have seen an increase in the number of chemists doing theoretical and computational chemistry. The fast evolution of computers has allowed to perform complex calculations and to obtain very significant

information about geometrical structures and properties of molecules and solids. Consequently, the computational chemistry is the application of chemical, mathematical and computing skills to the solution of interesting chemical problems for the case of Homogeneous Catalysis.^{52,53}

Note that the words *exact* and *perfect* do not appear here, as very few aspects of chemistry can be computed exactly, but almost every aspect of chemistry has been described in a qualitative or approximate quantitative computational scheme. Thus, computational chemistry has become a useful method for chemists that carry out predictions before running the actual experiments so that they can be better prepared for making observations. It is also widely employed to interpret and complement experimental results.

Using computational chemistry software you can in particular perform:

- Electronic structure determinations
- Geometry optimizations
- Frequency calculations
- Definition of transition structures and reaction paths
- Protein calculations, i.e. docking
- Calculations of potential energy surfaces (PES)
- Calculations of rate constants for chemical reactions (kinetics)
- Thermodynamic calculations – heat of reactions, energy of activation, etc
- IR, NMR, UV spectroscopy analysis
- Excited state chemistry studies
- Chemical dynamics analysis
- Other physical and chemical properties

The most important numerical techniques are *ab initio*, *empirical* or *semi-empirical* and *molecular mechanics*. These differ mainly according to how exactly the physics of the system is solved. Definitions of these terms are helpful in understanding the use of computational techniques for chemistry:

- *Ab initio*, (Latin for “from scratch”) a group of methods in which molecular structures can be calculated using nothing but the Schrödinger equation, the values of the fundamental constants and the atomic numbers of the atoms present. Due to the high computational cost, it is best for small systems (tens of atoms), or systems requiring rigorous accuracy.
- *Empirical* or *semi-empirical* techniques use approximations from empirical (experimental) parameters to provide the input into the mathematical models. These less accurate methods are based on the Hartree-Fock formalism and due to the less rigorous methods than *ab initio*, these techniques are best for medium-sized systems (hundreds of atoms).
- *Molecular mechanics* uses classical physics and empirical or semi-empirical (predetermined) force fields to explain and interpret the behaviour of atoms and molecules. They are the best for large systems (~1000 of atoms).

In this chapter, the *ab initio* Hartree-Fock (HF) method will be explained first because it is the most simple theory and it is used as starting point for the post Hartree-Fock methods. Because of the latter are computationally expensive, they can not be used for large systems as those studied in this thesis and consequently they will not be detailed in this chapter, but excellent reviews for them can be found in references section.^{54,55,56} In addition, the DFT methods will be described. These methods allow performing more complex calculations on large molecules because of their low computational cost.

1.2.1. The Hartree-Fock approximation

The most common type of *ab initio* calculation is the *Hartree-Fock* (HF) approach, the most frequent method for calculating the electron wavefunction of atoms and molecules. It is the best approximation for these wavefunctions constructed by placing an electron into a spin-orbital, the picture that most chemists use to rationalize chemistry. The HF approximation is, furthermore, the usual preliminary point for more accurate calculations.

The HF algorithm is typically used to solve the Schrödinger equation for a multi-electron atom or molecule, which is the main objective of quantum mechanics. The HF is an extension of the molecular orbital theory in which the Coulombic electron-electron repulsion is not specifically taken into account, however, its average effect is included in the calculation. But it has an important task as a starting point for more accurate approximations that include electron correlation. It assumes that the motion of each electron can be described by a simple function called orbital which is not explicitly dependent of the motion of other electrons.

The *Born-Oppenheimer (BO) approximation* is inherently assumed when the wavefunction of a molecule is broken into its electronic and nuclear (vibrational, rotational and translational) components.

$$\Psi_{\text{total}} = \Psi_{\text{electronic}} \cdot \Psi_{\text{nuclear}} \quad (1.1)$$

Thus, the wavefunction of the many-electron molecule is a function of electron and nuclear coordinates: $\Psi(R, r)$ (R = nuclear coordinates, r = electron coordinates). The motions of the electrons and nuclei are coupled. However, the nuclei are much heavier than the electrons ($m_p \sim 2000 m_e$) and consequently nuclei move much more slowly than electrons ($E=1/2mv^2$). To the electrons the nuclei appear basically fixed. Thus, instead of solving the full Schrödinger equation:

$$\hat{H}\Psi_{\text{total}}(\vec{r}; \vec{R}) = E_{\text{total}}\Psi_{\text{total}}(\vec{r}; \vec{R}) \quad (1.2)$$

In the BO approximation, this equation is separated into the following two equations:

$$\begin{aligned} \hat{H}_{\text{el}}\psi_{\text{el}}^n(\vec{r}; \vec{R}) &= U_n(\vec{R})\psi_{\text{el}}^n(\vec{r}; \vec{R}) \\ (\hat{T} + U_n)(\vec{R})\psi_{\text{nucl}}^n(\vec{R}) &= E_{\text{total}}\psi_{\text{nucl}}^n(\vec{R}) \end{aligned} \quad (1.3)$$

The first is the so-called electronic Schrödinger equation that describes the electronic motion considering fixed nuclei. The second, which is the nuclear Schrödinger equation, contains the nuclear motion under the potential (U_n) created by the electrons.

The full electronic Hamiltonian (\hat{H}_{el}) for a system of N electrons in the presence of M nuclei with charge Z_A is:

$$H^{\text{exact}} = \sum_i^N \hat{h}(i) + \sum_i^N \sum_{j>i}^N \frac{1}{r_{ij}} \quad (1.4)$$

where

$$\hat{h}(i) \equiv -\frac{1}{2} \nabla_i^2 - \sum_A^M \frac{Z_A}{r_{iA}}$$

Solving the Schrödinger equation with this Hamiltonian is very difficult because the term $1/r_{ij}$ correlates the motion of all the electrons.

The HF method makes two major simplifications in order to deal with this task:

- a) After the Born-Oppenheimer approximation, the next important approximation is to use a Slater determinant as a wavefunction:

$$\Phi_0 = \frac{1}{\sqrt{N!}} \begin{bmatrix} \varphi_1\alpha(1) & \varphi_1\beta(1) & \varphi_2\alpha(1) & \cdots & \varphi_M\beta(1) \\ \vdots & \vdots & \vdots & \ddots & \vdots \\ \varphi_1\alpha(N) & \varphi_1\beta(N) & \varphi_2\alpha(N) & \cdots & \varphi_M\beta(N) \end{bmatrix} \quad (1.5)$$

where:

- α/β are spin-functions (spin-up/spin-down)
- φ_i are spatial functions (molecular orbitals)
- $\varphi_i\alpha$ and $\varphi_i\beta$ are called spin-orbitals
- N electron system
- Slater determinant gives proper anti-symmetry (Pauli Principle) with respect to interchange of any two electrons⁵⁷

b) Slater determinants are built from molecular orbitals, but how do we define these orbitals? We expand each molecular orbital (MO) as a Linear Combination of Atomic Orbitals (LCAO-MO), which are usually (but not always) chosen to be orthogonal. The finite basis set is assumed to be approximately complete.

$$\varphi_i = \sum_k^M c_{ki} \chi_k \quad (1.6)$$

where:

- c_{ki} are molecular orbital coefficients.
- the basis functions, χ_k , are atom-centered functions that mimic solutions of the H-atom (s orbitals, p orbitals,...)

Therefore, the larger the expansion the more accurate and expensive the calculations become.

The one-electron functions $\{\varphi_i\}$ are called *spin orbitals* and these are chosen to be orthonormal.

$$\langle \varphi_i | \varphi_j \rangle = \delta_{ij} \quad (1.7)$$

The *variational principle* specifies that the best set of spin orbitals is the one that minimizes the electronic energy. This principle consists in choosing a “trial wavefunction” depending on one or more parameters, and finding the values of these parameters for which the expectation value of the energy is the lowest possible. The wavefunction obtained by fixing the parameters to such values is then an approximation to the ground state wavefunction, and the expectation value of the energy in that state is an upper bound to the ground state energy.

$$E_{\text{HF}} = \langle \Phi_0 | \hat{H} | \Phi_0 \rangle = \sum_i^N \langle i | \hat{h} | i \rangle + \frac{1}{2} \sum_i^N \sum_j^N \langle ij | jj \rangle - \langle ij | ji \rangle \quad (1.8)$$

The HF equation determines the best spin-orbitals (those that make the energy be a minimum):

$$f_i \cdot \varphi_i = \varepsilon_i \cdot \varphi_i \quad (1.9)$$

Where f_i is the Fock operator that it is defined as:

$$\hat{f}(k) = \hat{h}(k) + \sum_b \hat{J}_b(k) - \hat{K}_b(k) \quad (1.10)$$

The first part $\hat{h}(k)$ includes the kinetic energy and the attractive electron-nucleus potential; $\hat{J}_b(k)$ is the Coulomb operator, defining the electron-electron repulsion energy, and $\hat{K}_b(k)$ the exchange operator, defining the electron exchange energy.

The HF method also receives the name of the Self-Consistent Field method (SCF) where a set of spin-orbitals is required to start the progression of solving the Fock equations,⁵⁸ which step by step will obtain a new set of orbitals until we will found the coefficients in eq. (1.6) that lead to a minimum of the energy.

The SCF method has a physical limitation since it does not give an accurate description of most of the chemical systems. It is because of the average potential does not describe the correlation of the motion of the electrons and it is usually solved through the introduction of a finite basis set to expand the molecular orbitals. This electronic correlation has to be included to improve the results and for this reason the post-HF methods were introduced.

An important consequence of the only approximate treatment of the electron-electron repulsion is that the true wavefunction function of a many electron system is never a single Slater determinant. The correlation energy is described as the difference between the exact non-relativistic Born-Oppenheimer energy for a determined basis set and the HF expression.

$$E_{corr} = E_{exact} - E_{HF} \quad (1.11)$$

An additional issue that affects the accuracy of the computed results is the form chosen for the basis functions. The actual form of the single electronic molecular wavefunction (molecular orbital) is of course not known. The forms, used for the

basis functions, can provide a better or worse approximation to the exact numerical single electron solution of the HF equation. The basis functions used most often are combinations of either Slater type orbitals ($\exp(-r)$) or Gaussian type orbitals ($\exp(-r^2)$), abbreviated STO and GTO, respectively, where r is the distance of the electron from the atomic nucleus.

The expression for the GTOs, only introduces the quadratic dependence of r in the exponential part. This fact makes GTOs inferior to the STOs in two aspects (see Figure 1.7). GTOs have problems representing the proper behaviour near the nucleus and the other problem is that the GTO falls off rapidly far from the nucleus compared with an STO and therefore, the wavefunction is consequently represented poorly at long distances from the nuclei. The main advantage of using GTOs is that analytical expressions for all kinds of integrals are known, and consequently they are computationally much more efficient.

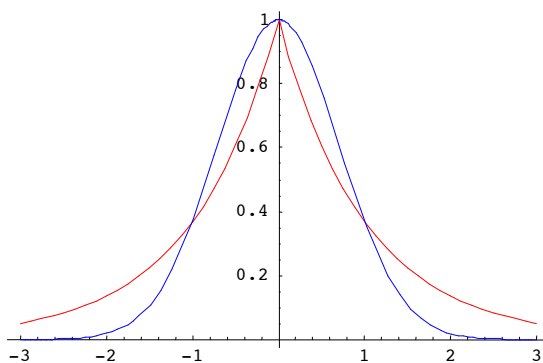


Figure 1.7. Behaviour of Gaussian Type Functions (blue) and Slater Type Function (red)

1.2.2. The Density Functional Theory

An alternative to *ab initio* methods is Density Functional Theory (DFT), in which the total energy is expressed in terms of the total electron density, rather than the wavefunction. We will review some of the fundamental aspects of electronic structure theory in order to lay the foundations for the theoretical discussion on DFT. This method will be described based on the books *Introduction to Computational Chemistry*⁵⁵ and *A Chemist's Guide to Density Functional Theory*.⁵⁹

DFT method is a quantum mechanical theory that gives accurate results and it the best choice to study large molecules, as with a moderate computational cost DFT gives a good prediction for the molecular properties.

Traditional methods in electronic structure theory, in particular the *HF theory* and its descendants, are based on the complicated many-electron wavefunction, as discussed before. Then the main objective of DFT is to replace the many-body electronic wavefunction with the electronic density as the basic quantity. Whereas the many-body wavefunction function is dependent on $3N$ variables, the density is only a function of three variables and is a simpler quantity to deal with both conceptually and practically. Therefore the DFT gives a different approach for solving the Schrödinger equation, and it is based on the *Hohenberg and Kohn (HK) theorems*.

Hohenberg-Kohn Theorem (1964)

The first HK theorem states that the electronic density fully determines the energy of a non-degenerate electronic ground state.⁶⁰ In fact, there exists a one-to-one relationship between the electronic density and the Hamiltonian, since not only the energy but also any other observable property of the system can be determined.

Further, the second HK theorem establishes the variational principle for DFT and it proves that the energy of the system $E(\rho)$ is a minimum E_0 when the exact electronic density of the system ρ_0 is considered

$$E_0[\rho_0] \leq E[\rho] \quad (1.12)$$

Thus the variational equation is obtained,

$$\frac{\delta E[\rho]}{\delta \rho(r)} - \mu = 0 \quad (1.13)$$

where μ is the electronic chemical potential given as the derivative of the energy $E(\rho)$ in front of the electronic density, ρ . In fact, μ is the Lagrange multiplier that ensures the normalization of the electronic density.

$$\int dr. \rho(r) = N \quad (1.14)$$

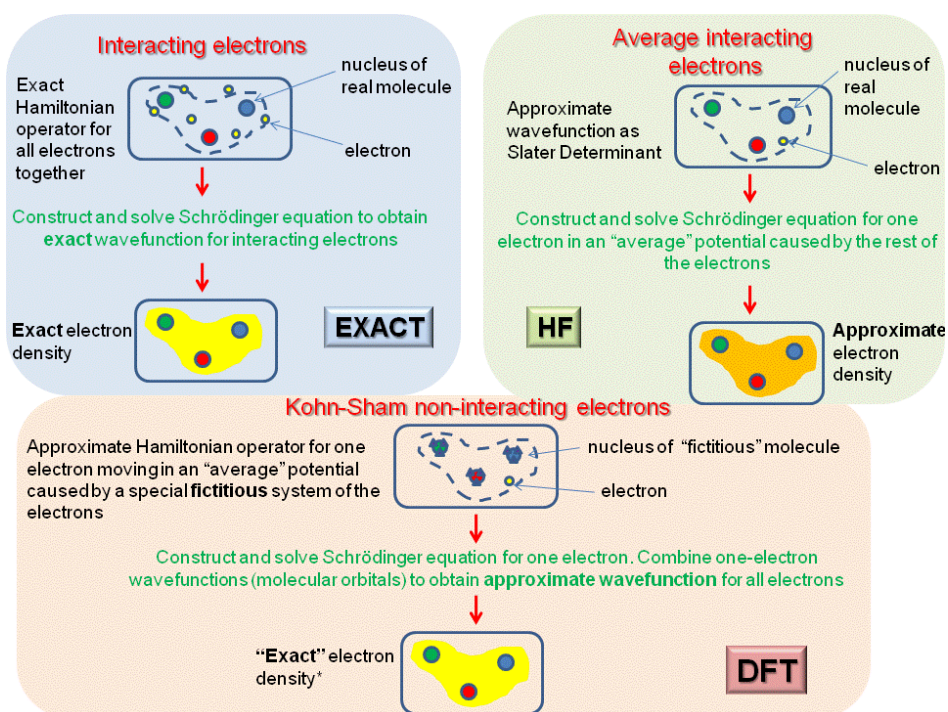
Kohn-Sham Formulation (1965)

The most common implementation of DFT is through the *Kohn-Sham (KS) method*,⁶¹ who proposed a self-consistent method similar to the SCF for the HF theory. The KS orbitals may be expanded in a set of basis functions, analogous to the HF method.

$$\varphi_i = \sum_k^M c_{ki} \chi_k \quad i = 1, 2 \dots M \quad (1.15)$$

To compute the kinetic energy this method uses a reference state formed by a system of N non-interacting electrons. In this way, the major part of the kinetic energy can be computed with good accuracy. The remainder is merged with the non-classical contributions to the electron-electron repulsion, which are also unknown. By means of this method as much information as possible is computed exactly, leaving only a small part of the total energy to be determined by an approximate functional.

Therefore, the key to KS theory is thus the calculation of the kinetic energy under the assumption of *non-interacting* electrons. But in reality the electrons are interacting, and this equation does not provide the total kinetic energy. However, just as HF theory provides ~99% of the correct answer, the difference between the exact kinetic energy and that calculated by assuming non-interacting orbitals is small. The next figure (Figure 1.8) represents distinct situations depending on the wavefunction takes into account the interacting or non-interacting electrons.



* It means a formally exact and practically approximate but cheap way to access the correlation energy = $E_{\text{exact}} - E_{\text{HF}}$

Figure 1.8. Exact, HF and DFT approaches to solve the electronic Schrödinger equation

The division of the electron kinetic energy into two parts, is one of the approximations to correct this term. Therefore, the kinetic energy is absorbed into an exchange-correlation term, and a general DFT energy expression can be written as,

$$H_\lambda = T + V_{ext}(\lambda) + \lambda V_{ee} \quad 0 \leq \lambda \leq 1 \quad (1.16)$$

Where T is the kinetic energy, V_{ee} the Coulomb repulsion and λ a coupling parameter that varies from 0 (non-interacting system) to 1 (interacting system). The external potential $V_{ext}(\lambda)$ is equal to the electron-nuclear attraction V_{ne} for $\lambda = 1$, i.e. an electron interacting system is considered. The Born-Oppenheimer approximation is still considered, therefore, the repulsion potential between nuclei is computed apart and directly added to the final expression of the energy. Finally the electronic correlation can be separated into a Coulomb and exchange part, leading the next equation:

$$E(\rho) = T(\rho) + E_{ne}(\rho) + J(\rho) + K(\rho) \quad (1.17)$$

Consequently, the energy functional can also be written in the following form:

$$E(\rho) = T_s(\rho) + \int \rho(r)v(r)dr + \frac{1}{2} \int drdr' \frac{\rho(r)\rho(r')}{|r-r'|} + E_{xc}(\rho) \quad (1.18)$$

The first term of the equation may be considered the kinetic energy functional for non-interacting electron system, while the second term contains the electron-nucleus interaction. The third term of the equation represents the classical $J(\rho)$ Coulomb repulsion of the electron cloud, and finally the last term $E_{xc}(\rho)$ is the exchange-interaction energy functional which includes non classical effects of the electronic correlation and it involves contributions to the potential energy of the system, but it contains also a portion belonging to the kinetic energy, corresponding to the difference $T(\rho) - T_s(\rho)$.

If the previous equation is rearranged and we now apply the *variational principle*, the effective potential Kohn-Sham $v_{eff}(r)$ is obtained.

$$v_{eff}(r) + \frac{\delta T_s(\rho)}{\delta \rho(r)} = \mu$$

$$v_{eff}(r) = v(r) + \frac{\delta J(\rho)}{\delta \rho(r)} + \frac{\delta E_{xc}(\rho)}{\delta \rho(r)} \quad (1.19)$$

Then, the effective KS potential together with the kinetic energy operator from the Hamiltonian for the non-interacting system is:

$$\hat{H}_s = \sum_{i=1}^N \left[-\frac{1}{2} \nabla_i^2 + v_{eff}(r) \right] \quad (1.20)$$

and the equation that must be solved is:

$$\left[-\frac{1}{2} \nabla_i^2 + v_{eff}(r) \right] \varphi_i = \epsilon_i \varphi_i \quad (1.21)$$

Thus, once we know the various contributions to this equation, we have a grid on the potential $v_{eff}(r)$ which we need to insert into the one-particle equations, which in turn determine the orbitals and hence the ground state density and the ground state energy by employing the energy expression (1.18).

The solution of \hat{H}_s forms the set of the orbitals $\{\varphi_i\}$ whose associated electron density is equal to the exact one.

Therefore, it is clear that there are many similarities between the KS operational procedure to the SCF method for the HF theory, where it consists in constructing an exchange correlation potential, making a guess for the orbitals $\{\varphi_i\}$, building the electron effective potential, and solving the iterative equation (1.21) until self-consistency to finally obtain the DFT energy from equation (1.18).

If the form of the exchange-correlation functional $E_{xc}(\rho)$ were known, DFT theory would provide the *exact* total energy, including the electron correlation. The use of electronic density has an advantage in relation to the wavefunction, because DFT

methods have the potential of including the computationally difficult part in wave mechanics, the correlation energy, at a computational effort similar to that for determining the uncorrelated HF energy. Although this is certainly the case for approximations to $E_{xc}(\rho)$, this is not necessarily true for the exact $E_{xc}(\rho)$. It may well be that the exact $E_{xc}(\rho)$ functional is so complicated that the computational effort for solving the KS equations will be similar to that required for solving the Schrödinger equation with a wave mechanics approach. Since exact solutions are generally not available in either approach, the important fact is the computational cost for generating a solution of certain accuracy. In this respect DFT methods have very favourable characteristics.

Expression for the exchange-correlation functional

The exchange-correlation energy is given by:

$$E_{xc}(\rho) = \int \rho(r) \varepsilon_{xc}[\rho(r)] dr \quad (1.22)$$

It is possible to prove that the exchange-correlation potential is a unique functional, valid for all the systems, but a precise functional form of this potential has been elusive. Therefore, we are obligated to make approximations.

In the **Local Density Approximation (LDA)** it is assumed that the density locally can be treated as a uniform electron gas, or equivalently that the density is a slowly varying function. The X_α method,⁶² proposed by Slater can be considered the first method of LDA where the correlation part is neglected and the exchange term is given as,

$$\varepsilon_x^{LDA}[\rho(r)] = -\frac{9}{4}\alpha \left(\frac{3}{4\pi}\right)^{\frac{1}{3}} \rho(r)^{\frac{1}{3}} \quad (1.23)$$

On the other hand, for spin polarized systems, both the α and β electrons are considered independently, and the *local spin density* (LSD) approximation is obtained by:

$$\epsilon_x^{LSD}[\rho(r)] = -\frac{9}{4}\alpha\left(\frac{3}{4\pi}\right)^{\frac{1}{3}}\left[\rho_\alpha(r)^{\frac{1}{3}} + \rho_\beta(r)^{\frac{1}{3}}\right] \quad (1.24)$$

Later, *Vosko, Wilk and Nusair* (VWN) proposed an expression⁶³ for the correlation part, and the final equation of the exchange-correlation energy functional is:

$$\epsilon_{xc}^{LSD}[\rho(r)] = \int \rho(r)\left[\epsilon_x^{LSD}[\rho(r)] + \epsilon_c^{LSD}[\rho(r)]\right] dr \quad (1.25)$$

Note that the LDA approximation assumes that the exchange-correlation effects are local and depend only on the value of electron density at each point. Despite the simplicity of the model upon which they are based, usually the LDA methods works rather well for all kinds of systems. Specifically, they yield good geometries although the bond distances appear somewhat underestimated, good vibrational frequencies, and reasonable charge densities, except in the regions close to nuclei. Nevertheless, they are not accurate enough for systems with weak bonds or for making reliable thermochemical predictions. Thus, these methods have a general tendency to overstate the strength of the bonds, overestimating the bond energy by approximately 30%.⁶⁴

Improvements over the LDA (or LSD) approach have to consider a non-uniform electron gas. A step in this direction is to make the exchange and correlation energies dependent not only on the electron density, but also on derivatives of the density. These methods are known as **Gradient Corrected or Generalized Gradient Approximation (GGA)** methods.

Perdew and Wang (PW86)⁶⁵ not only considered the local density, but also they took into account their local gradients.

$$E_{xc}^{GGA}[\rho] = \int dr f^{GGA}(\rho_\sigma, \vec{\nabla}\rho_\sigma); \quad \sigma = \alpha, \beta \quad (1.26)$$

There have been two different strategies to design suitable approximations for the function f^{GGA} . First of all, Becke proposed a widely-used *semi-empirical* exchange density functional (B or B88)⁶⁶ where a parameter is included which is chosen on the basis of a least-squares fit to the exact HF exchange energy of the noble gases. This exchange functional is usually used with either the correlation functional proposed by Lee, Yang and Parr⁶⁷ (and the BLYP functional is achieved) or the gradient correction proposed by Perdew⁶⁸ in 1986, which is known by the acronym P86 (which together with the Becke exchange functional represents the BP86).

Using the latter (GGA) very excellent results for molecular geometries and ground state energies have been achieved. Potentially more accurate than the GGA functionals are hybrids and meta-GGA functions. These latter functionals include a further term in the expansion, depending on the density, the gradient of the density and the Laplacian (second derivative) of the density following the next form,

$$E_{xc}^{mGGA}[\rho] = \int dr f^{mGGA}(\rho_\sigma, \nabla\rho_\sigma, \nabla^2\rho_\sigma, \tau_\sigma); \quad \sigma = \alpha, \beta \quad (1.27)$$

Where τ_σ is the Kohn-Sham orbital kinetic energy density for electrons of spin σ .

There is little guidance from theory how such functionals should be chosen, and consequently many different potentials have been proposed. Perhaps, the most used DFT functional is the hybrid B3LYP, proposed by Becke.⁶⁹

The DFT chosen to achieve the present study has been a hybrid exchange-correlation functional that it is usually a linear combination of the HF exchange (E_x^{HF}) and some other one or combination of exchange and correlation functionals. The parameters relating the amount of each functional can be arbitrarily assigned and is usually fitted to reproduce well some set of observables (bond lengths, ionization potentials, electron affinities, band gaps, etc.). In this case, the B3LYP (Becke, three parameter, Lee-Yang-Parr) exchange-correlation functional is:

$$E_{xc}^{B3LYP} = E_{xc}^{LDA} + a_0 (E_x^{HF} - E_x^{LDA}) + a_x (E_x^{GGA} - E_x^{LDA}) + a_c (E_c^{GGA} - E_c^{LDA}) \quad (1.28)$$

where $a_0 = 0.20$, $a_x = 0.72$, and $a_c = 0.81$ are the three empirical parameters; E_x^{GGA} and E_c^{GGA} are the generalized gradient approximation formulated with Becke 88⁶⁶ exchange functional and the correlation functional of Lee, Yang and Parr,^{67,70} and E_c^{LDA} the VWN correlation functional (local density approximation).

Next figure (Figure I.9) shows the increasing of quality and computational cost depending on the correlation-exchange functional used:

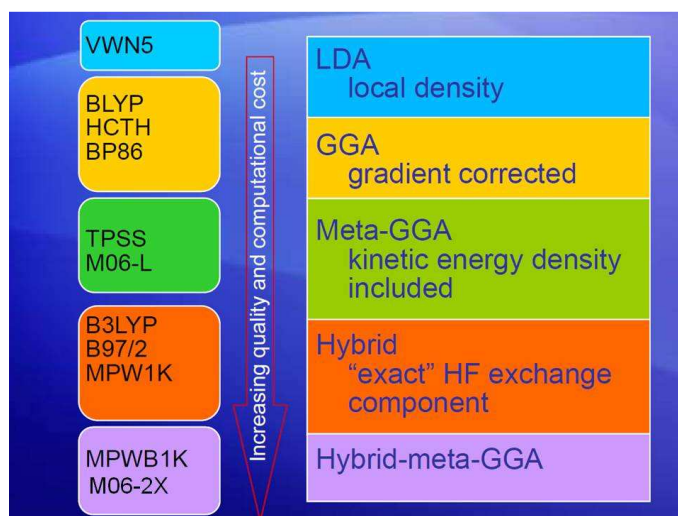


Figure I.9. Correlation-exchange functionals

Note that there is no consensus on whether meta-GGA is better or not that the hybrid-meta-GGA, although a recent publication reveal that the last one is still appropriate for many studies of organic reaction mechanisms.⁷¹

1.2.3. Computational details

In the present research work, all the calculations have been carried out using the hybrid DFT method, B3LYP, as implemented in the Gaussian 03 package,⁷² which is considered a reliable quantum chemical method for large molecules. The choice of DFT method is based on previous studies, which have shown that DFT (and in particular, the relative inexpensive B3LYP method) provides a reliable description of reaction mechanisms of many processes⁷³ and, in particular, of pericyclic reactions.^{74,75}

All of geometries have been fully optimized, without symmetry constraints except otherwise noted. Harmonic frequencies have been calculated at the same level to characterize the stationary points and to determine the zero-point energies. Therefore, the minimum structures reported in this thesis show positive eigenvalues of the Hessian matrix, whereas transition states (TSs) have one negative eigenvalue. To corroborate which are the corresponding minima linked by the considered TS, intrinsic reaction coordinate (IRC) routes⁷⁶ in both reactant and product directions were performed on these TS structures.

The thermodynamic functions (ΔH , ΔS , and ΔG) were estimated within the ideal gas approximation, assuming a temperature of 298.15 K and a pressure of 1 atm according to Equations (1.27) and (1.28) .

$$\Delta G_{298} = \Delta H_{298} - T\Delta S_{298} \quad (1.29)$$

and

$$\Delta H_{298} = \Delta E + \Delta E_{vib}^0 + \Delta E_{trans}^{298} + \Delta E_{rot}^{298} + \Delta(\Delta E_{vib}^0)_{298} + \Delta(pV) \quad (1.30)$$

1.2.3.1. Basis Functions

Some of the most used basis sets are those developed by *Dunning* and coworkers,⁷⁷ since they are designed to converge systematically to the complete basis set limit using extrapolation techniques. For first- and second-row atoms, the basis sets are cc-

pVNZ where N=D,T,Q,... (D=double, T=triple, Q=quadruple, etc.). The “cc-p”, stands for “correlation consistent polarized” and the “V” indicates that only the valence has splitted basis functions. They include successively larger shells of polarization (correlating) functions (d, f, g, etc.). More recently these *correlation consistent polarized* basis sets have become widely used and are the current state of the art for correlated or *post HF* calculations. Examples of these are:

- cc-pVDZ – Double-Zeta
- cc-pVTZ – Triple-Zeta
- cc-pVQZ – Quadruple-Zeta
- cc-pV5Z – Quintuple-Zeta, etc.
- aug-cc-pVDZ, etc. – Augmented versions of the preceding basis sets with added diffuse functions.

For third-row atoms, additional functions are necessary; these are the cc-pV(N+d)Z basis sets. Larger atoms require the cc-pVNZ-PP where PP stands for pseudopotential.

In our case, the basis set selected to carry out the studies is the *cc-pVDZ* basis set including a double- ζ valence for the non-metal atoms in the substrate molecule and the *cc-pVDZ-PP* basis set with effective core potential is used for Rh.

1.2.3.2. Pseudopotentials

For systems involving elements from the third row or higher in the periodic table there is a large number of core electrons which in general are unimportant in a chemical sense. However, it is necessary to use a large number of basis functions to expand the corresponding orbitals, otherwise the valence orbitals will not be properly described (due to a poor description of the electron-electron repulsion). These

problems may be “solved” by introducing an *Effective Core Potential* (ECP) (also called *pseudopotential*) to represent all the core electrons.

In quantum mechanics, the pseudopotential approximation is an attempt to replace the complicated effects of the motion of the core (non-valence) electrons of an atom and its nucleus with an effective potential, or pseudopotential, so that the Schrödinger equation contains a modified term instead of the terms for core electrons normally found in the Schrödinger equation. The pseudopotential approximation was first introduced by *Hans Hellmann* in the 1930s.⁷⁸ By construction of this pseudopotential, the valence wavefunction generated is also guaranteed to be orthogonal to all the core orbitals.

For transition metals, better results can be obtained if the orbitals in the next lower shell in the valence space are treated explicitly and are not included in the pseudopotential. The gain by using ECPs is largest for atoms in the lower part of the periodic table, especially those where relativistic effects are important.

The performance of ECPs is somewhat difficult to evaluate by comparison with other calculations, but they often reproduce known experimental results, justifying the approach.

1.2.4. Computational Chemistry in the lab

When using computational chemistry to answer a chemical question, the obvious problem is that you need to know how to use the software. Then, you need to have some information and/or intuition, concerning the quality of the answer, and you have to be able to make rational decisions about the possibility to sacrifice accuracy for efficiency.

Here is a check list to follow:

- *What do you want to know? How accurately? Why?*

If you can't answer these questions, then you don't even have a research project yet.

- *How accurate the answer predicted will be?*

The way to estimate your error is to compare a number of similar computations to the experimental answers. There are articles and compilations of many studies. If none exist, you will have to guess which method should be reasonable, and then do a study with this method of some experimentally known situation to get an idea of how good your calculation is.

- *How long do you expect it to take?*

Sometimes computational chemistry calculations (especially *ab initio* ones) can be so time consuming that it would take months to do a single calculation, even if you had a very powerful machine with enough memory and disk space. However, a number of methods exist that are appropriate for different situations. The trick is to determine which one is best for your project. Again, the answer is to look into the literature or perform some preliminary studies.

- *What approximations are being made? Which are significant?*

Some cases require making approximations of the real studied system in order to reduce the computational cost. These simplifications may allow a faster answer of the study with high reliability or not. Thus, it is important to have into account if the taken approximations can affect the final result with great magnitude or not.

Once you have finally answered all of these questions, you are ready to actually do a calculation. Now you must determine which is the best software available for your calculations, what it costs and how to use it.

1.2.4.1. Geometry optimization

The geometry of the molecules by computational calculations is obtained after applying a series of iterations which modify the geometry until the energy of the system has reached a minimum. We can distinguish between minima and saddle-points (Figure 1.10) who describe the Potential Energy Surfaces (PES) of the reaction mechanism studied.

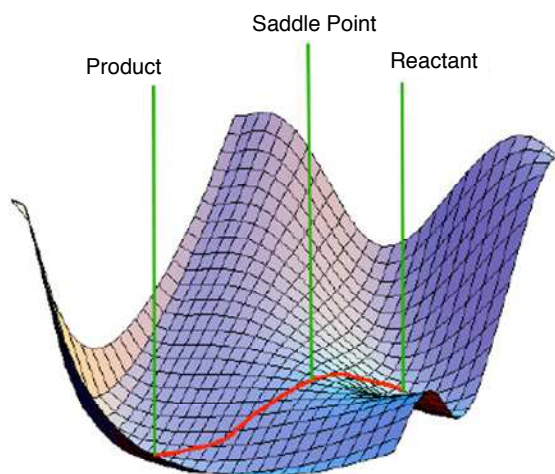


Figure 1.10. Representation of a Potential Energy Surface with minima and saddle point

Note that to find the minima in computational calculations, it involves solving the first derivatives of the energy respect to the Cartesian or any other system of coordinates, called the *gradient*. When the slope is equal to zero, a stationary point has been found. If the computed Hessian has only positive eigenvalues then a minimum (reactant,

product, or intermediate) has been located, while if the computed Hessian has a unique negative eigenvalue then it has been located a transition state. This is the procedure principle behind the geometry optimization of computational methods.

Molecular geometry can be described by three measurements (Figure 1.11):

- bond length (l), usually reported in Angstroms ($1\text{\AA} = 10^{-10}\text{m} = 100\text{ pm}$)
- bond angle (α), measured in degrees.
- dihedral angle (θ), in degrees.

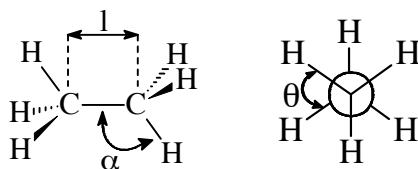


Figure 1.11. Representation of the three measurements: bond length (l), bond angle (α) and dihedral angle(θ)

But atoms are in constant motion, even at absolute zero. Therefore, how do we define the distance between them? (Figure 1.12) Several vibrational and rotational states are populated for each electronic state. The geometry optimization determines the *equilibrium* bond length.

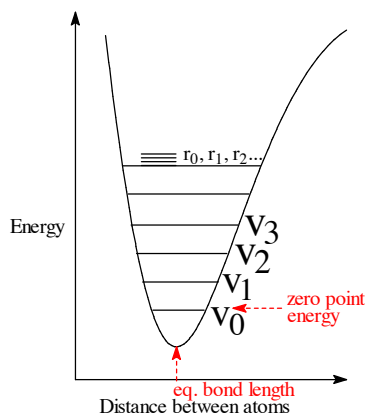


Figure 1.12. Representation of equilibrium bond length where V (vibrational state) and r (rotational state) are populated for each electronic state.

So in computational calculations the minimum is an equilibrium structure of one or several molecules.

On the other hand, the isolation of TSs is slightly different as the localization of minima in the potential energy surface. This is described as a maximum along the reaction coordinate, but a minimum in the other orthogonal directions. Again the *gradient* is used to locate TS geometries, but the second derivatives (or *Hessian*) of the energy are also required. Working with large molecules needs approaches such as the Bofill updating method⁷⁹ or mediating eigenvector following.⁸⁰

A global method normally used for finding TS is an interpolation between reactant and product, *Linear Synchronous Transit* (LST). This approach is a search for a maximum along a linear path between reactants and products (Figure 1.13).

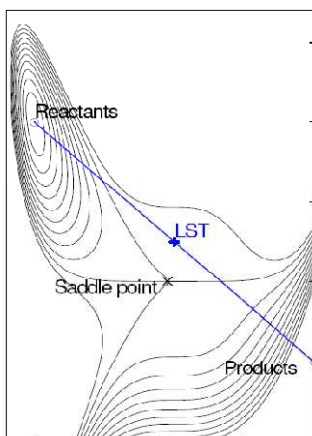


Figure I.13. Representation of linear synchronous transit (LST)

And there is another algorithm for finding TSs which called *Quadratic Synchronous Transit (QST)*. This case consists searching for a maximum along an arc connecting reactants and products, and for a minimum in all directions perpendicular to the arc (Figure I.14).

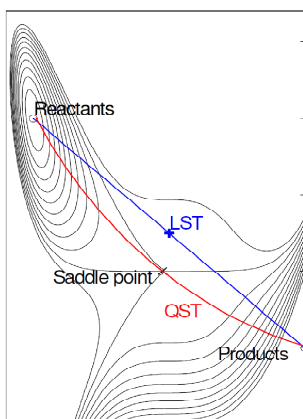


Figure I.14. Representation of quadratic synchronous transit (QST)

But how we know if the TS found is the correct? First of all, look at the transition state eigenvector to make sure it's the right one. Then, we can follow reaction path to be sure that the transition state connects the correct reactants and products. Steepest descent path from TS to reactants and products is the Internal Reaction Coordinate (IRC).

Thermodynamics and kinetics of the reaction can be obtained from the energies found for reactants, products or transition states (Figure 1.15).

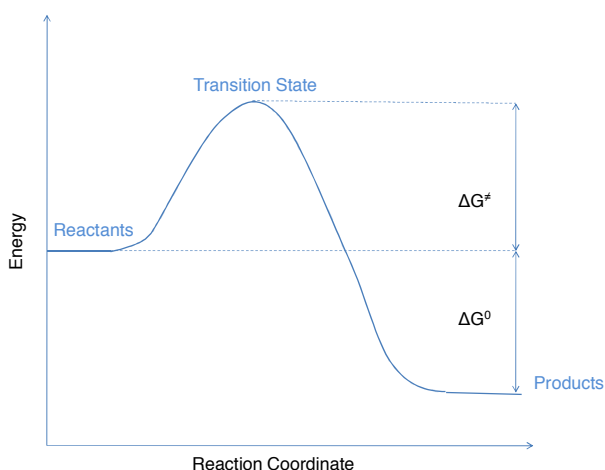


Figure 1.15. Schematic reaction Gibbs energy profile where minima (reactants, products) and saddle point (transition state) are represented as well as the activation energy (ΔG^\ddagger) and reaction energy (ΔG^0)

The next equations (1.29 and 1.30) correspond to the activation energy ΔG^\ddagger and the reaction energy ΔG^0 of a particular process. These expressions are valid for electronic energies, enthalpies and Gibbs energies, but the latter is the best representation when the number of reacting molecules changes along the reaction coordinate (because entropy effects are included).

$$\Delta G^0 = G_{products}^0 - G_{reactants}^0 \quad (1.31)$$

$$\Delta G^\ddagger = G_{transition\ state}^\ddagger - G_{reactants}^0 \quad (1.32)$$

Analysis of the binding energies

The bonding energy, ΔE_{total} , can be decomposed along the reaction coordinate into the strain ΔE_{strain} associated with deforming the individual reactants plus the actual interaction ΔE_{int} between the deformed reactants.

$$\Delta E_{total} = \Delta E_{strain} + \Delta E_{int} \quad (1.33)$$

The strain ΔE_{strain} is determined by the rigidity of the reactants and on the extent to which groups must reorganize in a particular reaction mechanism, whereas the interaction ΔE_{int} between the reactants depends on their electronic structure and on how they are mutually oriented as they approach each other. It is the interplay between ΔE_{strain} and ΔE_{int} that determines if and at which point along the reaction coordinate a barrier arises. The activation energy of a reaction ΔE^\ddagger consists of the activation strain $\Delta E_{strain}^\ddagger$ plus the TS interaction ΔE_{int}^\ddagger .

$$\Delta E^\ddagger = \Delta E_{strain}^\ddagger + \Delta E_{int}^\ddagger \quad (1.34)$$

The interaction ΔE_{int} between the strained reactants is further analyzed in the conceptual framework provided by the Kohn-Sham molecular orbital (KS-MO) model.

⁸¹⁻⁸³ To this end, it is further decomposed into three physically meaningful terms:

$$\Delta E_{int} = \Delta V_{elstat} + \Delta E_{Pauli} + \Delta E_{oi} \quad (1.35)$$

The term ΔV_{elstat} corresponds to the classical electrostatic interaction between the unperturbed charge distributions of the deformed reactants and is usually attractive. The Pauli repulsion ΔE_{Pauli} comprises the destabilizing interactions between occupied orbitals and is responsible for any steric repulsion (see Ref. 83 for an exhaustive discussion). The orbital interaction ΔE_{oi} accounts for charge transfer (interaction between occupied orbitals on one moiety with unoccupied orbitals of the other, including HOMO–LUMO interactions) and polarization (empty–occupied orbital mixing on one fragment due to the presence of another fragment). Since the Kohn–Sham MO method of density-functional theory (DFT) in principle yields exact energies and, in practice, with the available density functionals for exchange and correlation, rather accurate, we have the special situation that a seemingly one-particle model (an MO method) in principle fully accounts for the bonding energy.^{82,83}

Decomposition of energy is an effective tool to understand the behaviour of several chemical reactions. In this thesis, it will be useful to give an explanation of some experimental results.

Chapter 2. **OBJECTIVES**

The starting goals of this thesis have been developed taking into account the precedents outlined in *Chapter 1*. The following statements are the initial proposals of this work. Compound numbers used in the original publications have been reflected here in this chapter despite occasional repetitions.

Taking into account the precedents which have been described in Chapter 1, the main goal of the present thesis is to understand the properties and reactivity of unsaturated substrates with alkynes and alkenes moieties through [2+2+2] cycloadditions catalyzed by Wilkinson's complex, $\text{RhCl}(\text{PPh}_3)_3$.

Experimental techniques have been used and DFT approaches have been employed to give an explanation of the experimental results and also to make suggestions for further experimental work.

To this end, we have designed a series of experiments, each of them having their own objectives. In particular, the following goals were established for this thesis:

Project I.

Since we are interested in theoretical studies of [2+2+2] cycloaddition reactions catalyzed by Wilkinson's complex, we were concerned in the substitution of PPh_3 by PH_3 in the theoretical model in order to reduce the computational cost of the subsequent studies.

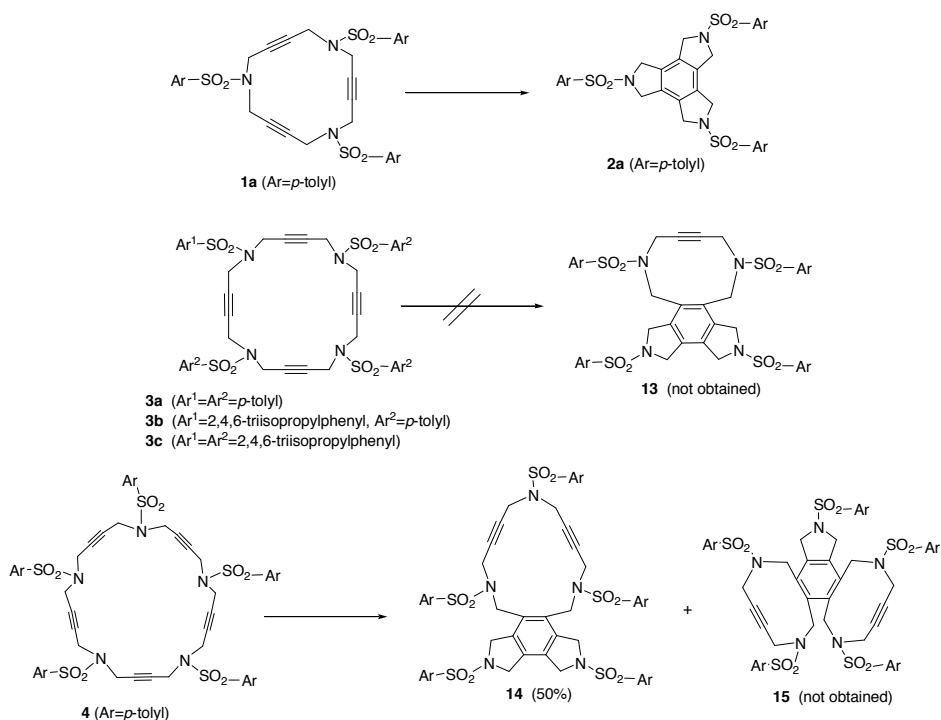
Thus, comparison of the reaction mechanisms catalyzed by the $\text{RhCl}(\text{PPh}_3)_3$ and $\text{RhCl}(\text{PH}_3)_3$ complexes and the discussion whether the substitution of PPh_3 by PH_3 leads to very different or comparable energy profiles were the main goals of this project.

Finally, as a third goal, we wanted to discuss the similarities and differences between the intermolecular [2+2+2] cycloaddition of three acetylene molecules and the simplest intramolecular [2+2+2] cycloaddition of a 15-membered azamacrocyclic triyne, both catalyzed with the same model catalyst, $\text{RhCl}(\text{PH}_3)_3$.

Project 2.

As we have described in previous chapter, the [2+2+2] cycloaddition reaction of the 20-membered tetraacetylenic azamacrocycle catalyzed by Wilkinson's complex did not lead to the expected cyclotrimerized products. Therefore, the main goal of this project was to investigate the origin of the lack of reactivity of the 20-membered macrocycle (**3**, Scheme 2.1) unlike the 15- and 25-membered azamacrocycles (**1a** and **4**, Scheme 2.1) carrying out theoretical calculations using density functional theory (DFT) with a hybrid functional (B3LYP).

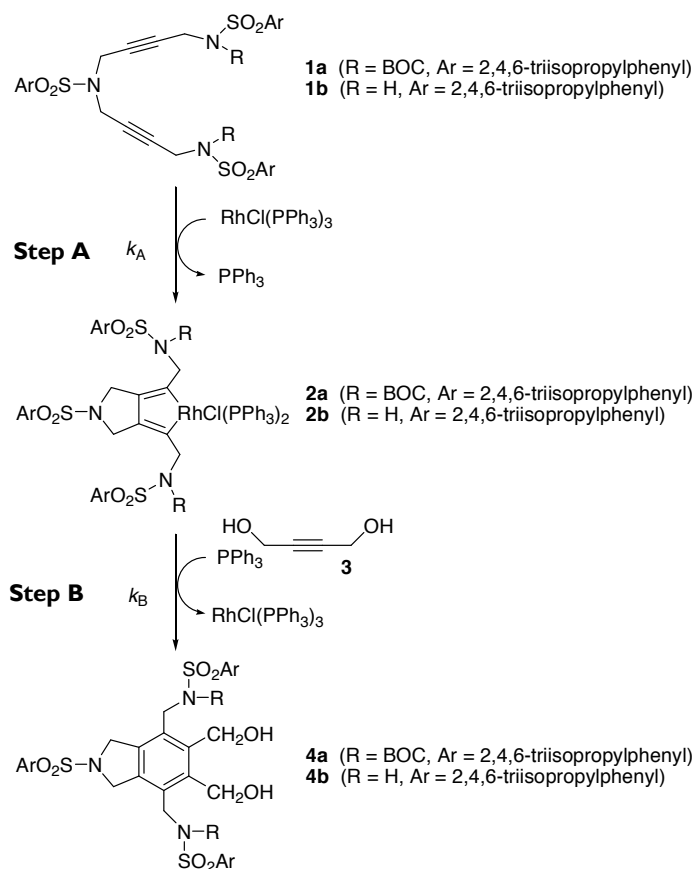
An additional goal was to study the chemoselectivity of the cycloaddition in the case of the pentaacetylenic azamacrocycles (**4**, Scheme 2.1) for which more than a single product can be obtained as cycloaddition can occur between three adjacent (**14**) or non-adjacent triple bonds (**15**).



Scheme 2.1. [2+2+2] Cycloaddition reactions of the 15-, 20- and 25-membered azamacrocycles

Project 3.

Given that no kinetic data of the catalytic cycle of the [2+2+2] cycloaddition reaction was available in the literature, our objective was to study the main steps of the catalytic cycle of the cycloaddition between a symmetric diyne (**1**) and a symmetric monoalkyne (**3**) catalyzed by Wilkinson's catalyst $\text{RhCl}(\text{PPh}_3)_3$ (Scheme 2.2) to obtain the greatest amount of mechanistic information (kinetics and characterization of the catalytic species) using electrochemical techniques, NMR spectroscopy, and electro spray ionization mass spectrometry (ESI-MS).

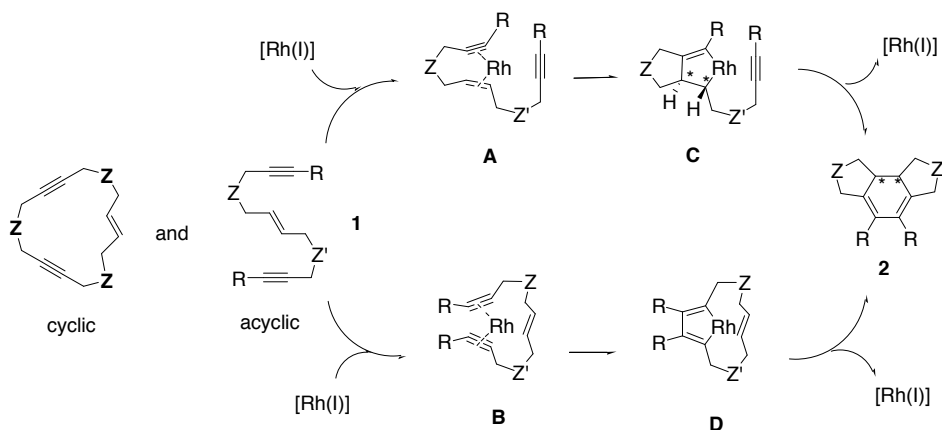


Scheme 2.2. Rh(I)-Catalyzed [2+2+2] cycloaddition of diynes with monoalkynes

Project 4.

The oxidative coupling step of enediynes, which is usually the rate-determining step in the intramolecular cycloaddition processes, can take place following two possible reaction pathways as indicated in Scheme 2.3. One is through the oxidative coupling of the enyne moiety affording metallacyclopentene **C** ($1 \rightarrow \mathbf{A} \rightarrow \mathbf{C}$) and the other through the oxidative coupling of the two alkyne moieties affording metallacyclopentadiene **D** ($1 \rightarrow \mathbf{B} \rightarrow \mathbf{D}$). The existence of these two paths provide a possible explanation for the difference of enantiomeric excess (ee) observed in the cycloaddition process to form enantioenriched cyclohexadienes with two chiral carbon centers.

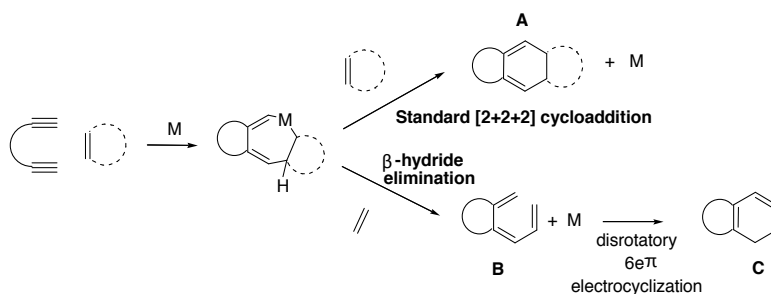
The main goal of this study was to analyze the reaction pathway in the oxidative coupling step as a function of the enediyne tethers and the substituent of the alkyne termini used (R) in order to determine the preferred coupling in acyclic and cyclic enediynes. For this purpose we performed density functional theory (DFT) calculations of the oxidative coupling step for several species **1** (Scheme 2.3).



Scheme 2.3. Possible routes for the [2+2+2] cycloaddition process in enediynes

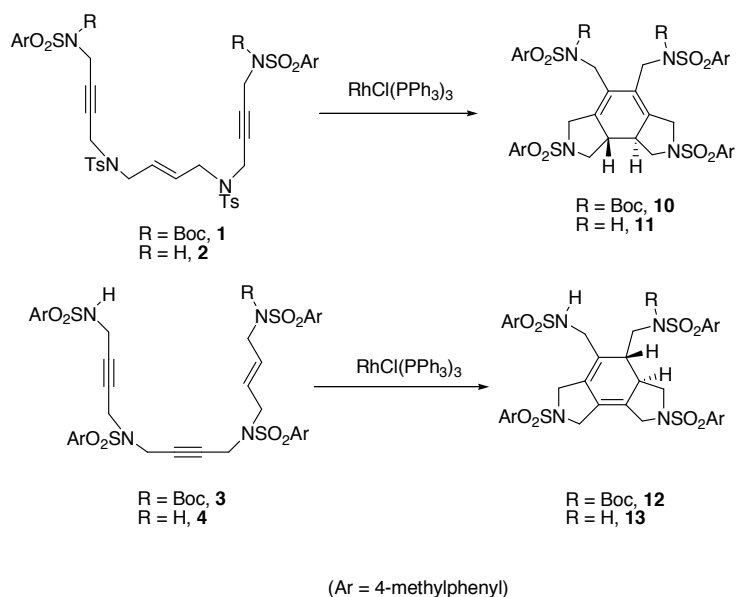
Project 5.

Recently, Saá et al.²⁸ studied the cycloaddition reaction of diynes with alkenes using a Ru-complex to give cyclohexadiene derivative products. With cyclic alkenes, the standard [2+2+2] cycloaddition pathway prevailed, leading to 1,3-cyclohexadienes **A** (Scheme 2.4). However, when the alkene moiety was linear an isomer of cyclohexadiene **A** was obtained, **C** (Scheme 2.4). In consonance with the discovery of this new reaction pathway exhibited, Aubert, Gandon et al.²⁹ reported this same behaviour for the [CpCoL₂] complex.



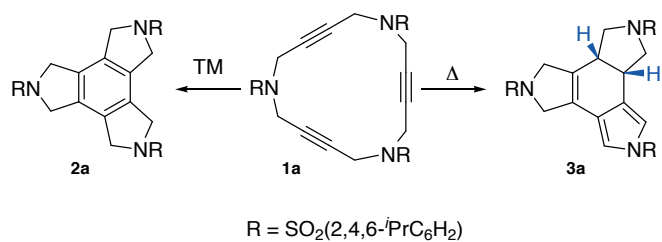
Scheme 2.4. Two possible reaction pathways for cycloaddition of diynes and alkenes

Thus, the aim of this study was the preparation of a set of enediynes (**1-4**, Scheme 2.5), to be reacted in an intramolecular way, where the two alkynes and one alkene moiety are part of the compound, modifying the position of the olefin in the structure. Secondly, to study the course of their [2+2+2] cycloaddition reactions catalysed by Wilkinson's complex to see whether we find a similar behaviour to that reported by Saá et al. and Aubert, Gandon et al. DFT studies were performed to understand the experimental results.

Scheme 2.5. $\text{RhCl}(\text{PPh}_3)_3$ -catalyzed cycloaddition of enediynes **1-4****Project 6.**

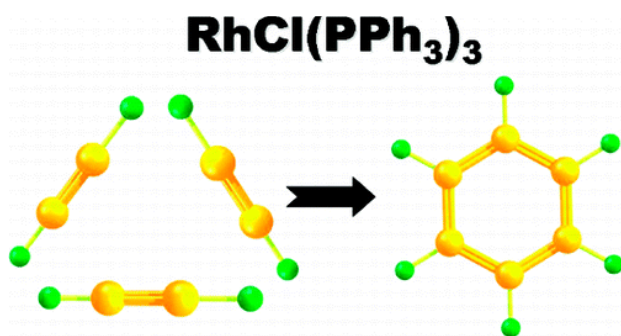
During our study of the metal-catalyzed [2+2+2] cycloadditions of macrocyclic scaffolds of type **1** to give tetra fused structures of type **2** (Scheme 2.6), we found a new product in moderate yield when the catalytic system tested was unable to promote [2+2+2] cycloaddition. After purification of the tarry material obtained when reacting macrocycle **1a**, a detailed NMR analysis revealed a new tetra fused structural isomer **3a** (Scheme 2.6). Macrocycle **1a** was then treated excluding any catalyst, and product **3a** was isolated from decomposition products and some starting material.

The main goal of this project was the study of the reaction mechanism of this process by means of DFT calculations.



Scheme 2.6. Transition-metal catalyzed vs thermally-induced cycloadditions

Chapter 3. **Density Functional Study of the
[2+2+2] Cycloaddition of Acetylene
Catalyzed by Wilkinson's Catalyst,
 $\text{RhCl}(\text{PPh}_3)_3$**



Dachs, A., Osuna, S., Roglans, A., Solà, M. "Density functional study of the [2+2+2] cyclotrimerization of acetylene catalyzed by Wilkinson's catalyst, $\text{RhCl}(\text{PPh}_3)_3$ ". *Organometallics*. Vol. 29, issue 3 (2010) : p. 562-569

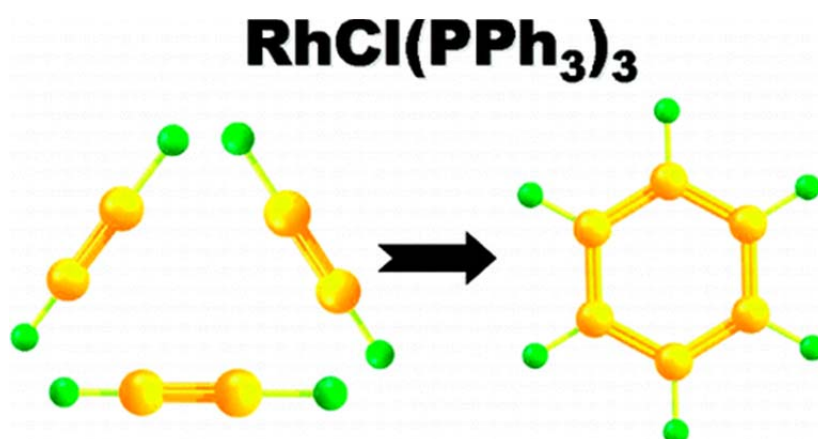
<http://pubs.acs.org/doi/full/10.1021/om900836b>

DOI: <http://dx.doi.org/10.1021/om900836b>

Publication Date (Web): January 11, 2010

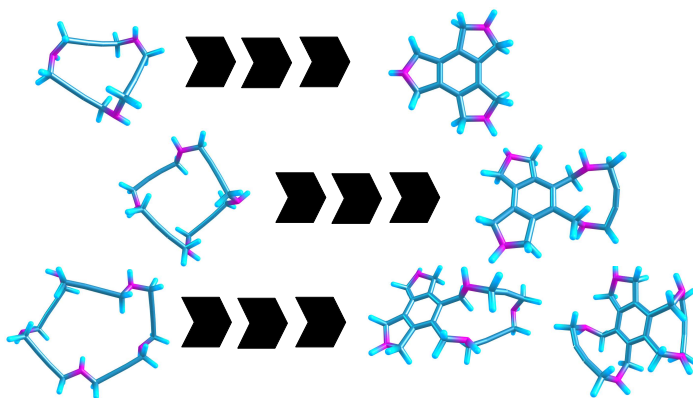
Copyright © 2010 American Chemical Society

Abstract



In this work we report density functional calculations at the B3LYP level of the [2+2+2] intermolecular cyclotrimerization of three acetylene molecules catalyzed by Wilkinson's catalyst. This process corresponds to the simplest [2+2+2] cyclotrimerization reaction. The results obtained show that this reaction is thermodynamically very favorable and that the rate-determining step is the initial oxidative coupling between two acetylene molecules with a relatively low Gibbs free energy barrier of $19.8 \text{ kcal}\cdot\text{mol}^{-1}$. The energy profile derived from the real $[\text{RhCl}(\text{PPh}_3)_3]$ Wilkinson's catalyst is compared with that obtained with a model of the catalyst in which the PPh_3 ligands have been substituted by the smaller and computationally less expensive PH_3 molecules. Our results show that, at least for this reaction, this substitution has little influence on the thermodynamics obtained, while the barrier of the rate-determining step is somewhat increased (about $5 \text{ kcal}\cdot\text{mol}^{-1}$) in the model system. These results justify the use of this simplified model of the catalyst in theoretical studies of more complex cyclotrimerizations. Finally, we compare the results of the [2+2+2] intermolecular cyclotrimerization of three acetylene molecules catalyzed by $[\text{RhCl}(\text{PH}_3)_3]$ with those of the [2+2+2] intramolecular cyclotrimerization in a 15-membered azamacrocyclic triyne recently reported (*Chem.-Eur. J.* **2009**, *15*, 5289). This comparison shows that the entropic term changes the preference for the intermolecular cyclotrimerization at low temperatures to the intramolecular one at high temperatures.

Chapter 4. **Rhodium(I)-Catalyzed
Intramolecular [2+2+2] Cycloadditions of
15-, 20-, and 25-Membered
Azamacrocycles. Experimental and
Theoretical Mechanistic Studies**



Dachs, A., Torrent, A., Roglans, A., Parella, T., Osuna, S., Solà, M. "Rhodium(I)-catalysed intramolecular [2+2+2] cyclotrimerisations of 15-, 20- and 25-membered azamacrocycles. Experimental and theoretical mechanistic studies". *Chemistry: a European journal*. Vol. 15, issue 21 (May 18, 2009) : p. 5289-5300

<http://onlinelibrary.wiley.com/doi/10.1002/chem.200802548/full>

DOI: <http://dx.doi.org/10.1002/chem.200802548>

Article first published online: 22 APR 2009

Copyright © 2009 WILEY-VCH Verlag GmbH & Co. KGaA, Weinheim

Abstract

Number of members makes a difference: The [2+2+2] intramolecular cyclotrimerisation of a new series of 20- and 25-membered azamacrocycles catalysed by the Wilkinson's catalyst are reported (see scheme). The 20- and 25-membered azamacrocycles show different reactivity. Why? Theoretical calculations give insight into the reactivity differences observed for the 20- and 25-membered macrocycles.

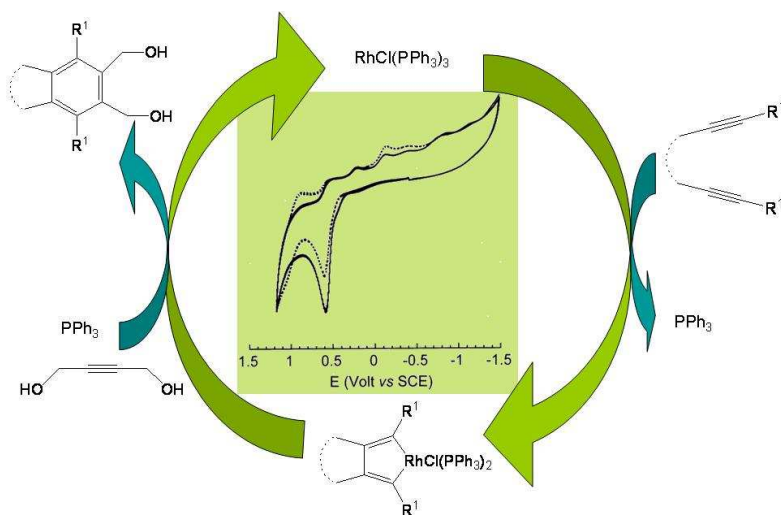
A new series of 20- and 25-membered polyacetylenic azamacrocycles have been satisfactorily prepared and completely characterised by spectroscopic methods. Various [2+2+2] cyclotrimerisation processes catalysed by the Wilkinson's catalyst, $[\text{RhCl}(\text{PPh}_3)_3]$, were tested in the above-mentioned macrocycles. The 25-membered azamacrocycle (like the previously synthesised 15-membered azamacrocycle) led to the expected cyclotrimerised compound in contrast to the 20-membered macrocycle, which is characterised by its lack of reactivity. The difference in reactivity of the 15-, 20- and 25-membered macrocycles has been rationalised through density functional theory calculations.

S'ha sintetitzat i caracteritzat espectroscòpicament una nova sèrie de macrocicles nitrogenats poliactilènics de 20- i 25-membres. Amb aquests macrocicles s'han dut a terme les reaccions de ciclotrimerització [2+2+2] catalitzades pel catalitzador de Wilkinson, $[\text{RhCl}(\text{PPh}_3)_3]$. El macrocicle nitrogenat de 25-membres (de la mateixa manera que el macrocicle nitrogenat de 15-membres) permet l'obtenció del compost ciclotrimeritzat. Per contra, el macrocicle de 20-membres es caracteritza per la seva falta de reactivitat. El diferent comportament de reactivitat dels macrocicles de 15-, 20-, i 25-membres ha estat estudiat mitjançant càlculs teòrics basats en la teoria del funcional de la densitat.

Keywords

- cyclotrimerization;
- density functional calculations;
- macrocycles;
- reaction mechanisms;
- rhodium

Chapter 5. **Rates and Mechanism of Rhodium-Catalyzed [2+2+2] Cycloaddition of Bisalkynes and a Monoalkyne**



Dachs, A., Torrent, A., Pla-Quintana, A., Roglans, A., Jutand, A. "Rates and mechanism of Rhodium-catalyzed [2+2+2] cycloaddition of bisalkynes and a monoalkyne".

Organometallics . Vol. 28, issue 20 : p. 6036–6043

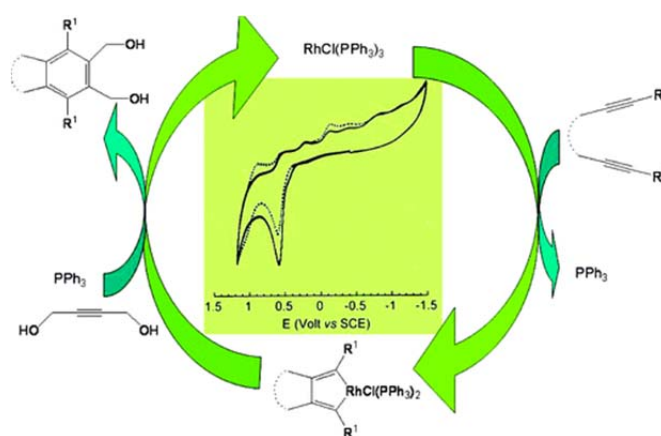
<http://pubs.acs.org/doi/abs/10.1021/om900544u>

DOI: <http://dx.doi.org/10.1021/om900544u>

Publication Date (Web): October 2, 2009

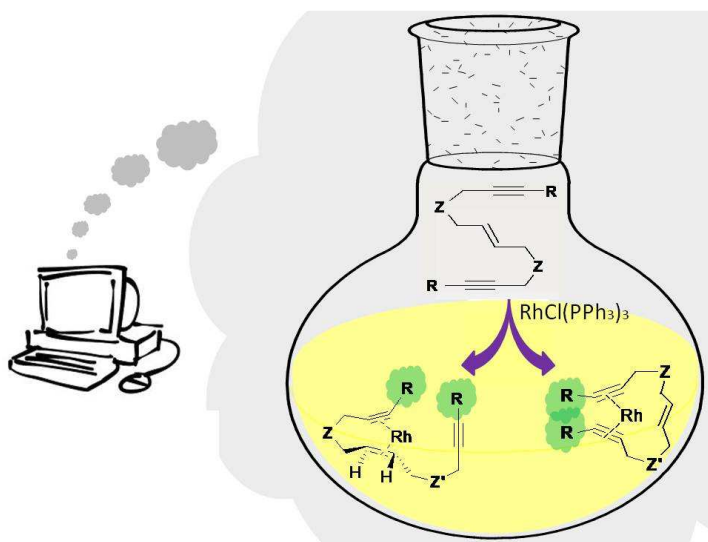
Copyright © 2009 American Chemical Society

Abstract



The mechanism of $\text{RhCl}(\text{PPh}_3)_3$ -catalyzed [2+2+2] cycloaddition of alkynes is investigated in the case of the reaction of symmetrical diynes **1a** and **1b** with the monoalkyne **3** ($\text{HOCH}_2\text{-C}\equiv\text{C-CH}_2\text{OH}$), leading to highly substituted benzene derivatives in dichloromethane at 25 °C. The two main steps of the catalytic cycle are characterized. The intermediate rhodacyclopentadiene Rh^{III} complexes **2a** and **2b** (formed by oxidative coupling after the coordination of the diynes **1a** and **1b** to $\text{RhCl}(\text{PPh}_3)_2$) are characterized by cyclic voltammetry, conductivity measurements, ^{31}P NMR, and ESI-MS. The formation of complexes **2a** and **2b** (step A) and their further reactions with the monoalkyne **3**, which deliver $\text{RhCl}(\text{PPh}_3)_3$ and the final product (step B), are followed by means of electrochemical techniques that deliver kinetic data for the two successive separately investigated steps. From the relative values of the half-reaction times of step A ($t_{\text{A}1/2} = 650$ and 75 s for **1a** and **1b**, respectively) and step B ($t_{\text{B}1/2} = 130$ and 680 s for **2a** and **2b**, respectively) determined under stoichiometric conditions, it emerges that step A (coordination of the two $\text{C}\equiv\text{C}$ bonds of **1**, followed by oxidative coupling) is rate-determining in the reaction involving **2a**, whereas step B (reaction of the intermediate complexes **2** with the monoalkyne **3**) is rate-determining in the reaction involving **1b**. Kinetic data for the catalytic cycle of a $\text{RhCl}(\text{PPh}_3)_3$ -catalyzed [2+2+2] cycloaddition of alkynes are thus presented for the first time.

Chapter 6. **RhCl(PPh₃)₃-Catalyzed
Intramolecular Cycloaddition of
Enediyne: the Nature of the Tether and
Substituents Controls the Reaction
Mechanism**



Dachs, A., Torrent, A., Solà, M. "RhCl(PPh₃)₃-catalyzed intramolecular cycloaddition of enediynes: the nature of the tether and substituents control of the reaction mechanism". *Organometallics* . Vol. 30, issue 11 : p. 3151-3159

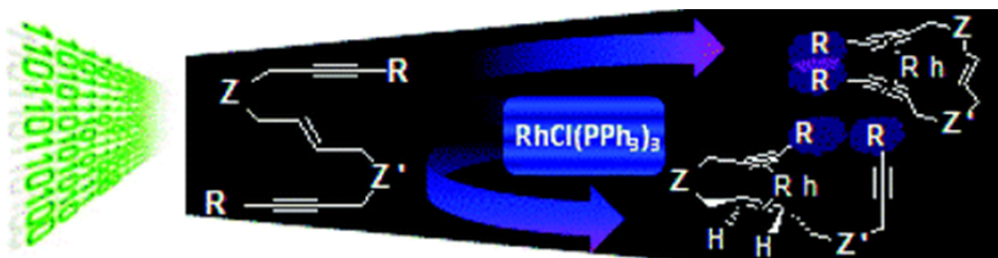
<http://pubs.acs.org/doi/full/10.1021/om200227e>

DOI: <http://dx.doi.org/10.1021/om200227e>

Publication Date (Web): May 4, 2011

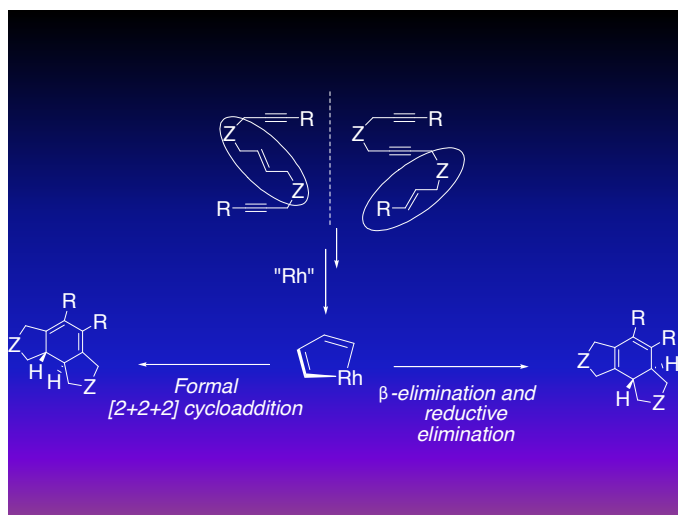
Copyright © 2011 American Chemical Society

Abstract



In this study we analyze a series of intramolecular [2+2+2] cycloadditions of enediynes catalyzed by the Wilkinson's complex with the B3LYP method. We are interested in the changes observed in the rate-determining oxidative coupling step of acyclic and cyclic enediynes as a function of the type of enediyne tether and the substituents present in the alkyne moieties in the case of acyclic systems. Our results show that the oxidative coupling step occurs between the two alkyne groups when the active catalyst is the RhCl(PH₃)₃ species, irrespective of the tether, the substituents of the alkyne groups, and the cyclic or acyclic nature of the enediynes. The same alkyne–alkyne coupling is favored in the cycloaddition of cyclic enediynes catalyzed by RhCl(PH₃)₂ as the active catalyst. With this catalyst, however, the preferred coupling in acyclic enediynes depends on the nature of the tether and substituents. Carbon-, oxygen-, and nitrogen-tethered enediynes with terminal alkynes favor the alkyne–alkyne oxidative coupling, whereas when the alkynes have an alkyl substituent, the enyne coupling is favored.

Chapter 7. **Intramolecular [2+2+2]**
Cycloisomerizations of yne-yne-ene and
yne-ene-yne Ene-diyne Catalyzed by
Rh(I): Experimental and Theoretical
Mechanistic Studies



Intramolecular [2+2+2] Cycloadditions of *Yne-ene-yne* and *Yne-yne-ene* Ene-diyne Catalyzed by Rh(I): Experimental and Theoretical Mechanistic Studies[†]

Anna Dachs,^{a,b} Anna Pla-Quintana,^a Teodor Parella,^c

Miquel Solà*^{a,b} and Anna Roglans*^a

^a Department of Chemistry, Universitat de Girona, Campus de Montilivi, s/n. E-17071-Girona, Spain

^b Institut de Química Computacional, Universitat de Girona, Campus de Montilivi, s/n. E-17071-Girona, Spain

^c Servei de RMN, Universitat Autònoma de Barcelona, 08193- Cerdanyola, Barcelona, Spain

anna.roglans@udg.edu, miquel.sola@udg.edu

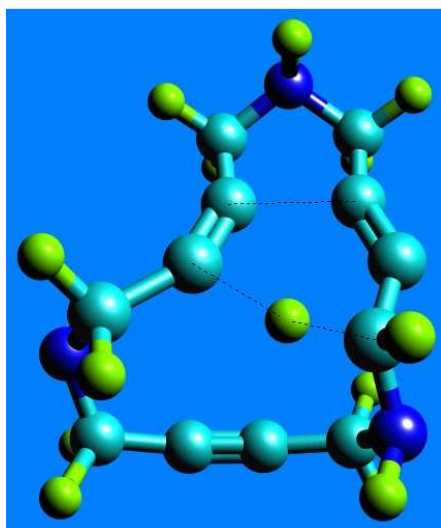
Abstract

N-Tosyl linked open-chained yne-ene-yne enediynes **1** and **2** and yne-yne-ene enediynes **3** and **4** were satisfactorily prepared. The [2+2+2] cycloaddition process catalyzed by the Wilkinson's catalyst (RhCl(PPh₃)₃) was tested in the above-mentioned substrates resulting in the production of high yields of the cycloadducts. Ene-diyne **1** and **2** gave standard [2+2+2] cycloaddition reactions whereas enediynes **3** and **4** suffered β-hydride elimination followed by a reductive elimination of the Wilkinson's catalyst giving cycloadducts **14** and **15** that are isomers from those that would be obtained through standard [2+2+2] cycloaddition reactions. The different reactivity of these two types of enediynes was rationalised through density functional theoretical calculations.

KEYWORDS [2+2+2] Intramolecular Cycloadditions · Wilkinson's Catalyst · Ene-diyne · Density Functional Theory · Reaction Mechanisms

[†] Dedicated to the memory of Prof. Rafael Suau (1945-2010) in recognition of his outstanding contribution to the field of organic chemistry.

Chapter 8. **Ene Reactions Between Two Alkynes? Doors Open to Thermally Induced Cycloisomerization of Triynic and Enediynic Macrocycles**



Ene reactions between two alkynes? Doors open to thermally induced cycloisomerization of macrocyclic triynes and enediynes†

Iván González,^a Anna Pla-Quintana,^a Anna Roglans,^{*a} Anna Dachs,^{ab} Miquel Solà,^{ab} Teodor Parella,^c Jordi Farjas,^d Pere Roura,^d Vega Lloveras^e and José Vidal-Gancedo^e

Received (in Cambridge, UK) 15th December 2009, Accepted 12th February 2010

First published as an Advance Article on the web 9th March 2010

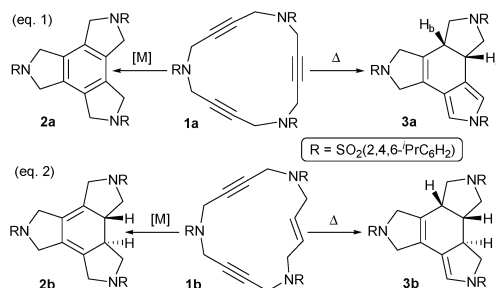
DOI: 10.1039/b926497c

A domino process is described combining an ene reaction between two alkynes and a Diels–Alder cycloaddition of the vinylallene formed. The process accounts for the thermally induced cycloisomerization of macrocyclic triynes and enediynes to give fused tetracycles in a stereoselective manner.

A highly efficient way of constructing complex organic molecules consists in the use of domino reactions.¹ When pericyclic transformations, endowed with complete atom economy and regio- and stereochemical control, are linked in a domino process, this as a whole will share these characteristics, achieving highly efficient chemical processes. In this communication we present a domino process consisting of two pericyclic steps: an unprecedented ene reaction between alkynes and a Diels–Alder cycloaddition.

Triaza macrocyclic scaffolds of type **1** have previously been transformed by a rhodium catalyzed [2+2+2] cycloaddition into tetra-fused structures of type **2** (Scheme 1).² A moderate yield of a new product, **3a**, was obtained when the catalytic system tested was unable to promote the [2+2+2] cycloisomerization of **1a**. The new isomer featured a pyrrole ring fused to a central cyclohexene ring with its double bond conjugated to those of the pyrrole. The process was stereoselective since the saturated azacyclopentyl ring had a *cis* ring fusion (H_a, H_b in Scheme 1). Macrocycle **1a** was then treated without any catalyst and product **3a** was isolated from decomposition products and some starting material with a 32% yield (Entry 1, Table 1). Remarkably, the formation of compound **2a** was not detected in any case so excluding the possibility of both a thermal [2+2+2] cycloaddition process and an isomerization of **3a** to **2a**.

To check the generality of this reaction, macrocyclic enediyne **1b** was submitted to the same conditions (Entry 2, Table 1). Again the cyclohexadiene tetra-fused product **2b**



Scheme 1 Metal-catalyzed vs. thermally-induced cycloisomerizations.

Table 1 Thermal cycloadditions of **1a** and **1b**^d

Entry	Substrate	Additive ^b	Reaction time	Product/Yield (%)
1	1a	—	30 h	3a /32
2	1b	—	6 days	3b /45
3	1a	1,4-CHD	60 h	3a /77
4	1b	1,4-CHD	6 days	3b /78

^a Reactions were run in toluene at 110 °C. ^b 20 equiv.

obtained in the metal-catalyzed process was not isolated but rather a 45% yield of a much more asymmetrical isomer **3b** was obtained in a stereoselective manner (Scheme 1). Almost half of the starting material decomposed during the prolonged heating time, but no isomer **2b** was detected in the NMR spectra of the crude reaction mixture.

On excluding metal catalysis, the possibility of there being a radical mechanism proposed for thermally induced intramolecular cycloisomerization of open-chain triynes³ was examined. Since radical species were engaged as intermediates for the formation of the isomerized products, the effect of an excess of 1,4-cyclohexadiene (1,4-CHD) added to the reaction mixture was evaluated. An increase in the yield of the cycloisomerized products **3a** and **3b** was obtained (entries 3–4, Table 1) although no formal addition of H occurred in the overall reaction.

To further understand the scope of the reaction, cycloaddition of macrocycle **1c**, bearing a phenyl substituent on the double bond, was studied. Two isomeric products with an overall 81% yield were obtained, which after isolation were assigned to structures **3c** and **3c'** (Scheme 2). The reaction was again stereoselective.

To further study yield enhancement by 1,4-CHD, we conducted an EPR study (Table 2). The use of a spin trap,

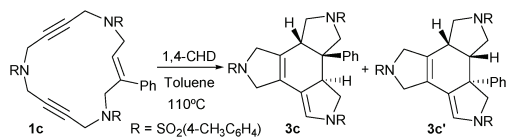
^a Dept. de Química, Universitat de Girona (UdG), Campus de Montilivi, s/n, E-17071-Girona, Spain. E-mail: anna.roglans@udg.edu; Fax: +34972418150; Tel: +34972418275

^b Institut de Química Computacional, UdG
^c Servei de RMN, Universitat Autònoma de Barcelona (UAB), Cerdanyola, E-08193-Barcelona, Spain

^d Dept. de Física, UdG, Campus de Montilivi, s/n, E-17071-Girona, Spain

^e Institut de Ciència de Materials de Barcelona (CSIC), Campus de la UAB, Cerdanyola, E-08193-Barcelona, Spain

† Electronic supplementary information (ESI) available: Experimental procedures, NMR and EPR spectra, B3LYP/cc-pVDZ xyz Cartesian coordinates and DSC thermograms. See DOI: 10.1039/b926497c



Scheme 2 Thermally-induced cycloaddition of macrocycle **1c**.

either 2-methylnitrosopropane (MNP) or α -phenyl-*N*-*tert*-butyl nitrene (PBN), was necessary as no radical was detected when the EPR experiment was recorded for the macrocycle alone (Entry 1). The addition of an excess of MNP allowed two radical adducts to be detected which were centred at the same position. These were ascribed to species **A** and **B** (Entry 2, Fig. S36[†]). The former is an adduct of the spin trap MNP and a *tert*-butyl radical resulting from its own decomposition. The blank experiment excluding macrocycle **1** (Entry 3) showed the formation of **A** to be independent of the presence of the substrate. However, species **B** originates from the reaction of MNP and a benzyl radical formed during the process. The formation of benzyl radicals was confirmed by the use of the more thermally stable PBN allowing the detection of spin adduct **C** (Entry 4), which was not formed in a blank experiment without macrocycle **1a** (Entry 5, Fig. S37[†]). Hence, the EPR experiments did not detect any radical species in **1a** but showed that benzyl radicals were formed in the reaction media, presumably due to H abstraction from toluene *via* homolytic cleavage. At this point, a deuteration experiment was undertaken. Macrocycle **1a** was heated at 110 °C in toluene-d⁸ but no incorporation of deuterium was observed either by NMR or ESI-MS.

Once a radical mechanism was discarded, the role of the radicals needed to be understood (Table 3). First, the reaction medium was switched to chlorobenzene, which is less prone to radical homolytic cleavage, and the yield for both **3a** and **3b** was substantially increased (compare Entries 1–2, Table 3 with Entries 1–2, Table 1). Then, benzoyl peroxide was added to the reaction mixture and complete decomposition of the starting material was observed by TLC and NMR after 24 h of reaction (Entries 3–4). The experiments confirm the detrimental behavior of radicals, which decompose the starting material. This hypothesis was reinforced by DFT calculations,⁴ which showed that the reaction of toluene with **1a** to yield the benzyl

Table 2 Radicals detected in the spin-trapping experiments

Entry	Mixture	g factor	LW (Gauss)	hfcc (Gauss)	Detected radical adduct structure
1	1a	—	—	—	—
2	1a + MNP	2.0062	1.1	a_N 15.2	O^\bullet (A) $^t\text{Bu-N}^t\text{Bu}$
		2.0062	0.9	a_N 15.2 a_H 7.4	O^\bullet (B) $^t\text{Bu-N-CH}_2\text{-Ph}$
3	MNP	2.0061	1.0	a_N 15.3	O^\bullet (A) $^t\text{Bu-N}^t\text{Bu}$
4	1a + PBN	2.0061	1.2	a_N 14.5 a_H 2.7	Ph O^\bullet (C) $\text{Ph-CH}_2\text{-CH-N}^t\text{Bu}$
5	PBN	—	—	—	—

Table 3 Effect of the radicals on the cycloisomerization reaction^a

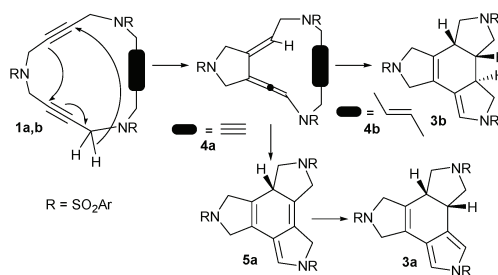
Entry	Substrate	Solvent/Additive	React. time	Prod./Yield
1	1a	Chlorobenzene/none	30 h	3a /62%
2	1b	Chlorobenzene/none	60 h	3b /60%
3	1a	Toluene/benzoyl peroxide ^b	24 h	Decomposes
4	1b	Toluene/benzoyl peroxide ^b	24 h	Decomposes

^a Reactions were run at 110 °C. ^b A steady supply of radicals was generated by adding benzoyl peroxide at fixed time intervals.

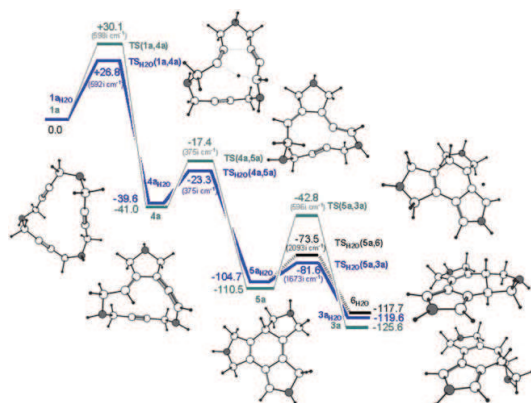
radical plus [**1a-H**] (formed by reaction of one of the N atoms in the macrocycle **1a** with a H) is endergonic by 38.4 kcal mol⁻¹ suggesting that such a transformation is feasible at the reaction temperature. Therefore, the addition of 1,4-CHD increases the yield by neutralizing the radicals generated in the reaction media and so it effectively acts as a radical scavenger.

Given the lack of radical involvement, a mechanistic proposal was made for the reaction based on a domino process composed of an unprecedented intramolecular ene reaction between two alkynes⁵ followed by a Diels–Alder reaction (Scheme 3). To the best of our knowledge, such an ene reaction has not been previously described, although acetylenic enophiles as well as acetylenic “enes” have been shown to participate in intramolecular ene-reactions,⁶ and more recently an ene reaction of arynes with alkynes has been published.⁷ This ene reaction affords a vinylallene intermediate **4** which may undergo a Diels–Alder reaction with the third unsaturation. If this is a triple bond (**4a**), the Diels–Alder reaction gives a 1,4-cyclohexadiene (**5a**) which undergoes a hydrogen rearrangement to yield **3a**. If the third unsaturation is a double bond (**4b**), the Diels–Alder reaction directly yields **3b**. In the case of macrocycle **1c**, the same mechanism accounts for both **3c** and **3c'**, each arising from one of the two non-equivalent alkynes participating as the ene or enophile in the reaction.

We then performed DFT calculations⁴ to evaluate the feasibility of the mechanism. The energy profile is presented in Scheme 4. We analyzed whether the reaction occurs both with and without a water molecule (blue/green profile, respectively). As a single water molecule was found to be needed to assist the final hydrogen transfer, only data related to this profile will be discussed. The overall reaction is exergonic by *ca.* 120 kcal mol⁻¹. Initially, two triple bonds approach each other so that the distance between the propargylic hydrogen and the enophilic alkyne is suitable (bond lengths of C₆–C₉ and C₁₀–H are 2.077 and 1.682 Å,



Scheme 3 Mechanistic proposal for the thermally induced process.



Scheme 4 Reaction Gibbs free energy profile (green: without water molecule/blue: with one water molecule) for the domino ene/Diels-Alder reaction. All energies in kcal mol⁻¹ are referred to **1a** or **1a** + H₂O.



Fig. 1 Optimized structure (B3LYP/cc-pVDZ) for TS_{H₂O}(**1a,4a**).

respectively, Fig. 1) to permit the six-electron pericyclic process, with suprafacial orbital interaction. The Gibbs free activation barrier of this process is 26.8 kcal mol⁻¹, which is the rate-determining step. The process from **1a** through the TS(**1a,4a**) gives the vinylallene species **4a**, from which the second pericyclic process takes place.

The transformation from **4a**H₂O into **5a**H₂O has a barrier of 16.3 kcal mol⁻¹ and is exergonic by 65.1 kcal mol⁻¹. Finally, a hydrogen rearrangement is required. A thermal [1,3]-H sigmatropic rearrangement through TS(**5a,3a**) with a suprafacial orbital interaction with a high barrier (67.7 kcal mol⁻¹) due to the extremely strained four-membered ring formed in the TS was rejected. However, when a water molecule was added to the theoretical model to assist the H rearrangement via TS_{H₂O}(**5a,3a**) (Fig. 2), the barrier was much lower (23.1 kcal mol⁻¹). We also studied the possibility of forming product **6** with a *trans* ring fusion. In this case the energy barrier TS_{H₂O}(**5a,6**) (Fig. 2) is 31.2 kcal mol⁻¹, 8.1 kcal mol⁻¹

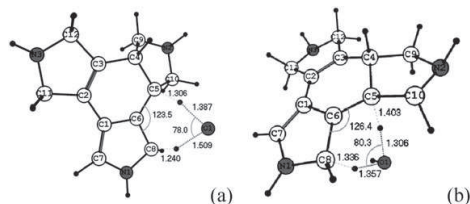


Fig. 2 Optimized structure (B3LYP/cc-pVDZ) for (a) TS_{H₂O}(**5a,3a**) and (b) TS_{H₂O}(**5a,6**).

higher compared to TS_{H₂O}(**5a,3a**), thus explaining the formation of only **3a**, which is thermodynamically and kinetically favoured with respect to **6**.⁸

The assistance of a water molecule was experimentally supported by conducting the reaction of **1a** in anhydrous chlorobenzene with added D₂O. The product showed quantitative deuterium incorporation in H_a (Scheme 1) as observed both in NMR and ESI-MS spectroscopies (see SI†).

Experimental support for the proposed mechanism was also obtained from DSC measurements. As expected for thermally activated processes, the peak temperature *T_p* of the first process increases with the heating rate (Fig. S39†). For **1a** the Kissinger plot⁹ of *T_p* exhibits the characteristic linear dependence related to processes governed by an Arrhenius-type rate constant *k*(*T*), (*k*(*T*) = *A*exp(-*E_a*/*RT*)) where *E_a* is the activation energy and *A* the preexponential term. An activation energy of 30.4 kcal mol⁻¹ was obtained from the fit to the Kissinger plot, which is in reasonable agreement with DFT calculations that yield 25.0 kcal mol⁻¹ for this activation energy obtained from the calculated enthalpy barrier Δ*H*[‡] plus the *RT* term calculated at 298 K. A reaction enthalpy of 120.8 kcal mol⁻¹ for the complete transformation was determined by integrating the heat released, which agrees quite well with the DFT enthalpy of 118.3 kcal mol⁻¹.

Financial support from MICINN (CTQ2008-05409, -03077, CTQ2006-06333, -01080, MAT2009-08385) of Spain, “Generalitat de Catalunya” (2009SGR637) and the University of Girona (grant to I. G.) is acknowledged.

Notes and references

- Domino Reactions in Organic Synthesis*, ed. L. F. Tietze, G. Brasche and K. M. Gericke, Wiley-VCH, Weinheim, 2006.
- A. Pla-Quintana, A. Roglans, A. Torrent, M. Moreno-Mañas and J. Benet-Buchholz, *Organometallics*, 2004, **23**, 2762–2767; A. Torrent, I. González, A. Pla-Quintana, A. Roglans, M. Moreno-Mañas, T. Parella and J. Benet-Buchholz, *J. Org. Chem.*, 2005, **70**, 2033–2041; S. Brun, L. Garcia, I. González, A. Torrent, A. Dachs, A. Pla-Quintana, T. Parella and A. Roglans, *Chem. Commun.*, 2008, 4339–4341; A. Dachs, A. Torrent, A. Roglans, T. Parella, S. Osuna and M. Solà, *Chem.–Eur. J.*, 2009, **15**, 5289–5300.
- For selected references: J. Marco-Contelles, *Chem. Commun.*, 1996, 2629–2630; M. G. Kociolk and R. P. Johnson, *Tetrahedron Lett.*, 1999, **40**, 4141–4144; S. Saaby, I. R. Baxendale and S. V. Ley, *Org. Biomol. Chem.*, 2005, **3**, 3365–3368; P. J. Parsons, A. J. Waters, D. S. Walter and J. Board, *J. Org. Chem.*, 2007, **72**, 1395–1398.
- Geometry optimizations and energy calculations were performed with the GAUSSIAN 03 program package using the hybrid DFT B3LYP method and the cc-pVDZ basis set. Reported energies are relative Gibbs free energies obtained at 298 K and 1 atm. The SO₂-Ar moieties present in the experimental species were substituted by H to reduce the computational effort. See SI† for details and references.
- K. Mikami and M. Shimizu, *Chem. Rev.*, 1992, **92**, 1021–1050.
- W. Oppolzer, E. Pfenninger and K. Keller, *Helv. Chim. Acta*, 1973, **56**, 1807–1812.
- R. R. Jayanth, M. Jeganmohan, M.-J. Cheng, S.-Y. Chu and C.-H. Cheng, *J. Am. Chem. Soc.*, 2006, **128**, 2232–2233.
- The **5a**H₂O → **2a**H₂O transformation assisted by a water molecule was also examined. It presents a large barrier (TS_{H₂O}(**5a,2a**), Fig. S38†) of 46.9 kcal mol⁻¹, 23.8 kcal mol⁻¹ higher in comparison with TS_{H₂O}(**5a,3a**). So, **2a**H₂O is the most stable product (is more stable than **3a**H₂O by 3.3 kcal mol⁻¹) but it is not kinetically accessible.
- H. E. Kissinger, *Anal. Chem.*, 1957, **29**, 1702–1706.

Chapter 9. **Results and Discussion**

A general outlook of the work presented in Chapters 3-8 is provided here. The most important results will be briefly summarized and extra information not included in the papers but relevant for purposes of comparison is also added and discussed. This chapter tries to connect the previously proposed objectives (Chapter 2) and the experimental results obtained. Compound numbers used in the original publications have been reflected here in this chapter despite occasional repetitions.

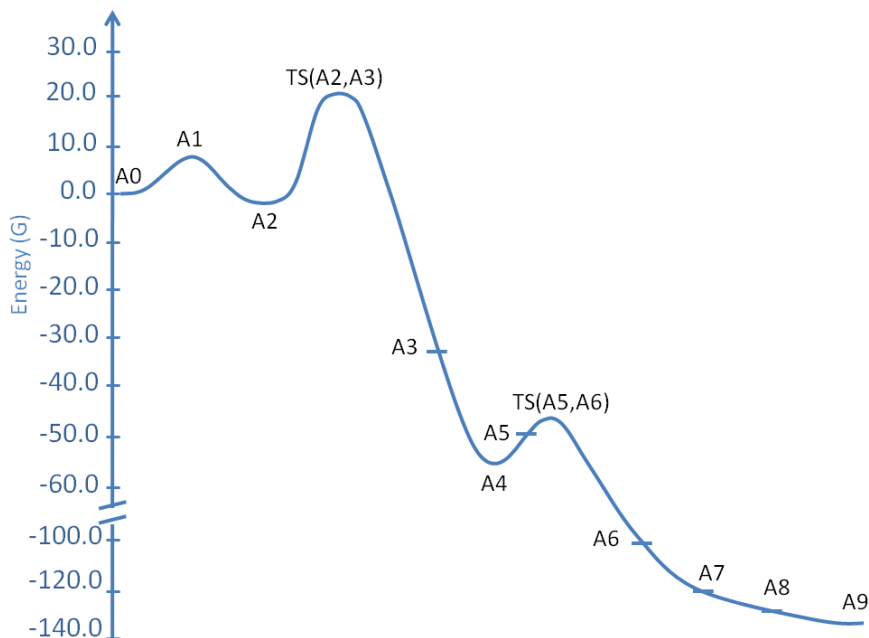
The results obtained and previously presented as separate papers (from chapters 3-8) will be now discussed in a more reduced way.

9.1. Density Functional Study of the [2+2+2] Cyclootrimerization of Acetylene Catalyzed by Wilkinson's Catalyst, $\text{RhCl}(\text{PPh}_3)_3$

The metal-catalyzed [2+2+2] cycloaddition of three acetylenes has been theoretically studied in the case of cobalt, ruthenium and rhodium catalysts but, to the best of our knowledge, not for the Wilkinson's catalyst. Therefore, we decided to initiate a study of the mechanism of the $[\text{RhCl}(\text{PPh}_3)_3]$ -catalyzed [2+2+2] cycloaddition of acetylene to benzene to analyze similarities and differences between the mechanism found for the Wilkinson's catalyst and the mechanisms proposed in previous works using other catalysts.

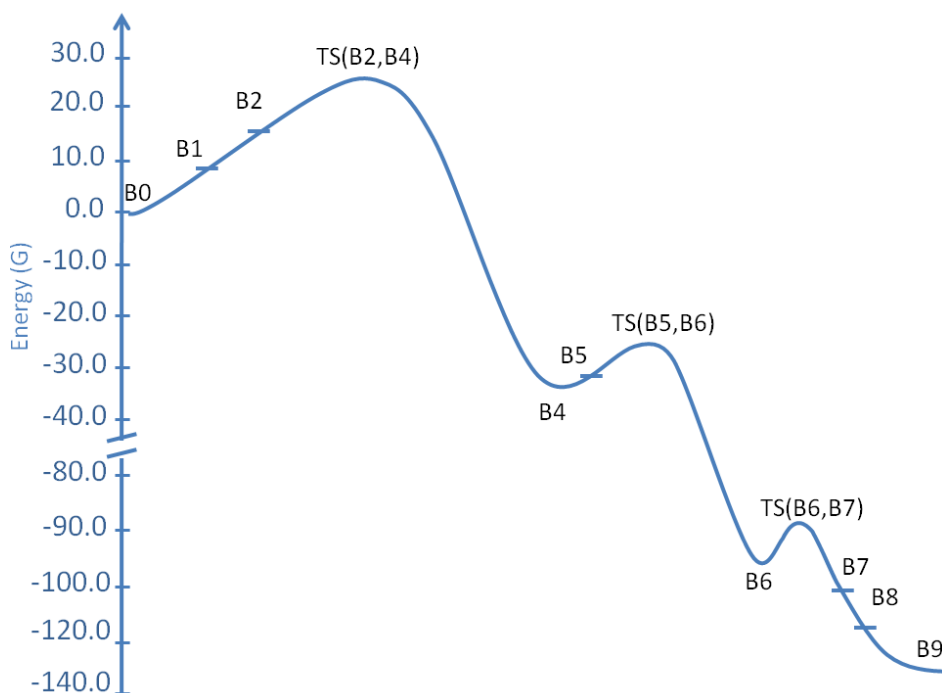
In many theoretical studies involving the Wilkinson's complex or similar catalysts, the PPh_3 ligands are replaced by PH_3 molecules. PPh_3 is substituted by PH_3 in DFT studies to reduce the computational cost. Thus, it is known that the electronic and steric effects produced by the PPh_3 ligands are quite different from those created by the PH_3 ligands. Thus, we have compared the reaction mechanisms catalyzed by the $[\text{RhCl}(\text{PPh}_3)_3]$ and $[\text{RhCl}(\text{PH}_3)_3]$ complexes due to our interest in theoretical studies using the Wilkinson's complex as a catalyst of different [2+2+2] cycloaddition reactions that we have carried out in this thesis.

The Gibbs energy profile at 298 K of cycloaddition of three acetylene molecules catalyzed by the Wilkinson's complex, $\text{RhCl}(\text{PPh}_3)_3$, is depicted in Scheme 9.1. The whole reaction is thermodynamically very favourable by 134.5 kcal/mol and the rate-determining step of the process is the oxidative coupling ($\text{TS}(\text{A2},\text{A3})$) between two acetylene moieties to give the rhodacyclopentadiene complex (A3) with an energy barrier of 19.8 kcal/mol respect to the initial reactants (ΔG^0) and 25.9 kcal/mol respect to the intermediate A2 (ΔG^\ddagger).



Scheme 9.1. Reaction Gibbs energy profile for the [2+2+2] cycloaddition of acetylene catalyzed by $\text{RhCl}(\text{PPh}_3)_3$ (in kcal/mol)

Scheme 9.2 depicts the Gibbs energy profile obtained with the $\text{RhCl}(\text{PH}_3)_3$ catalyst. As can be seen when comparing the results of Scheme 9.1 and Scheme 9.2, the thermodynamics of the whole process does not change as the reaction is exoergonic in the two cases by exactly the same amount (134.5 kcal/mol) since it is a catalytic process.



Scheme 9.2. Reaction Gibbs energy profile for the [2+2+2] cycloaddition of acetylene catalyzed by $\text{RhCl}(\text{PH}_3)_3$ (in kcal/mol)

The oxidative coupling through TS(B2,B4) (Figure 9.1) remains the rate-determining step with a Gibbs energy barrier of $\Delta G^0 = +24.7$ kcal/mol. In fact, both reaction energies and barriers for the rate-determining step differ by less than 1 kcal/mol if the entropic effects have not taken into account. Differences in the Gibbs energy barrier are not greater (1.2 kcal/mol) if we take as the minimum the intermediate A2 for TS(A2,A3) and the initial reactants B0 for TS(B2,B4).

Note that TS(A2,A3) has only one PPh_3 ligand attached to the Rh, while TS(B2,B4) has two PH_3 ligands. So in order to compare with the same phosphine ligands, the TS(B2,B3) is presented here (Figure 9.1), where the Rh has only one PH_3 ligand. The energy barrier of this process is higher (24.9 kcal/mol) in comparison to that found for TS(B2,B4) (11.9 kcal/mol), but the Gibbs energy barriers are similar, 23.9 kcal/mol for TS(B2,B3) and 24.7 kcal/mol for TS(B2,B4). So we observed that the entropic effects are much more important for TS(B2,B4) than TS(B2,B3) because of the presence of one more PH_3 ligand, as we expected.

From the geometric point of view, TS(A2,A3) and TS(B2,B3) have similar distances and angles, and with regards to the Gibbs energy barriers, TS(B2,B3) is only 2.0 kcal/mol lower than TS(A2,A3). Thus, all these results make $\text{RhCl}(\text{PH}_3)_3$ a good model of the Wilkinson's catalyst.

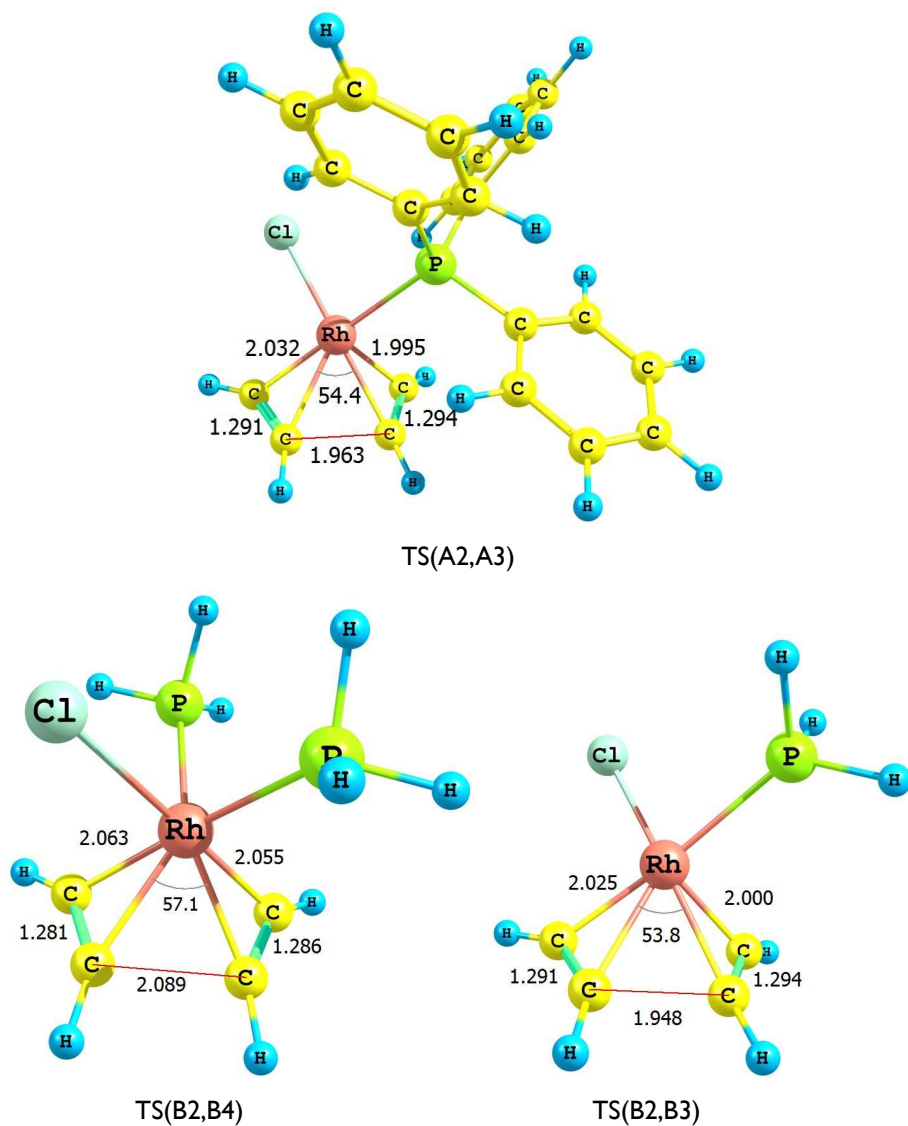


Figure 9.1. Oxidative coupling step of the two acetylene moieties with catalytic species: $\text{RhCl}(\text{PPh}_3)$ (above), $\text{RhCl}(\text{PH}_3)_2$ (below, left) and RhClPH_3 (below, right).

Selected bond distances (Å) and angles (deg.) are represented

It is worth noting that we found some differences between the two reaction mechanisms. In particular, they differ in the initial step of the reaction (compare Scheme 9.1 and Scheme 9.2) where the substitution process of phosphines by acetylenes is exothermic with PPh_3 ligands, while it is endothermic with PH_3 ligands. In line with this context, we have to mention that Macgregor, Roe et al.⁸⁴ reported a new study of which phosphine dissociates faster from Wilkinson's catalyst. They concluded that the dissociation from a position that is *trans* to another PPh_3 is significantly more accessible than from the position that is *trans* to Cl.

Moreover, another difference is an alternative pathway for the attack of the third acetylene molecule to the rhodacyclopentadiene (A4) that is found to be operative for the Wilkinson's catalyst but not in the modeled $[\text{RhCl}(\text{PH}_3)_3]$ one. This second route has similar or slightly higher energy requirements to those shown in Scheme 9.1, but it is likely that both pathways are operative for the $\text{RhCl}(\text{PPh}_3)_3$ catalyst. However, the small energy differences found justify the use of the simplified model of the catalyst in theoretical studies of more complex cycloadditions in order to reduce the computational cost significantly.

Finally, we also compared the thermodynamic and kinetic results of the simplest intermolecular [2+2+2] cycloaddition of three acetylene molecules with those of one of the simplest intramolecular [2+2+2] cycloaddition in a 15-membered azamacrocyclic triyne (Chapter 4). Here we compared between the intra- and intermolecular versions in order to analyze their behaviour in distinct temperature conditions. By analyzing the Gibbs energy barrier of the rate-determining step we have found that the entropic term changes the preference for the intermolecular cyclotrimerization at low temperatures to the intramolecular one at high temperatures. In the case of 0 K, the difference between Gibbs energy barriers of the intra- and intermolecular process is only 0.4 kcal/mol in favour of the intermolecular reaction. At 298 K, the Gibbs energy barrier of the intramolecular process is lower in comparison with the intermolecular one by as much as 3 kcal/mol. This result is due to a more favourable entropic contribution for the intramolecular reaction than the intermolecular one.

9.2. Rhodium(I)-Catalyzed Intramolecular [2+2+2] Cyclotrimerizations of 15-, 20-, and 25-Membered Azamacrocycles: Experimental and Theoretical Mechanistic Studies

As was mentioned in Chapter 1, our research group has developed, over the last few years, an efficient rhodium(I)-catalyzed [2+2+2] cycloaddition process of 15-, 16- and 17-membered triynic and enediyinic azamacrocycles of type 1 in Figure 9.2.

Due to the good results obtained in above mentioned studies, it was interesting to see the behaviour of [2+2+2] cycloaddition reaction of larger macrocycles with more unsaturations. Therefore, in this study we reported an efficient stepwise preparation of 20- and 25-membered macrocycles (**3** and **4**, respectively, Figure 9.2) featuring four and five triple bonds, respectively, with different arylsulfonyl moieties in their structure. All new compounds were completely characterized by spectroscopic methods and additional evidence for structure was secured by X-ray diffraction.⁸⁵

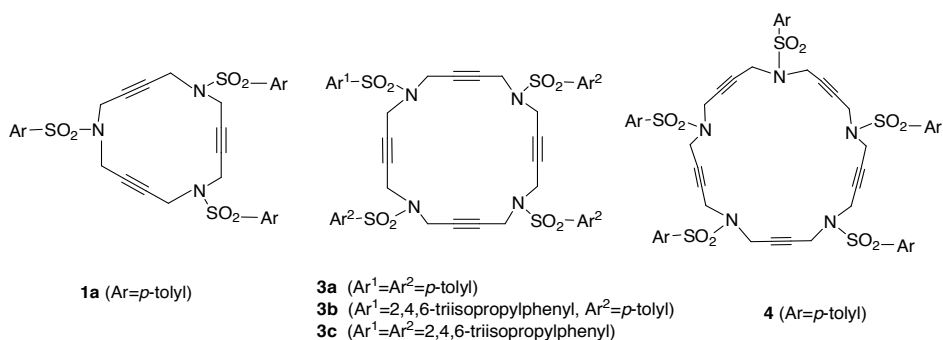
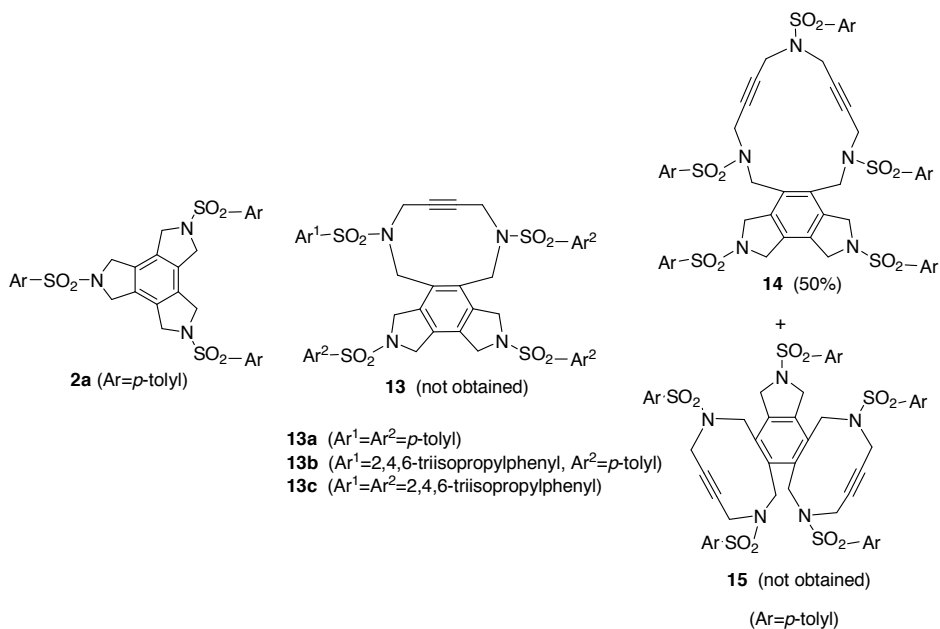


Figure 9.2. Structure of the 15-, 20- and 25-azamacrocycles

After preparing the macrocycles, the next step was to study how to obtain fused tetracycles by cycloaddition reactions. There is one possible way for macrocycles **3** to

cyclise to afford a fused benzene derivative (product **13** in Scheme 9.3), but the reaction did not take place when it was treated with the Wilkinson's catalyst. However, in the case of the 25-membered ring, **4**, there are two possible ways of cyclization; that is cycloaddition between three consecutive triple bonds to afford compound **14** (Scheme 9.3) or between non-consecutive triple bonds to afford compound **15** (Scheme 9.3). Experimentally, product **14** was obtained as the only product of the process.

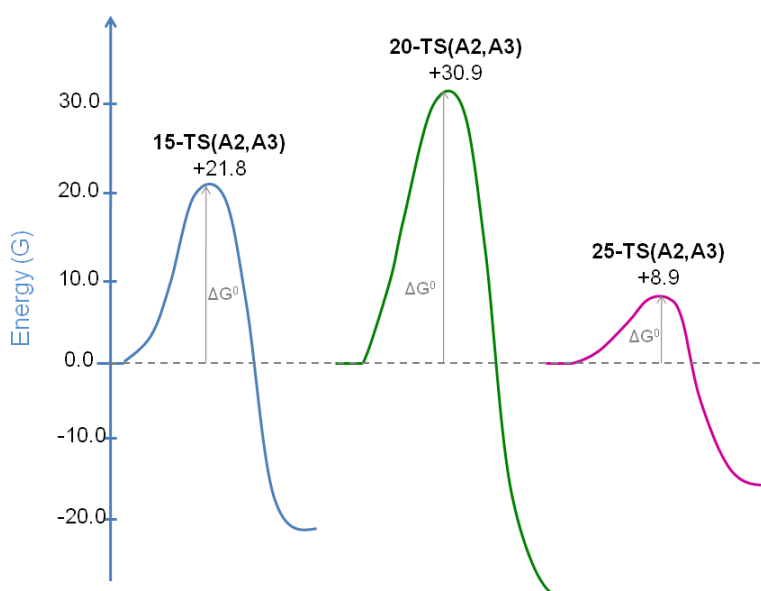


Scheme 9.3. Fused tetracycle products

Therefore, experimentally we observed that the 5,5,15-fused core (**14**) is more favourable than the 5,10,10-fused system (**15**). For this reason, we noted that the formation of a strained ten-membered ring during the cycloaddition, for example in compounds **13** and **15**, might disfavour the process.

DFT calculations revealed the whole reaction mechanism of the 15-, 20- and 25-membered azamacrocycles (MAA). As reported in previous studies, we also found that the rate-determining step in the [2+2+2] cycloaddition of macrocycles is the

initial oxidative coupling to yield the rhodacyclopentadiene intermediate. The Gibbs energy barriers obtained for this process in the 15-, 20- and 25-MAA are calculated to be 21.8, 30.9 and 8.9 kcal/mol with respect to separated reactants (Scheme 9.4). The values obtained were in line with the experimental observations, where the 20-membered macrocycle has clearly larger values than those found for the same rate-determining step in the 15- and 25-MAA.



Scheme 9.4. Representation of the oxidative coupling step barriers for the 15-, 20- and 25-membered azamacrocycles (energy barriers in kcal/mol)

It was interesting to discuss the results obtained by theoretical calculations as to the two possible products coming from the 25-MAA. Thermodynamically, product **14** is more stable than **15** (by 22.8 kcal/mol). Furthermore, the process that leads to the

product obtained (**14**), which implies the cycloaddition of three consecutive alkynes, is kinetically preferred.

To investigate the origin of the barriers, we decomposed the energy barrier of the rate determining step into deformation energy and interaction energy ($\Delta E_{def} + \Delta E_{int}$). The deformation energy in the TS was not the origin of the larger barrier for the 20-TS(A2,A3). However, the interaction energy for the 20- and 25-TS(A2,A3) were quite different between the two cases, -62.4 and -95.7 kcal/mol, respectively. So when the main interaction in the TS(A2,A3) was found to be between the LUMO of the catalyst and the HOMO of the macrocycle, the HOMO-LUMO overlaps that were detected were fairly similar in both cases. Thus, the HOMO in the deformed 20-MAA showed a higher electron-delocalization in comparison with the HOMO in the deformed 25-MAA (Figure 9.3), which apparently was responsible for its greater stabilization and, as a consequence, its lower reactivity.

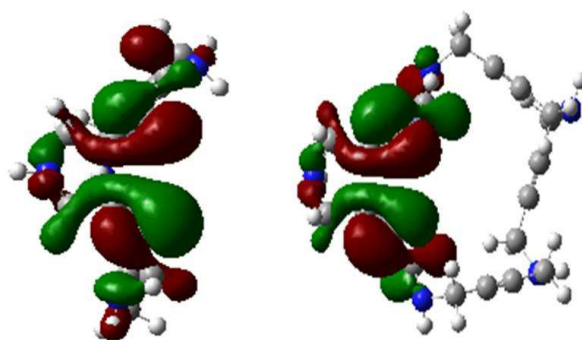
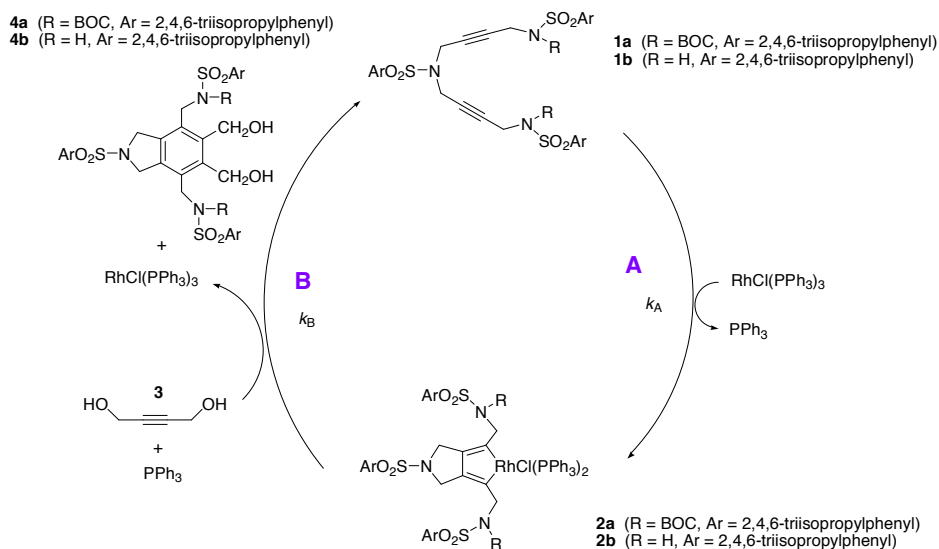


Figure 9.3. 3D-representation of the HOMOs for the 20-(left) and 25-MAA (right) at the geometry of the macrocycles have in the 20- and 25-TS(A2,A3). Isosurface values are ± 0.192 and ± 0.172 au, respectively.

9.3. Rates and Mechanism of Rhodium-Catalyzed [2+2+2] Cycloaddition of Bisalkynes and a Monoalkyne

Until now, several [2+2+2] cycloaddition processes have been carried out to study the reaction mechanism with different experimental techniques and also with DFT calculations, but no electrochemical data appears in the literature. We therefore applied this technique in collaboration with Prof. Anny Jutand from Paris.

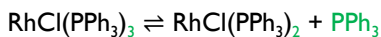
We studied the two main steps of the catalytic cycle of the $\text{RhCl}(\text{PPh}_3)_3$ -catalyzed [2+2+2] cycloaddition of the symmetrical diynes **1a** and **1b** with the monoalkyne **3** in dichloromethane at room temperature. The reactions of the diynes **1a** and **1b** with $\text{RhCl}(\text{PPh}_3)_3$ were followed by cyclic voltammetry, ^{31}P NMR, and ESI-MS (step A, Scheme 9.5). The rhodacyclopentadiene complexes **2a** and **2b** formed in these reactions were characterized by the same techniques.



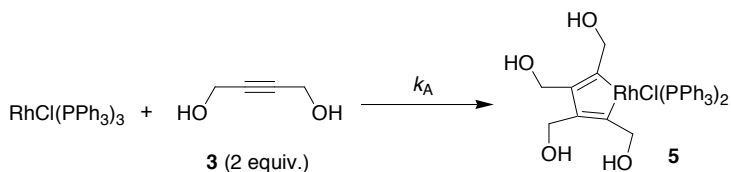
Scheme 9.5. [2+2+2] Cycloaddition reactions studied by CV, ^{31}P NMR, and ESI-MS

The reaction of complexes **2a** and **2b** with the monoalkyne **3**, which delivers the final product together with $\text{RhCl}(\text{PPh}_3)_3$ (step B, Scheme 9.5), was followed by electrochemical techniques.

The redox chemistry of the $\text{RhCl}(\text{PPh}_3)_3$ was characterized. First, the compound exhibited two successive irreversible oxidation peaks (**a**, Figure 9.4) at the scan rate of 0.5 Vs^{-1} . The oxidation peak current of the major peak ($E_{\text{O}_2}^{\text{P}} = +0.633 \text{ V vs SCE}$) increased at the expense of the oxidation peak current of the first minor and broader oxidation peak ($E_{\text{O}_1}^{\text{P}} = +0.483 \text{ V}$) upon addition of $\text{RhCl}(\text{PPh}_3)_3$ (0.5 equiv.). O_2 was the only oxidation peak observed in the presence of 10 equiv. of PPh_3 . This proved that $\text{RhCl}(\text{PPh}_3)_3$ (oxidized at O_2) was involved in an equilibrium with $\text{RhCl}(\text{PPh}_3)_2$ (oxidized at O_1) and PPh_3 :



Second, the cyclic voltammetry (CV) allowed us to characterize the standard oxidation potential (E^0) of the rhodacyclopentadiene complexes **2b** (Scheme 9.5) and **5** (Scheme 9.6) as a reversible oxidation peak (**b**, Figure 9.4).



Scheme 9.6. Oxidative coupling of the monoalkyne **3** studied by CV, ^{31}P -NMR, and ESI-MS

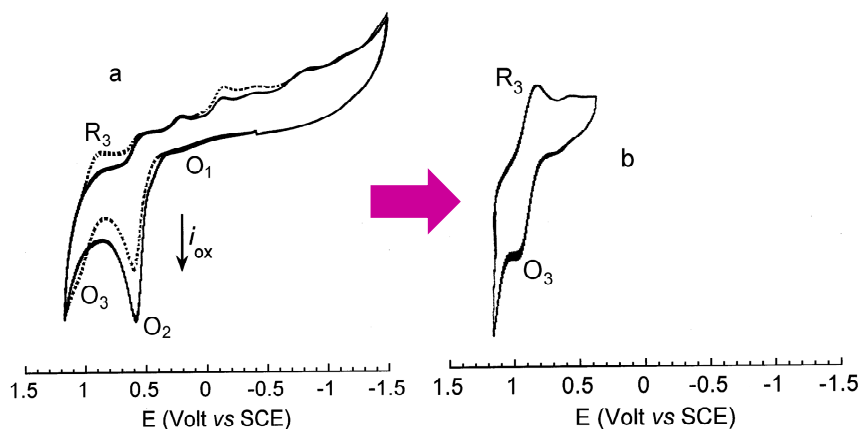


Figure 9.4. Cyclic voltammetry performed in CH_2Cl_2 containing nBu_4NBF_4 (0.3M) at steady gold disk electrode ($d = 2$ mm) at the scan rate of 0.5 Vs-1 at 25 °C. **a)** (—) $\text{RhCl}(\text{PPh}_3)_3$ (1.5 mM) oxidation first. (----) $\text{RhCl}(\text{PPh}_3)_3$ (1.5 mM) in the presence of **1a** (1.5 mM) after 15 min. **b)** after full reaction with **1a**

Moreover, the ^{31}P NMR allowed to associate a doublet to each rhodacyclopentadiene (**2a-c** and **5**), which correspond to two magnetically equivalent PPh_3 . The higher J_{Rhp} constant found was for the complex **2a** ($J_{\text{Rhp}} = 185\text{Hz}$), attributed to a difference of geometry induced by the bulky BOC protecting groups. The rhodacyclopentadiene complexes **2a-c** and **5** were also confirmed by electrospray ionization mass spectrometry (ESI-MS).

The kinetics of the reaction of the Wilkinson's catalyst with **1** in CH_2Cl_2 (step A in Scheme 9.5) was monitored by recording the decay of the oxidation plateau current i_{ox} of $\text{RhCl}(\text{PPh}_3)_3$ measured at a rotating gold disk electrode polarized at +1V, after addition of a stoichiometric amount of **1** to avoid further reactions.

From the values of the half-reaction times $t_{A/2}$ and $t_{B/2}$ of steps A and B, respectively, it was found that step A (coordination of the two C≡C bonds of **1**, followed by oxidative coupling) was the rate-determining step for the reaction of the bulky **1a**. In contrast, step B, reaction of **2b** (generated from the non-protected and thus less bulky diyne **1b**) with the monoalkyne **3** with subsequent recovery of the Wilkinson's catalyst, was the rate-determining step.

So, we note that the reaction is sensitive to steric factors around the C≡C bonds, which affect their coordination to the Rh(I) centre prior to oxidative coupling. It emerges that the first step A is affected by the substitution on the N atom (NH versus NBOC): the more hindered, the less reactive. Step B is also affected by the substitution on the N atoms, but the more substituted **2a** is found to be more reactive than the less substituted **2b**. This can be explained by the fact that in step B the steric hindrance might be beneficial due to the favouring the release of one PPh₃ by steric decompression to facilitate the coordination of the C≡C bond of **3** in the Rh(III) centre. In other words, one phosphine would be more labile in the bulky **2a** than in the less bulky **2b**.

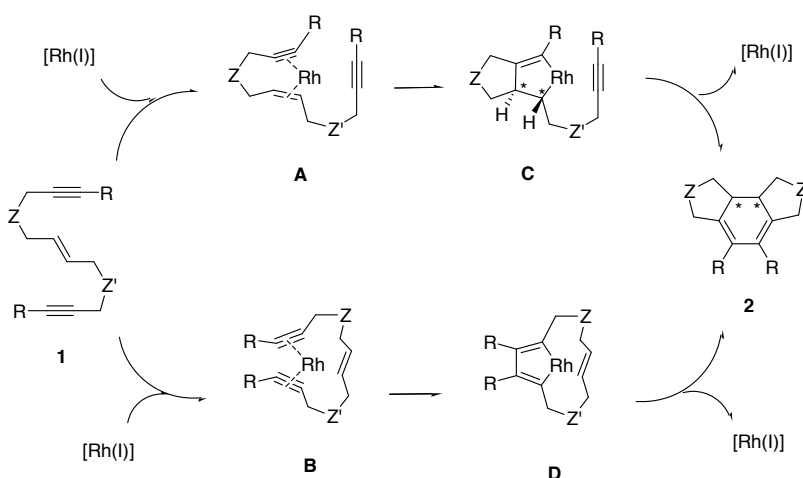
The kinetics of the reaction of RhCl(PPh₃)₃ with monoalkyne **3** was also investigated by means of the electrochemical techniques, as performed for bisalkynes **1**. From the value of $t_{A/2}$ for the formation of the rhodacyclopentadiene (**5**), it appears that the oxidative coupling from the dialkyne **1a** was twice as fast as that of the monoalkyne **3** (650 versus 1350 s, respectively).

These results suggested that the coordination of dialkynes **1** to RhCl(PPh₃)₃ was more favoured than that of the monoalkyne **3** due to intramolecular coordination.

9.4. $\text{RhCl}(\text{PPh}_3)_3$ -Catalyzed Intramolecular Cycloaddition of Eneidyne: the Nature of the Tether and Substituents Controls the Reaction Mechanism

The previous studies only involved alkyne moieties in the [2+2+2] cycloaddition reactions, but as we have seen in Chapter I, there are other unsaturations that can be involved in cycloaddition processes. Given this, we were interested in combining alkynes with alkenes in the initial reagent and studying the behaviour of these compounds with Wilkinson's model, $\text{RhCl}(\text{PH}_3)_3$, by DFT calculations.

The rate-determining oxidative coupling step in the intramolecular [2+2+2] cycloaddition of enediynes catalyzed by transition metals can take place through initial enyne (path **A** \rightarrow **C** \rightarrow **2** in Scheme 9.7) or alkyne-alkyne couplings (path **B** \rightarrow **D** \rightarrow **2** in Scheme 9.7). In this chapter we analyzed the reaction pathway in the oxidative coupling step as a function of the enediyne tethers and the substituent of the alkyne termini used. In particular, we analyzed different tethers (Z and $\text{Z}' = \text{O}, \text{NH}, \text{CH}_2, \text{CH}_3\text{SO}_2\text{N},$ and $\text{C}(\text{COOCH}_3)_2$) and two alkyne termini substituents ($\text{R} = \text{H}$ and CH_3).



Scheme 9.7. Possible routes for the [2+2+2] cycloaddition process in enediynes

The fact that the cycloaddition may proceed following one of the two paths has been considered to be the most likely explanation of the experimental difference of enantiomeric excesses observed in enediyne systems. When using chiral catalysts, the enyne coupling is expected to produce larger enantiomeric excesses (ee) than the alkyne-alkyne one.

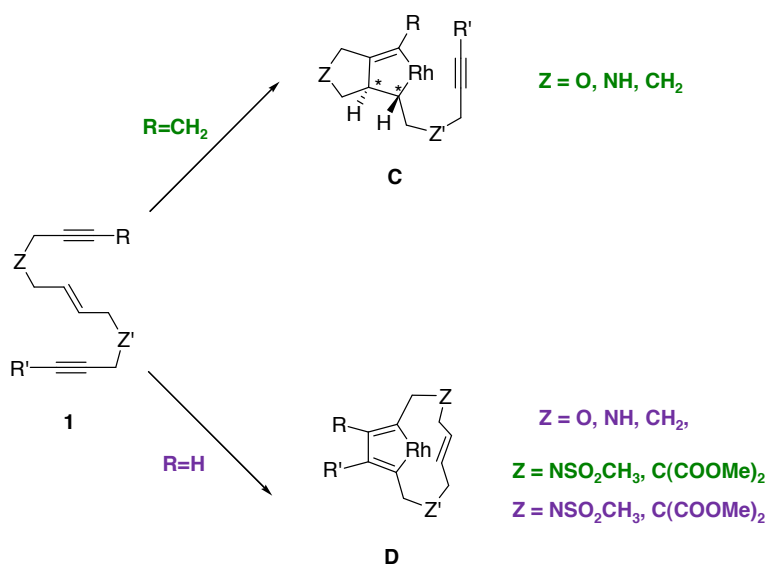
This aspect can be explained by the fact that if the selectivity is induced during the oxidative coupling step (**A** to **C**, via enyne coupling), which is the expected rate-determining step, relatively high barriers are expected and, consequently, the greater the energy differences between the transition states leading to the two different diastereoisomers resulting in a significant ee. In contrast, if the selectivity is induced after the rate-determining step (**D** to **2**, via alkyne-alkyne coupling), the ee will be small as all further steps after oxidative coupling involve low barriers, as we have seen in previous chapters, and the difference in TS energies leading the two different enantiomers will therefore be smaller.

The present study analyzes different factors that may have an influence on the preferred reaction pathway for the oxidative coupling in the [2+2+2] cycloaddition of enediynes. Thus, we have discussed the effect of different tethers and substituents in the alkyne moieties in the [2+2+2] cycloaddition of a series of cyclic and acyclic enediynes catalyzed by the $\text{RhCl}(\text{PH}_3)_2$ and RhClPH_3 active species.

Firstly, as has been corroborated in our previous study (Chapter 9.1), we have found that the substitution of the PPh_3 ligands by PH_3 reduces the energy barriers by about 15-20 kcal/mol for **Z** and **Z'** = **O**. This is not surprising given that PPh_3 has a larger σ -donation and smaller π -backdonation as compared to PH_3 . Thus, the RhClPPh_3 active catalyst has the same qualitative behaviour as those found with the RhClPH_3 complex. Therefore, to make the study computationally affordable, the *model* of the Wilkinson's catalyst ($\text{RhCl}(\text{PH}_3)_3$) can be exploited to study the preferred reaction pathway of enediynes of type **1**. Despite the fact that the energy barriers will be higher than those we would acquire using $\text{RhCl}(\text{PPh}_3)_3$, the qualitative results obtained with the *model*

catalyst are expected to be the same as those that would be achieved using the actual catalyst.

As far as the tether effect is concerned, we have found that the larger the electronegativity of the tethers, the lower the oxidative coupling energy barrier. Tethers have a small influence on the reaction path followed, except in the cases of substitution of NH and CH₂ tethers by the bulkier NSO₂CH₃ and C(COOCH₃)₂ tethers, which change the preferred pathway from enyne to alkyne-alkyne coupling (Scheme 9.8).



Scheme 9.8. Preferred pathway depending of the nature of the tether (Z) and the substituents of the terminal alkynes (R)

With respect to the alkyne moiety substituent, we have seen that substitution of H by CH₃ increases the energy barriers, especially that of the alkyne-alkyne coupling due to higher steric repulsion in the TSs. In cases where Z and Z' are O, NH or CH₂, this effect is enough to change the preferred pathway from alkyne-alkyne coupling for R = H to enyne coupling for R = CH₃.

As to the catalyst, the $\text{RhCl}(\text{PPh}_3)_3$ active species always prefers the alkyne-alkyne coupling since the destabilization due to methyl substitution in the alkyne moieties is not sufficient to reverse the preference for alkyne-alkyne coupling. However, for $\text{R} = \text{CH}_3$, energy differences between barriers for the alkyne-alkyne and enyne couplings become smaller and, therefore, a competition between the two reaction pathways is expected in this particular case. On the other hand, the $\text{RhCl}(\text{PPh}_3)_2$ catalyst favours the enyne coupling for the O, NH, and CH_2 tethers in the case of acyclic enediynes.

Finally, we have also found that while acyclic enediynes in some cases prefer the enyne coupling, the cyclic enediynes always favour the alkyne-alkyne coupling. It is found that geometrically, the enyne coupling is especially disfavoured due to high deformation energy required by the macrocycle to reach the TS geometry (Figure 9.5). In contrast, Figure 9.5 also revealed that the alkyne-alkyne coupling requires less deformation in cyclic systems due to the alkynes moieties being in the same plane and closer to each other.

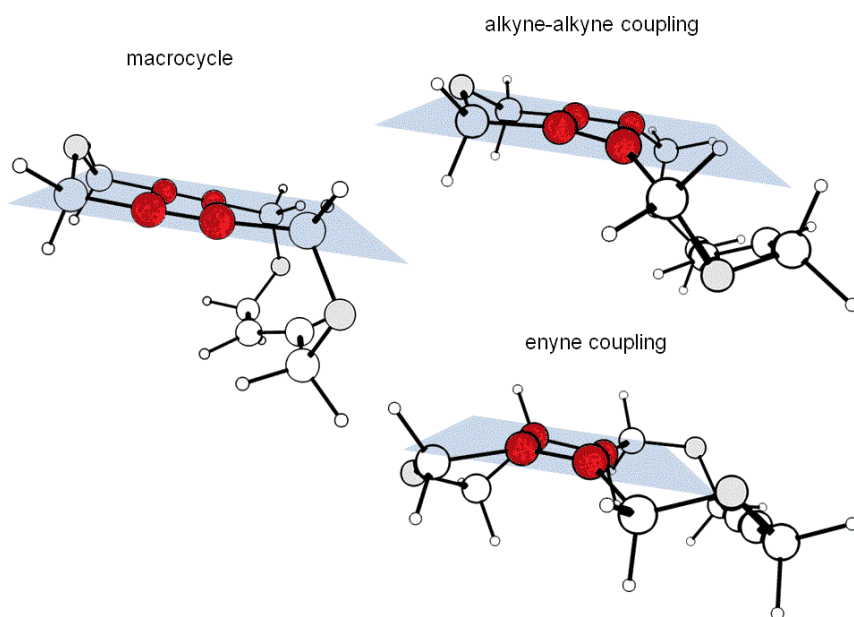
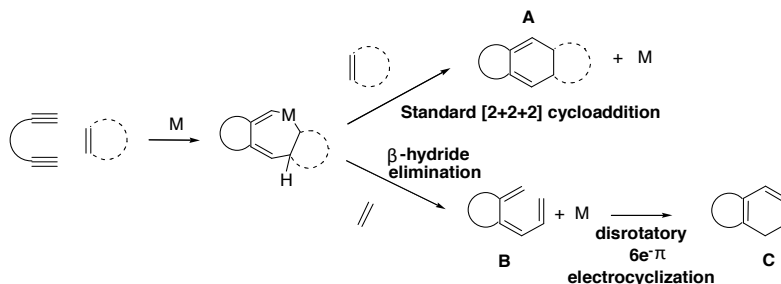


Figure 9.5. Optimized structures (B3LYP/cc-pVDZ-PP) for the macrocycle, alkyne-alkyne coupling and enyne coupling of the oxygen-tethered macrocyclic enediyne where key atoms are depicted in red

9.5. Intramolecular [2+2+2] Cycloadditions of *yne-yne-ene* and *yne-ene-yne* enediynes Catalyzed by Rh(I): Experimental and Theoretical Mechanistic Studies

The [2+2+2] cycloaddition of three alkynes is a well established method for the synthesis of polysubstituted benzenes and the cycloaddition of two alkynes with one alkene is a well known process for the formation of 1,3-cyclohexadienes.

Two possible reactions pathways for the cycloadditions of diynes with alkenes were explored by Saá et al.²⁸ with a Ru catalyst and Aubert, Gandon et al.²⁹ with a Co catalyst (Scheme 9.9). With cyclic alkenes, the standard [2+2+2] cycloaddition pathway prevailed, leading to 1,3-cyclohexadienes **A** (Scheme 9.9). However, when the alkene moiety was acyclic, a β -hydride elimination followed by a disrotatory $6e^- \pi$ -electrocyclization take place to afford an isomer of cyclohexadiene **A** was obtained (**C**).

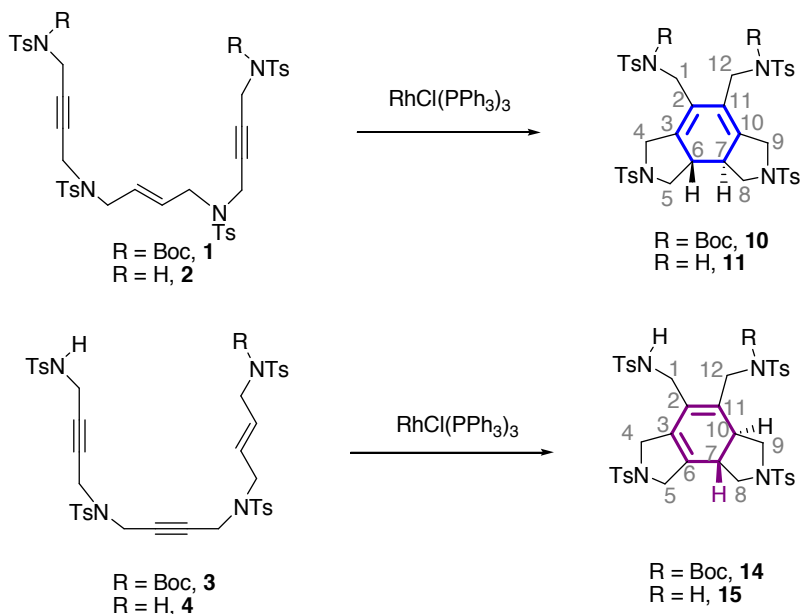


Scheme 9.9. Two possible reaction pathways for cycloaddition of diynes and alkenes

Our aim was to study the totally intramolecular [2+2+2] cycloaddition of enediynes when the alkene moiety is located in different positions and compare our cases with those of Saá and Aubert, Gandon et al.

Our experimental results showed that the reaction path of the Rh-catalyzed intramolecular [2+2+2] cycloaddition reaction of enediynes **1** to **4** to give the

corresponding cyclohexadienes varies with the position of the alkene moiety in the initial structure (Scheme 9.10).



Scheme 9.10. Rh(I)-catalyzed cycloadditions of compounds **1-4**

The full characterization of compounds **10,11,14** and **15** by 2D correlation NMR spectra confirmed the structure showed in Scheme 9.10. For instance, COSY data of **11** confirmed that the hydrogens of methylene groups 1 and 12 of the open-chain (δ 3.37 and 3.68 ppm) were only coupled with the amine NH proton (δ 7.74) (Figure 9.6). Consequently, there were no more H atoms closer to these methylenes coming from the cyclohexadiene ring. Moreover, NOE data were essential to determine the relative anti stereochemistry of the symmetrical centres in **10** and **11**.

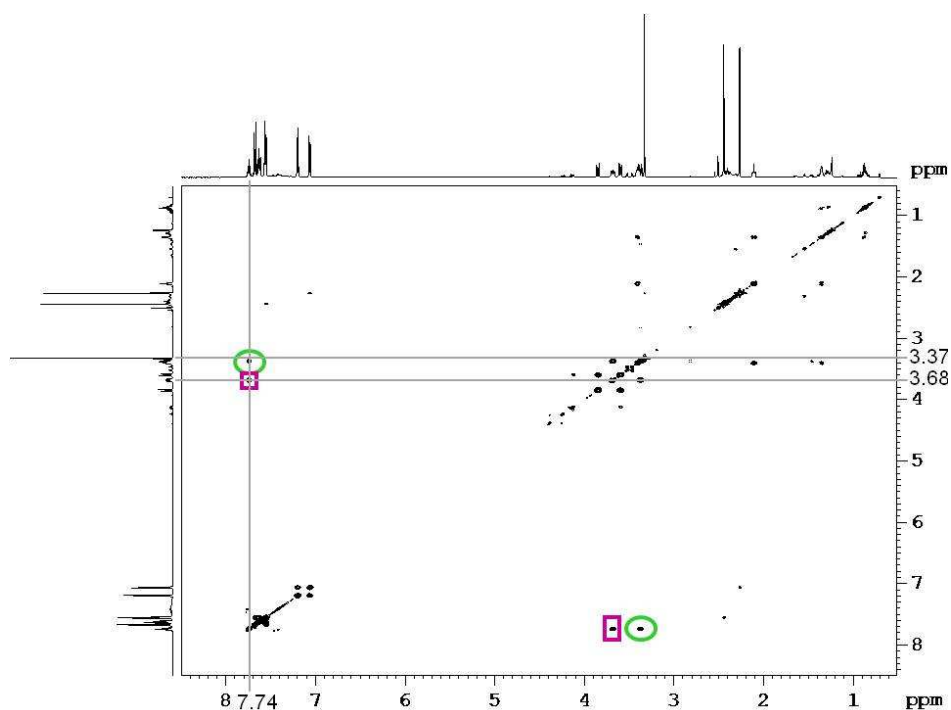
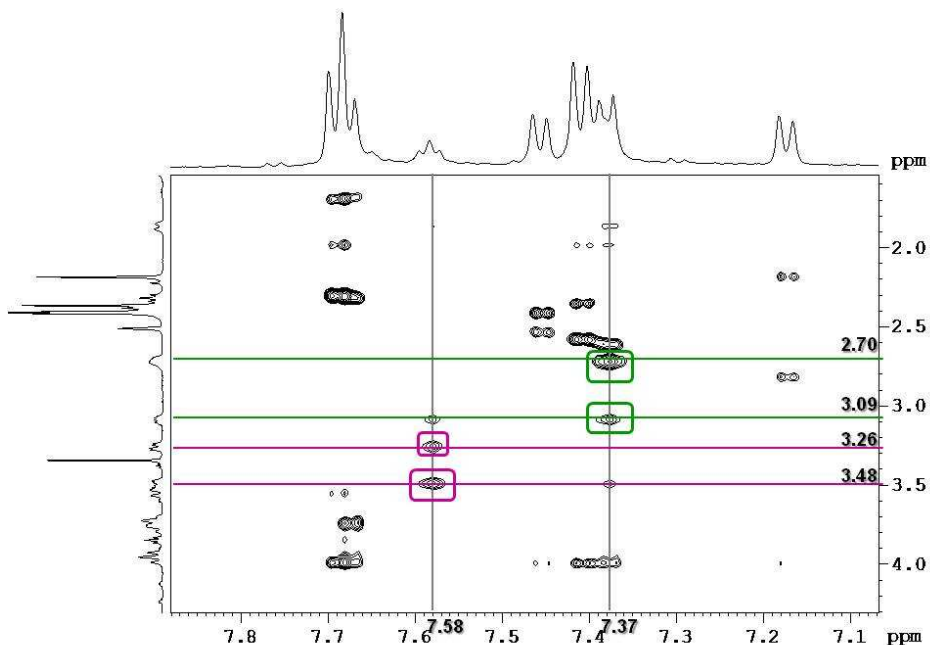
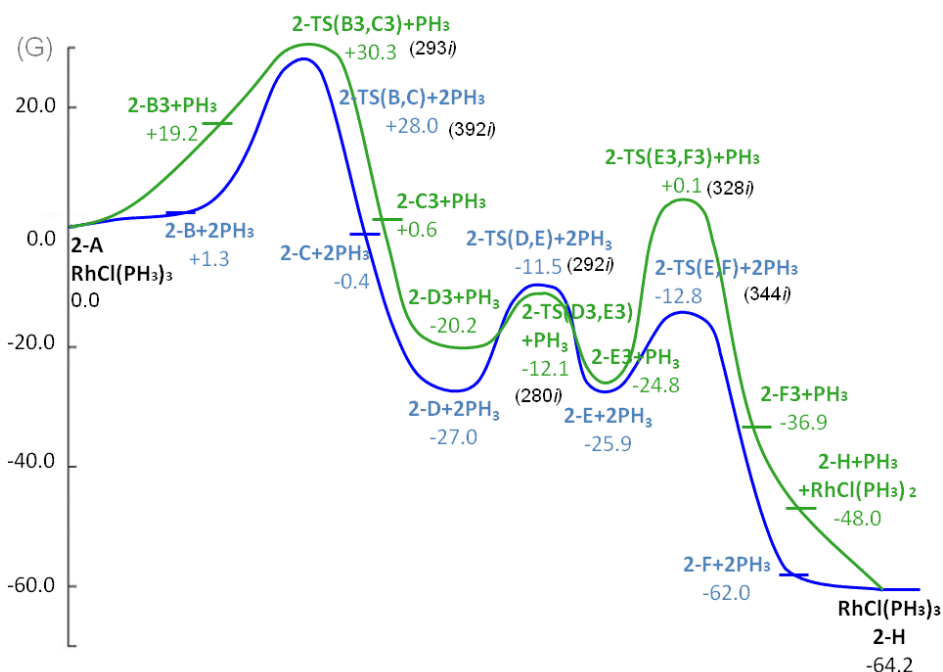


Figure 9.6. COSY spectra of product **11**

On the other hand, complete chemical shift assignment of **14** and **15** by 2D NMR techniques showed to be non-symmetric compounds. COSY data confirmed that the different methylene groups **1** (δ 2.70 and 3.09) and **12** (δ 3.26 and 3.48) of the compound **15** were only coupled with the amine NH protons (δ 7.37 and 7.58, respectively, Figure 9.7). Full characterization of these compounds can be found in the Supporting Information of the manuscript.

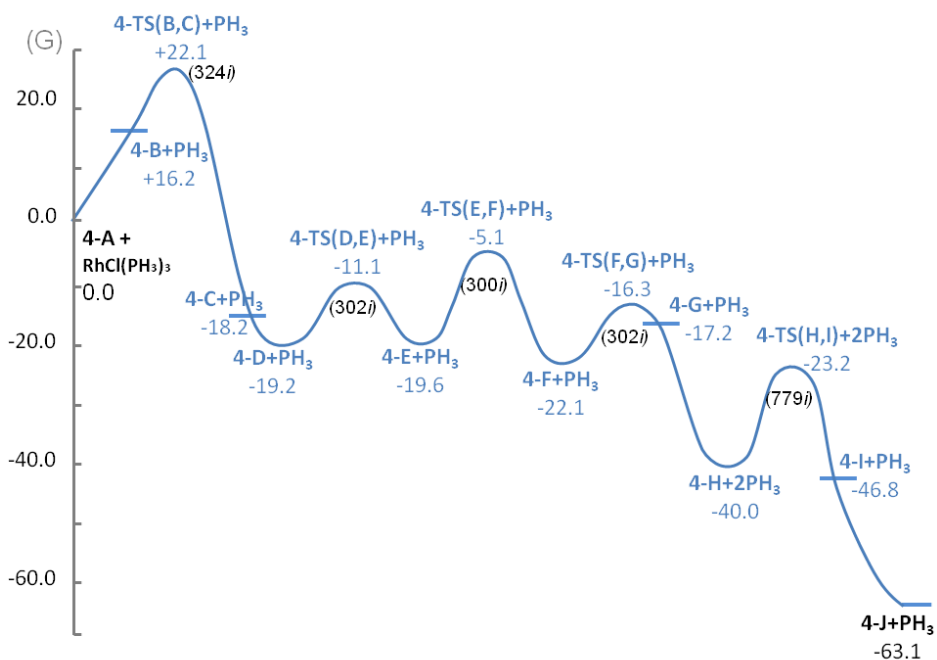
Figure 9.7. COSY spectra of product **15**

A DFT study allowed us to understand the different reactivity of the two enediynes: enediynes **1** and **2** (*yne-ene-yne*) prefer the conventional [2+2+2] cycloaddition reaction obtaining the expected cyclohexadienic products **10** and **11**, respectively (**2-H**, Scheme 9.11). Whereas enediynes **3** and **4** (*yne-yne-ene*) suffered β -hydride elimination followed by a reductive elimination of the Wilkinson's catalyst giving cycloadducts **14** and **15**, respectively (**4-J**, Scheme 9.12), which are isomers of those that would be obtained through standard [2+2+2] cycloaddition reactions.



Scheme 9.11. Reaction Gibbs energy profiles for the [2+2+2] cycloaddition of the enedynes **1** and **2** where the active catalyst is $\text{RhCl}(\text{PH}_3)_2$ (green line) or $\text{RhCl}(\text{PH}_3)_3$ (blue line). Relative Gibbs energy values with respect to separated reactants in kcal/mol. Imaginary frequencies [cm^{-1}] for the different transition states are given in brackets

Scheme 9.11 shows two different reaction pathways where both cases are achievable due to the rate-determining steps (oxidative coupling, **2-TS(B,C)** and **2-TS(B3,C3)**) are energetically similar. The next steps of the reaction mechanism do not show significant energy differences. Only the last step of the path shows a clear preference for **2-TS(E,F)** with respect to **2-TS(E3,F3)** by 12.9 kcal/mol.



Scheme 9.12. Reaction Gibbs energy profile for the [2+2+2] cycloaddition reaction of the enedynes **3** and **4**. Relative Gibbs energy values with respect to separated reactants in kcal/mol. Imaginary frequencies [cm⁻¹] for the different transition states are given in brackets

The Gibbs energy profile for the [2+2+2] cycloaddition reaction of enedynes **3** and **4** (Scheme 9.12) shows an accessible pathway to obtain the corresponding cycloadducts **14** and **15** (**4-J**).

The key intermediates are represented in Figure 9.8. The cycloheptadiene complex (**2-E3**) is especially important for the *yne-ene-yne* enedynes due to the fact that Rh is not able to eliminate the H in β -position due to the H $_{\beta}$ is too far (3.48 Å). Given this, the reaction pathway evolves as a formal [2+2+2] cycloaddition reaction. Quite the opposite, the complex **4-F** for the *yne-yne-ene* enedynes is essential to suffer a β -hydride elimination and consequently, the reaction pathway followed is completely different to the *yne-ene-yne* enedynes.

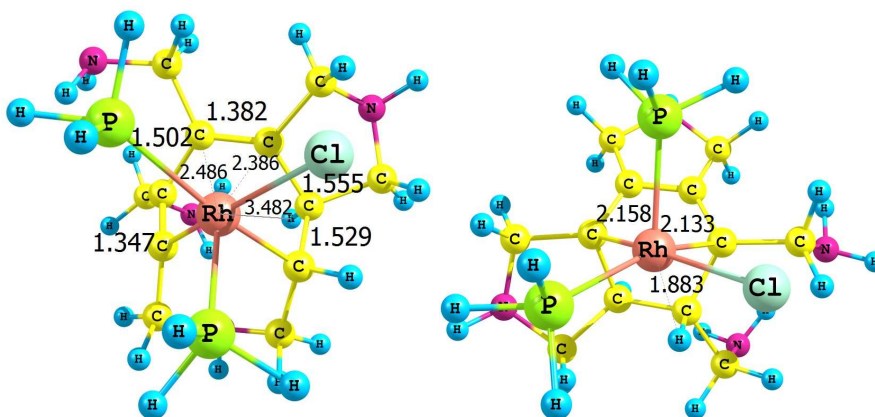
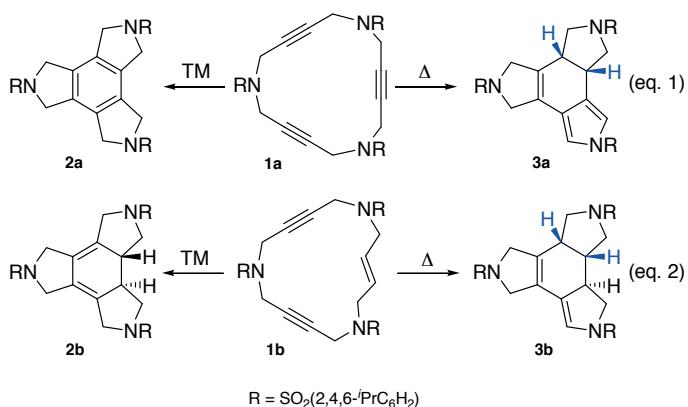


Figure 9.8. Optimized structure at B3LYP level of **2-E3** (left) of the model **2-A** and **4-F** (right) of the model **4-A** with selected bond distances (Å)

Therefore, the reaction mechanism where a β -hydride elimination is involved in the process, is in line with that found by the partially intramolecular version of the Ru catalyst²⁸ and the Co catalyst.²⁹ Thus, the partially intramolecular process requires a pure thermal disrotatory $6e\pi$ electrocyclization to give the final cyclohexadiene product and in our case, total intramolecular version, it is not necessary as the reductive elimination gives final products **14** and **15 (4-J)** satisfactorily as an exoergic processes with -63.1 kcal/mol.

9.6. Ene reactions between two alkynes? Doors open to thermally induced cycloisomerization of macrocyclic triynes and enediynes

As we have seen in the last chapters, [2+2+2] cycloadditions provide rapid access to polysubstituted six-membered rings. In the case of macrocycles **1a** and **1b** (Scheme 9.13), we have seen that the presence of active catalysts (TM) give polysubstituted compounds (**2a** and **2b**, Scheme 9.13), but when the TM is inactive, new kinds of polysubstituted products (**3a** and **3b**, Scheme 9.13) are obtained. This study describes a formal metal-free [2+2+2] cycloaddition strategy of macrocycles type **1** based on a thermally induced process (Scheme 9.13). This new reaction was stereoselective as both in products **3a** (with a yield of 32%) and **3b** (with a yield of 45%), where the saturated 5-membered ring has a *cis* ring fusion (H, blue in Scheme 9.13).⁸⁶



Scheme 9.13. Metal catalyzed vs. thermally induced cycloadditions of macrocycles **1a** and **1b**

We considered several possibilities in order to postulate a mechanism to explain the metal-free process. The option of a radical mechanism proposed for thermally induced intramolecular transformation by adding an excess of 1,4-cyclohexadiene (1,4-CHD), which is a radical hydrogen donor, was discarded because no incorporation of H in the final product was observed and an increase in the yield of the new products (**3a** and **3b**) was obtained.

To further study the yield enhancement by 1,4-CHD, we conducted an EPR study (Table 9.1). The use of a spin trap, either 2-methylnitrosopropane (MNP) or α -phenyl-N-*tert*-butyl nitron (PBN), was necessary as no radical was detected when the EPR experiment was recorded for the macrocycle alone (Entry 1). The addition of an excess of MNP allowed the detection of two radical adducts centered at the same position, which were ascribed to species **A** and **B** (Entry 2). The former is an adduct of the spin trap MNP and a *tert*-butyl radical resulting from its decomposition. The blank experiment excluding macrocycle **I** (Entry 3) showed the formation of **A** to be independent of the presence of the substrate and so, could not be related to any intermediate. However, species **B** originates from the reaction of MNP and a benzyl radical formed during the process. The formation of benzyl radicals was confirmed by the more thermally stable PBN allowing the detection of spin adduct **C** (Entry 4), which was not formed in a blank experiment without macrocycle **Ia** (Entry 5). Hence, the EPR did not detect any radical species in **Ia** but showed that benzyl radicals were formed in the cycloaddition, presumably due to H \cdot abstraction from toluene via homolytic cleavage.

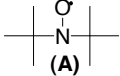
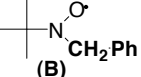
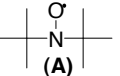
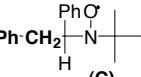
Entry	Mixture	g-factor	L	W	hfcc (Gauss)	Detected adduct structure	radical
1	Ia	-	-	-	-	-	-
2	Ia +MNP	2.0062	1.1		a_N 15.2		(A)
		2.0062	0.9		a_N 15.2 a_H 7.4		(B)
3	MNP	2.0061	1.0		a_N 15.3		(A)
4	Ia +PBN	2.0061	1.2		a_N 14.5 a_H 2.7		(C)
5	PBN	-	-		-	-	-

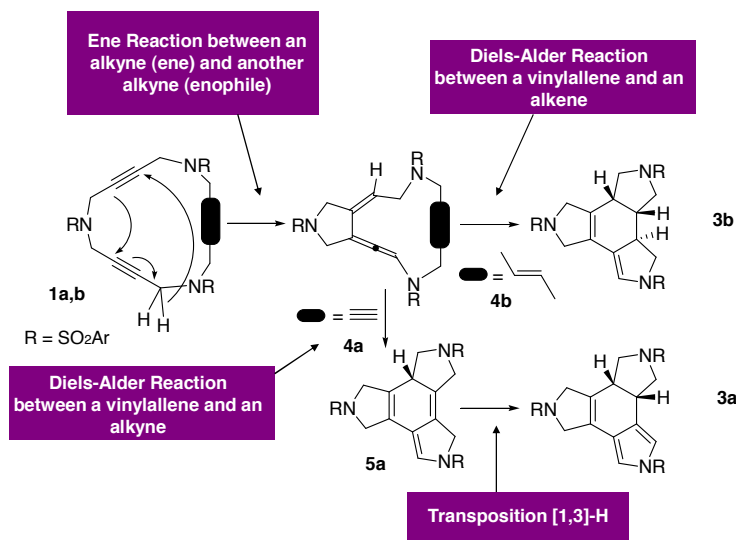
Table 9.1. Radicals detected in the spin-trapping experiments

Then, in order to understand the role played by the radicals observed, we changed the toluene for chlorobenzene, which is a solvent that is less conducive to homolytic breaking. The result was higher yields of the final products (**3a** and **3b**). After that, a radical initiator was added (benzoyl peroxide) and we observed the decomposition of the macrocycle. All of these experiments showed us that the radicals decompose the macrocycle or intermediates formed during the reaction, and moreover, that 1,4-CHD is a radical inhibitor.

Once a radical mechanism was discarded, a mechanistic proposal was made for the reaction (Scheme 9.14) based on a domino process composed of an unprecedented intramolecular *ene reaction* between two alkynes moieties followed by a *Diels-Alder reaction* between the intermediate (**4**) and the third unsaturation: an alkyne or alkene.

It should be noted that when the third unsaturation is a double bond, the *Diels-Alder reaction* leads to the final product. However, when the third unsaturation is a triple

bond, it is necessary to transpose the hydrogen (**5a** → **3a**) to obtain the experimental product.

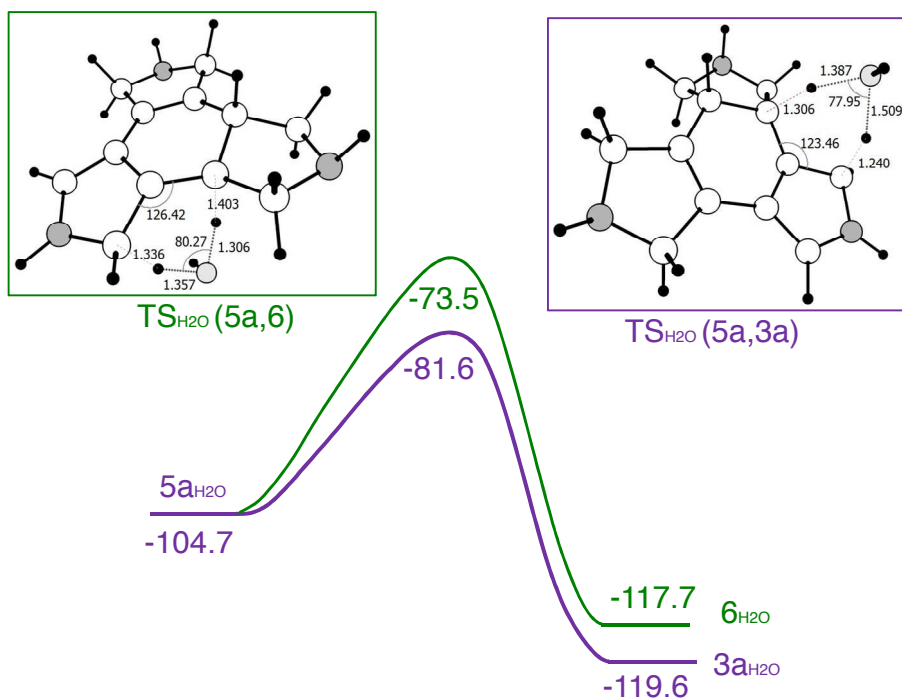


Scheme 9.14. Mechanistic proposal for the thermally induced cycloaddition of macrocycles **1**

We then performed DFT calculations to evaluate the feasibility of the mechanism. The overall reaction is exoergonic by 120 kcal/mol. The first step consists of a six-electron pericyclic process with an energy barrier of 26.8 kcal/mol, which is the rate-determining step of the reaction. The second pericyclic process comes from the intermediate **4a** into **5a** with a barrier of 16.6 kcal/mol. Finally, the last transformation suggested to us a 1,3-sigmatropic reaction of the transposition of the H marked in **5a** (Scheme 9.14), but the barrier obtained was too high (about 57 kcal/mol).

After that, we decided to study the possibility of a water-molecule assistance of the last process. In that case, we studied the two possibilities to obtain the product with

the two H in *cis* position (which is the experimental product) ($\text{TS}_{\text{H}_2\text{O}}(5\text{a},3\text{a})$, $\Delta G^\ddagger = 23.1$ kcal/mol, Scheme 9.15), or the formation of the product with the two H in *trans* position ($\text{TS}_{\text{H}_2\text{O}}(5\text{a},6)$, $\Delta G^\ddagger = 31.2$ kcal/mol, Scheme 9.15). These results confirmed that the formation of the product with H in *cis* position is preferred by 8.1 kcal/mol.



Scheme 9.15. Energy profile and optimized structures (B3LYP/cc-pVDZ) for $\text{TS}_{\text{H}_2\text{O}}(5\text{a},6)$ (left) and $\text{TS}_{\text{H}_2\text{O}}(5\text{a},3\text{a})$ (right)

Kinetically we were able to confirm that the transposition of this H requires a water molecule assistance and, moreover, that the selective formation of the experimental product (**3a**) is favoured over the other one (**6**).

The assistance of a water molecule was experimentally supported by running the reaction with the presence of D_2O and confirming by 1H -NMR spectroscopy the quantitative deuterium incorporation in **3a** (Figure 9.9).

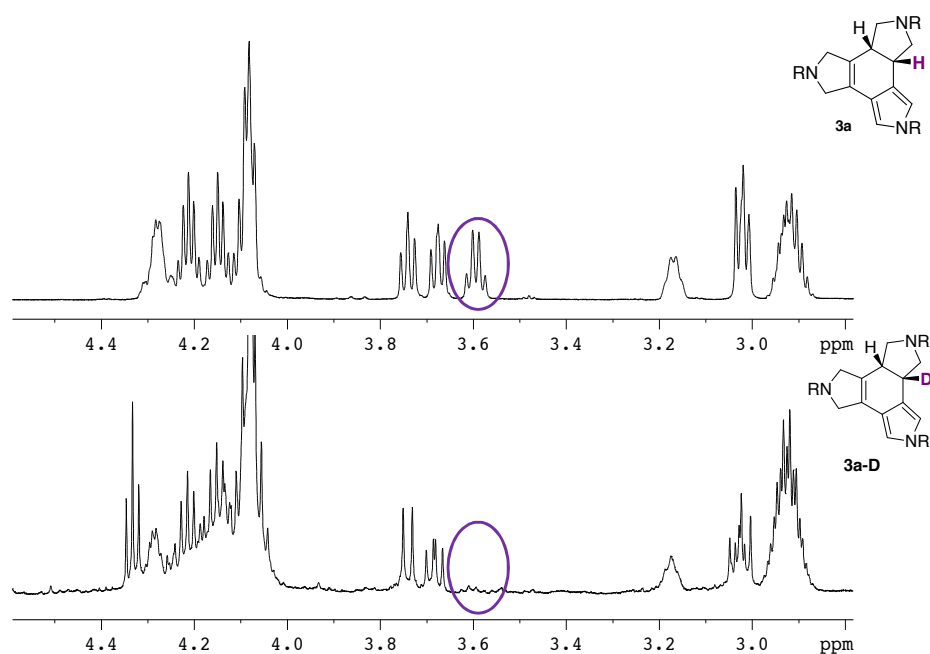


Figure 9.9. 1H -NMR (500.13MHz) spectra for deuterated **3a-D** (below) and 1H -NMR (600.13MHz) spectra for non-deuterated **3a** (above)

Besides from the disappearance of the 3.6 ppm signal, the multiplicity of the neighbouring protons at 3.02, 3.18 and 3.74 ppm is simplified. Moreover, the ESI-MS spectroscopy confirmed the presence of the deuterated product **3a** (**3a-D**) (Figure 9.10).

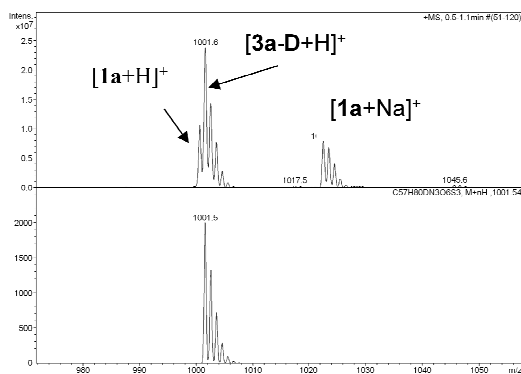


Figure 9.10. ESI-MS spectra for **3a-D** impurified with traces of unreacted starting macrocycle **1a**

In line with our findings, Danheiser et al.^{87a} reported a metal-free, bimolecular cycloaddition strategy based on the mechanism postulated above, as a cascade of two pericyclic processes. They established the utility of a bimolecular propargylic ene reaction/Diels-Alder cascade as a method for achieving formal thermal [2+2+2] cycloadditions leading to functionalized polycyclic compounds. This strategy was also described by Danheiser et al.^{87b} for the construction of polycyclic pyridine derivatives.

Chapter 10. **Conclusions**

The most important conclusions taken out from the studies of this thesis on [2+2+2] cycloaddition reactions will be briefly summarized in this chapter. Compound numbers used in the original publications have been reflected here in this chapter despite occasional repetitions.

Project 1:

We have found that modelling PPh_3 by PH_3 in the catalyst results in minor changes in the thermodynamics and kinetics at 0K. Both the reaction energies and the barriers in the rate-determining step differed by less than 1 kcal/mol when the entropic effects were not taken into account. However, this difference was a little bit higher (of about 5 kcal/mol) when the Gibbs energy was considered. Despite these results, we thought that this simplification could be exploited in subsequent studies to reduce the computational cost significantly.

In spite of this, we should note that there were some differences between the two reaction mechanisms: the initial step of the reaction was not the same and an alternative pathway for the attack of the third acetylene molecule on the formed rhodacyclopentadiene was found to be operative for the Wilkinson's catalyst but not in the modelled $[\text{RhCl}(\text{PH}_3)_3]$ one.

When the thermodynamic and kinetic results of the simplest intermolecular [2+2+2] cycloaddition of three acetylene molecules were compared with those of one of the simplest intramolecular [2+2+2] cycloaddition in a 15-membered azamacrocyclic triyne, the Gibbs energy barrier of the rate-determining step found confirmed that the entropic term changes the preference for the intermolecular cycloaddition at low temperatures to the intramolecular one at high temperatures.

Project 2:

We reported the preparation of 20- and 25-membered azamacrocycles featuring four and five triple bonds, respectively, and all new compounds were completely characterized by spectroscopic methods.

Moreover, an efficient $\text{RhCl}(\text{PPh}_3)_3$ -catalyzed [2+2+2] cycloaddition of 25-membered pentaacetylenic azamacrocyclic **4** afforded the cycloisomerized compound **14** resulting from the reaction of three adjacent alkynes instead of the cycloaddition between non-adjacent triple bonds. The DFT study confirmed this chemoselectivity showing that the reaction pathway to obtain product **14** is thermodynamically and kinetically preferred over that yielding the product **15**.

In contrast, the 20-membered tetracetylenic azamacrocyclic **3** did not lead to the expected cycloisomerized compound. DFT calculations allowed us to determine the reaction mechanism of the 20-MAA. The results obtained showed that there were two main factors that contribute to the lack of reactivity of the 20-MAA:

- a) the 20-MAA has a more stable and delocalized HOMO orbital
- b) the formation of a strained ten-membered ring during the cycloaddition of the 20-MAA.

These two factors increased the Gibbs energy barriers of the rate-determining step and hindered the intramolecular cycloaddition of the 20-MAA.

Project 3:

The [2+2+2] cycloaddition reaction of symmetrical diynes (**1a** and **1b**) with the monoalkyne **3** were followed by electrochemical techniques at room temperature. Other spectroscopic techniques like ^{31}P NMR and ESI-MS were also employed to obtain further information.

Two main steps were identified in this study: first, the formation of the rhodacyclopentadiene complexes **2a**, **2b** and **5** (Step A), and second, the reaction of complexes **2** with the monoalkyne **3** giving the final product together with $\text{RhCl}(\text{PPh}_3)_3$ (Step B).

Kinetic data on the two main steps of the catalytic cycle for a $\text{RhCl}(\text{PPh}_3)_3$ -catalyzed [2+2+2] cycloaddition of alkynes were thus available for the first time. From the results obtained, the half-reaction times $t_{A/1/2}$ and $t_{B/1/2}$ of steps A and B, respectively, it was found that step A (alkyne-alkyne coupling of **1**) was the rate-determining step for the bulky compound **1a**. In contrast, in step B, the reaction of **2b** complex (coming from the less bulky diyne **1b**) with the monoalkyne **3** to deliver the aromatic compound **2b**, was found to be the rate-determining step.

We concluded that either the first or second step might be the rate-determining step depending on the structure of the starting reagents.

Project 4:

When the [2+2+2] cycloaddition reaction takes place in an enediyne compound, the oxidative coupling can be observed between the two alkynes (alkyne-alkyne coupling) or between one alkyne and the alkene (enyne coupling) of the compound.

These two reaction pathways have to be considered to explain the experimental difference of enantiomeric excesses detected in enediynic systems. It has been established that the enyne coupling is expected to produce larger enantiomeric excesses (ee) than the alkyne-alkyne one, when a chiral catalyst is used.

Thus, we analyzed different factors that may have an influence on the preferred reaction pathway for the oxidative coupling in the [2+2+2] cycloaddition of enediynes catalyzed by the Wilkinson's catalyst.

In this study, we observed that the substitution of H by CH_3 increases the energy barriers, especially that of the alkyne-alkyne coupling. This fact is sufficient to change the preferred pathway from alkyne-alkyne coupling for $\text{R}=\text{H}$ to enyne coupling for $\text{R}=\text{CH}_3$.

With respect to the tethers of the enediyne, when the process took place with O, NH and CH₂ tethers, little influence on the reaction path followed was observed. A greater difference between the tethers studied is observed when the cases of NH and CH₂ tethers are substituted by the bulkier CH₃SO₂N and C(COOCH₃)₂ tethers, where the preferred pathway is changed from enyne to alkyne-alkyne coupling in substituted alkynes.

On the other hand, when the [2+2+2] cycloaddition reactions of acyclic enediynes, for which in some cases the enyne coupling was preferred, were compared with the cycloaddition of cyclic enediynes, it was observed that the latter always prefers the alkyne-alkyne coupling due to the lower deformation energy required.

Project 5:

The path of the RhCl(PPh₃)₃-catalyzed intramolecular [2+2+2] cycloaddition reaction of enediynes **1** to **4** to give the corresponding cyclohexadienes changed with the position of the alkene moiety in the initial compound.

DFT calculations gave an explanation of the different reactivity: enediynes type *yne-ene-yne* preferred the conventional [2+2+2] cycloaddition reaction, whereas enediynes type *yne-yne-ene* suffered β-hydride elimination followed by a reductive elimination of Wilkinson's catalyst giving cycloadducts **14** and **15**, which are isomers of those which would be obtained through standard [2+2+2] cycloaddition reactions.

Project 6:

The free transition metal-catalyzed processes are a novel method to obtain new polycyclic compounds.

When macrocycles **1a** and **1b** were unable to cyclotrimerize due to the low activity of the TM catalyst they reacted thermally, leading to isomers **3a** and **3b**. DFT calculations confirmed the mechanism proposed for this kind of systems, where an

ene reaction between an alkyne and another alkyne take place, followed by a Diels-Alder reaction between the intermediate formed above (vinylallene) and the third unsaturation (alkyne in **4a** and alkene in **4b**). A water molecule assisting the process is required for the 1,3-H transposition to give the final product, **3a**.

As a general reflection, after observing all the results and conclusions previously exposed, it is clear that the nature of the initial compounds which contains different saturations and substituents have a substantial influence on the reaction mechanism, and therefore, on the final product obtained, in the case of the Wilkinson's catalyst.

Supplementary Data

The material listed below is attached as supplementary data on the CD included in the thesis:

- Thesis: memory of the thesis in *.pdf* format.
- Supporting Information of Chapter 3
- Supporting Information of Chapter 4
- Supporting Information of Chapter 5
- Supporting Information of Chapter 6
- Supporting Information of Chapter 7
- Supporting Information of Chapter 8

Bibliography

- [1] Reppe, W.; Schweckendiek, W. J. *Justus Liebigs Ann. Chem.* **1948**, 560, 104.
- [2] For monographs on cycloaddition reactions see: (a) Schore, N.E. In *Comprehensive Organic Synthesis*; Trost, B. M., Fleming, I., Paquette, L. A., Eds.; Pergamon Press: Oxford, UK, **1991**; Vol. 5, pp 1129-1162. (b) Grotjahn, D.B. In *Comprehensive Organometallic Chemistry II*; Abel, E.W., Stone, F.G.A., Wilkinson, G., Hegedus, L., Eds.; Pergamon Press: Oxford, UK, **1995**; Vol. 12, pp 741-770. For reviews on [2+2+2] cycloaddition reactions see: (c) Müller, E. *Synthesis* **1974**, 761. (d) Vollhardt, K.P. *Acc. Chem. Res.* **1977**, 10, 1. (e) Vollhardt, K.P.C. *Angew. Chem. Int. Ed. Engl.* **1984**, 23, 539. (f) Schore, N.E. *Chem. Rev.* **1988**, 88, 1081. (g) Lautens, M.; Klute, W.; Tam, W. *Chem. Rev.* **1996**, 96, 49. (h) Saito, S.; Yamamoto, Y. *Chem. Rev.* **2000**, 100, 2901. (i) Varela, J.A.; Saá, C. *Chem. Rev.* **2003**, 103, 3787. (j) Kotha, S.; Brahmachary, E.; Lahiri, K. *Eur. J. Org. Chem.* **2005**, 4741. (k) Yamamoto, Y. *Curr. Org. Chem.* **2005**, 9, 503. (l) Gandon, V.; Aubert, C.; Malacria, M. *Chem. Commun.* **2006**, 2209. (m) Chopade, P.R.; Louie, J. *Adv. Synth. Catal.* **2006**, 348, 2307. (n) Tanaka, K. *Synlett*, **2007**, 13, 1977. (o) Heller, B.; Hapke, M. *Chem. Soc. Rev.* **2007**, 36, 1085. (p) Varela, J. A.; Saá, C. *Synlett* **2008**, 2571. (q) Shibata, T.; Tsuchikama, K. *Org. Biomol. Chem.* **2008**, 6, 1317. (r) Galan, B. R.; Rovis, T. *Angew. Chem. Int. Ed.* **2009**, 48, 2830. (s) Tanaka, K. *Chem. Asian. J.* **2009**, 4, 508.
- [3] (a) Welsch, T.; Tran, H.-A.; Witulski, B. *Org. Lett.* **2010**, 12, 5644. (b) Yuan, C.; Chang, C.-T.; Axelrod, A.; Siegel, D. *J. Am. Chem. Soc.* **2010**, 132, 5924. (c) Zou, Y.; Deiters, A. *J. Org. Chem.* **2010**, 75, 5355. (d) Kesenheimer, C.; Kalogerakis, A.; Meißner, A.; Groth, U. *Chem. Eur. J.* **2010**, 16, 8805. (e) Nicolaou, K.C.; Tang, Y.; Wang, J. *Angew. Chem. Int. Ed.* **2009**, 48, 3449. (f) Nicolaus, N.; Strauss, S.; Neudörfl, J.-M.; Prokop, A.; Schmalz, H.-G. *Org. Lett.* **2009**, 11, 341.
- [4] (a) Grigg, R.; Scott, R.; Stevenson, P. *Tetrahedron Lett.* **1982**, 23, 2691. (b) Grigg, R.; Scott, R.; Stevenson, P. *J. Chem. Soc. Perkin Trans. I* **1988**, 1357.

Bibliography

- [5] (a) Takahashi, T.; Xi, Z.; Yamazaki, A.; Liu, Y.; Nakajima, K.; Kotora, M. *J. Am. Chem. Soc.* **1998**, *120*, 1672. (b) Suzuki, D.; Urabe, H.; Sato, F. *J. Am. Chem. Soc.* **2001**, *123*, 7925.
- [6] (a) Cadierno, V.; García-Garrido, S.E.; Gimeno, J. *J. Am. Chem. Soc.* **2006**, *128*, 15094. (b) Tsuji, H.; Yamagata, K.; Fujimoto, T.; Nakamura, E. *J. Am. Chem. Soc.* **2008**, *130*, 7792.
- [7] (a) Yoshida, K.; Morimoto, I.; Mitsudo, K.; Tanaka, H. *Tetrahedron* **2008**, *64*, 5800. (b) Yoshida, K.; Morimoto, I.; Mitsudo, K.; Tanaka, H. *Tetrahedron Lett.* **2008**, *49*, 2363.
- [8] (a) Tanaka, K.; Shirasaka, K. *Org. Lett.* **2003**, *5*, 4697. (b) Tanaka, K.; Toyoda, K.; Wada, A.; Shirasaka, K.; Hirano, M. *Chem. Eur. J.* **2005**, *11*, 1145. (c) Hara, H.; Hirano, M.; Tanaka, K. *Org. Lett.* **2008**, *10*, 2537.
- [9] Recent references for Rh: (a) Kotha, S.; Khedkar, P. *Eur. J. Org. Chem.* **2009**, 730. (b) Tanaka, K.; Sawada, Y.; Aida, Y.; Thammathevo, M.; Tanaka, R.; Sagae, H.; Otake, Y. *Tetrahedron* **2010**, *66*, 1563. (c) Sedlák, D.; Kotora, M.; Bartůněk, P. *J. Med. Chem.* **2010**, *53*, 4290. (d) Wang, Y-H.; Huang, S-H.; Lin, T-C.; Tsai, F-Y. *Tetrahedron* **2010**, *66*, 7136. For Co: (e) Doszczak, L.; Fey, P.; Tacke, R. *Synlett* **2007**, 753. (f) Young, D.D.; Teske, J.A.; Deiters, A. *Synthesis* **2009**, 3785. For Ru: (g) Young, D.D.; Sripada, L.; Deiters, A. *J. Comb. Chem.* **2007**, *9*, 735. (h) Yamamoto, Y.; Hattori, K. *Tetrahedron* **2008**, *64*, 847.
- [10] (a) Ojima, I.; Vu, A.T.; McCullagh, J.V.; Kinoshita, A. *J. Am. Chem. Soc.* **1999**, *121*, 3230. (b) Kinoshita, H.; Shinokubo, H.; Oshima, K. *J. Am. Chem. Soc.* **2003**, *125*, 7784. (c) Yamamoto, Y.; Arakawa, T.; Ogawa, R.; Itoh, K. *J. Am. Chem. Soc.* **2003**, *125*, 12143. (d) Shibata, T.; Tsuchikama, K.; Otsuka, M. *Tetrahedron Asymmetry* **2006**, *17*, 614. (e) Songis, O.; Mísek, J.; Schmid, M.B.; Kollárovic, A.; Stará, I.G.; Saman, D.; Císarová, I.; Starý, I. *J. Org. Chem.* **2010**, *75*, 6889.
- [11] Barkovich, A.J.; Vollhardt, K.P.C. *J. Am. Chem. Soc.* **1976**, *98*, 2667.

- [12] (a) Sakurai, H.; Nakadaira, Y.; Hosomi, A.; Eriyama, Y.; Hirama, K.; Kabuto, C. *J. Am. Chem. Soc.* **1984**, *106*, 8315. (b) Sakurai, H. *Pure Appl. Chem.* **1996**, *68*, 327. (c) Ebata, K.; Matsuo, T.; Inoue, T.; Otsuka, Y.; Kabuto, C.; Sekiguchi, A.; Sakurai, H. *Chem. Lett.* **1996**, 1053.
- [13] (a) Moreno-Mañas, M.; Pleixats, R.; Roglans, A.; Sebastián, R.M.; Vallribera, A. *ARKIVOC* **2004**, (iv), 109 (b) Moreno-Mañas, M.; Pleixats, R.; Sebastián, R.M.; Vallribera, A.; Roglans, A. *J. Organomet. Chem.* **2004**, *689*, 3669.
- [14] (a) Pla-Quintana, A.; Roglans, A.; Torrent, A.; Moreno-Mañas, M.; Benet-Buchholz, J. *Organometallics*, **2004**, *23*, 2762. (b) Torrent, A.; González, I.; Pla-Quintana, A.; Roglans, A. *J. Org. Chem.* **2005**, *70*, 2033. (c) Pla-Quintana, A.; Torrent, A.; Dachs, A.; Roglans, A.; Pleixats, R.; Moreno-Mañas, M.; Parella, T.; Benet-Buchholz, J. *Organometallics*, **2006**, *25*, 5612. (d) Brun, S.; Garcia, L.; González, I.; Torrent, A.; Dachs, A.; Pla-Quintana, A.; Parella, T.; Roglans, A. *Chem. Commun.* **2008**, 4339.
- [15] Pla-Quintana, A.; Roglans, A. *Molecules* **2010**, *15*, 9230.
- [16] (a) Keith, J. M.; Larrow, J. F.; Jacobsen, E. N. *Adv. Synth. Catal.* **2001**, *343*, 5. (b) Nogradi, M. ed., *Stereoselective Synthesis, A Practical Approach*, 2nd edition, VCH, New York, 1995. (c) Finn, M. G.; Sharpless, K. B. eds., *Asymmetric Synthesis*, Academic Press, New York, 1985.
- [17] (a) Lin, G.-Q.; Li, Y.-M.; Chan, A. S. C. eds., *Principles and Applications of Asymmetric Synthesis*, John Wiley & Sons, New York, 2001. (b) Ojima, I. ed., *Catalytic Asymmetric Synthesis*, 2nd edition, Wiley-VCH, New York, 2000. (c) Jacobsen, E. N.; Pfaltz, A.; Yamamoto, H. eds., *Comprehensive Asymmetric Catalysis*, I-III, Springer, New York, 1999.
- [18] (a) Tanaka, K.; Osaka, T.; Noguchi, K.; Hirano, M. *Org. Lett.* **2007**, *9*, 1307. (b) Nishida, G.; Noguchi, K.; Hirano, M.; Tanaka, K. *Angew. Chem. Int. Ed.* **2007**, *46*, 3951. (c) Suda, T.; Noguchi, K.; Hirano, M.; Tanaka, K. *Chem. Eur. J.* **2008**, *14*, 6593. (d) Nishida, G.; Noguchi, K.; Hirano, M.; Tanaka, K. *Angew. Chem. Int. Ed.* **2008**, *47*, 3410. (e) Tanaka, K.; Fukawa, N.; Suda, T.; Noguchi, K. *Angew. Chem. Int. Ed.* **2009**, *48*, 5470.

Bibliography

- [19] (a) Tanaka, K.; Sagae, H.; Toyoda, K.; Noguchi, K.; Hirano, M. *J. Am. Chem. Soc.* **2007**, *129*, 1522. (b) Tanaka, K.; Sagae, H.; Toyoda, K.; Hirano, M. *Tetrahedron* **2008**, *64*, 831. (c) Mori, F.; Fukawa, N.; Noguchi, K.; Tanaka, K. *Org. Lett.* **2011**, *13*, 362.
- [20] Shibata, T.; Uchiyama, T.; Endo, K. *Org. Lett.* **2009**, *11*, 3906.
- [21] (a) Friedman, R.K.; Rovis, T. *J. Am. Chem. Soc.* **2009**, *131*, 10775. (b) Oinen, M.E.; Yu, R.T.; Rovis, T. *Org. Lett.* **2009**, *11*, 4934. (c) Dalton, D.M.; Oberg, K.M.; Yu, R.T.; Lee, E.E.; Perreault, S.; Oinen, M.E.; Pease, M.L.; Malik, G.; Rovis, T. *J. Am. Chem. Soc.* **2009**, *131*, 15717.
- [22] (a) Duong, H.A.; Cross, M.J.; Louie, J. *J. Am. Chem. Soc.* **2004**, *126*, 11438. (b) Duong, H.A.; Louie, J. *Tetrahedron* **2006**, *62*, 7552. (c) McCormick, M.; Duong, H.A.; Zuo, G.; Louie, J. *J. Am. Chem. Soc.* **2005**, *127*, 5030. (d) Tekavec, T.N.; Zuo, G.; Simon, K.; Louie, J. *J. Org. Chem.* **2006**, *71*, 5834. (e) Tekavec, T.N.; Louie, J. *Org. Lett.* **2005**, *7*, 4037. (f) Tekavec, T.N.; Louie, J. *J. Org. Chem.* **2008**, *73*, 2641.
- [23] Garcia, L.; Pla-Quintana, A.; Roglans, A.; Parella, T. *Eur. J. Org. Chem.* **2010**, 3407.
- [24] Selected references: (a) Ikeda, S.-I.; Mori, N.; Sato, Y. *J. Am. Chem. Soc.* **1997**, *119*, 4779. (b) Mori, N.; Ikeda, S.-I.; Sato, Y. *J. Am. Chem. Soc.* **1999**, *121*, 2722. (c) Hilt, G.; Paul, A.; Harms, K. *J. Org. Chem.* **2008**, *73*, 5187. (d) Obora, Y.; Satoh, Y.; Ishii, Y. *J. Org. Chem.* **2010**, *75*, 6046.
- [25] Suzuki, H.; Itoh, K.; Ishii, Y.; Simon, K.; Ibers, J. A. *J. Am. Chem. Soc.* **1976**, *98*, 8494.
- [26] Ikeda, S.-I.; Watanabe, H.; Sato, Y. *J. Org. Chem.* **1998**, *63*, 7026.
- [27] Yamamoto, Y.; Kitahara, H.; Ogawa, R.; Itoh, K. *J. Org. Chem.* **1998**, *63*, 9610.
- [28] Varela, J.A.; Rubín, S.G.; González-Rodríguez, C.; Castedo, L.; Saá, C. *J. Am. Chem. Soc.* **2006**, *128*, 9262.

-
- [29] Lebœuf, D.; Iannazzo, L.; Geny, A.; Malacria, M.; Vollhardt, K.P.C.; Aubert, C.; Gandon, V. *Chem. Eur. J.* **2010**, *16*, 8904.
- [30] Tanaka, K.; Nishida, G.; Sagae, H.; Hirano, M. *Synlett* **2010**, 1426.
- [31] (a) Oh, C.H.; Sung, H.R.; Jung S.H.; Lim, Y.M. *Tetrahedron Lett.* **2001**, *42*, 5493. (b) Yamamoto, Y.; Kuwabara, S.; Ando, Y.; Nagata, H.; Nishiyama, H.; Itoh, K. *J. Org. Chem.* **2004**, *69*, 6697. (c) Kezuka, S.; Okado, T.; Niou, E.; Takeuchi, R. *Org. Lett.* **2005**, *7*, 1711. (d) Evans, P. A.; Sawyer, J. R.; Lai, K. W.; Huffman, J. C. *Chem. Commun.* **2005**, 3971.
- [32] (a) Bennacer, B.; Fujiwara, M.; Ojima, I. *Org. Lett.* **2004**, *6*, 3589. (b) Bennacer, B.; Fujiwara, M.; Lee, S-Y.; Ojima, I. *J. Am. Chem. Soc.* **2005**, *127*, 17756. (c) Kaloko, J. J.; Teng, Y-H. G.; Ojima, I. *Chem. Commun.* **2009**, 4569.
- [33] (a) Slowinski, F.; Aubert, C.; Malacria, M. *Tetrahedron Lett.* **1999**, *40*, 707. (b) Slowinski, F.; Aubert, C.; Malacria, M. *Tetrahedron Lett.* **1999**, *40*, 5849. (c) Slowinski, F.; Aubert, C.; Malacria, M. *Adv. Synth. Catal.* **2001**, 343, 64. (d) Slowinski, F.; Aubert, C.; Malacria, M. *Eur. J. Org. Chem.* **2001**, 3491. (e) Slowinski, F.; Aubert, C.; Malacria, M. *J. Org. Chem.* **2003**, *68*, 378. (f) Schelper, M.; Buisine, O.; Kozhushkov, S.; Aubert, C.; de Meijere, A.; Malacria, M. *Eur. J. Org. Chem.* **2005**, 3000. (g) Geny, A.; Gaudrel, S.; Slowinski, F.; Amatore, M.; Chouraqui, G.; Malacria, M.; Aubert, C.; Gandon, V. *Adv. Synth. Catal.* **2009**, 351, 271.
- [34] (a) González, I.; Bouquillon, S.; Roglans, A.; Muzart, J. *Tetrahedron Lett.* **2007**, *48*, 6425. (b) González, I.; Pla-Quintana, A.; Roglans, A. *Synlett* **2009**, 2844.
- [35] In the systems where three alkynes are located in the same molecule, the term *cycloisomerization* can be used instead of *cyclotrimerization*.
- [36] Ma, S.; Ni, B. *J. Org. Chem.* **2002**, *67*, 8280.
- [37] Shibata, T.; Kurokawa, H.; Kanda, K. *J. Org. Chem.* **2007**, *72*, 6521.

- [38] (a) Müller, E. *Synthesis* **1974**, 761. (b) Iglesias, M.; Pino, C.; Ros, J.; García Blanco, S.; Carrera, S.M. *J. Organomet. Chem.* **1988**, 338, 89. (c) Bianchini, C.; Caulton, K.G.; Chardon, C.; Eisenstein, O.; Folting, K.; Johnson, T.J.; Meli, A.; Peruzzini, M.; Rauscher, D.J.; Streib, W.E.; Vizza, F. *J. Am. Chem. Soc.* **1991**, 113, 5127. (d) Nishiyama, H.; Niwa, E.; Inoue, T.; Ishima, Y.; Aoki, K. *Organometallics* **2002**, 21, 2572. (e) Uchimura, H.; Ito, J.-I.; Iwasa, S.; Nishiyama, H. *J. Organomet. Chem.* **2007**, 692, 481.
- [39] Schmid, R.; Kirchner, K.; *Eur. J. Inorg. Chem.* **2004**, 2609.
- [40] (a) Li, J.; Jiang, H.; Chen, M. *J. Org. Chem.* **2001**, 66, 3627.
- [41] (a) Peters, J.U.; Blechert, S. *Chem. Commun.* **1997**, 1983. (b) Witulski, B.; Stengel, T.; Fernández-Hernández, J.M. *Chem. Commun.* **2000**, 1965.
- [42] (a) Stockis, A.; Hoffmann, R. *J. Am. Chem. Soc.* **1980**, 102, 2952. (b) Bianchini, C.; Caulton, K.G.; Chardon, C.; Doublet, M.-L.; Eisenstein, O.; Jackson, S.-A.; Johnson, T.J.; Meli, A.; Peruzzini, M.; Streib, W.E.; Vacca, A.; Vizza, F. *Organometallics* **1994**, 13, 2010.
- [43] Hardesty, J. H.; Koerner, J. B.; Albright, T. A.; Lee, G.-Y. *J. Am. Chem. Soc.* **1999**, 121, 6055.
- [44] (a) Dahy, A. A.; Koga, N. *Bull. Chem. Soc. Jpn.* **2005**, 78, 781. (b) Dahy, A. A.; Suresh, C. H.; Koga, N. *Bull. Chem. Soc. Jpn.* **2005**, 78, 792.
- [45] 16-Electron d^8 -CpML species are known to exhibit triplet ground states, whereas the corresponding 18-electron CpML' complexes are usually singlets. See: (a) Siegbahn, P. E. M. *J. Am. Chem. Soc.* **1996**, 118, 1487. (b) Poli, R.; Smith, K. M. *Eur. J. Inorg. Chem.* **1999**, 877. (c) Su, M.-D.; Chu, S.-Y. *Chem. Eur. J.* **1999**, 5, 198. (d) Smith, K. M.; Poli, R.; Harvey, J. N. *Chem. Eur. J.* **2001**, 7, 1679. (e) Carreón-Macedo, J. -L.; Harvey, J. N. *J. Am. Chem. Soc.* **2004**, 126, 5789. (f) Petit, A.;

- Richard, P.; Cacelli, I.; Poli, R. *Chem.Eur. J.* **2006**, *12*, 813 and pertinent references cited therein.
- [46] (a) Gandon, V.; Agenet, N.; Vollhardt, K.P.C.; Malacria, M.; Aubert, C. *J. Am. Chem. Soc.* **2006**, *128*, 8509. (b) Agenet, N.; Gandon, V.; Vollhardt, K.P. C.; Malacria, M.; Aubert, C. *J. Am. Chem. Soc.* **2007**, *129*, 8860.
- [47] Kirchner, K.; Calhorda, M.J.; Schmid, R.; Veiros, L.F. *J. Am.Chem. Soc.* **2003**, *125*, 11721.
- [48] Dazinger, G.; Torres-Rodrigues, M.; Kirchner, K.; Calhorda, M. J.; Costa, P. J. *J. Organomet. Chem.* **2006**, *691*, 4434.
- [49] Yamamoto, K.; Kinpara, K.; Saigoku, T.; Takagishi, H.; Okuda, S.; Nishiyama, H.; Itoh, K. *J. Am. Chem. Soc.* **2005**, *127*, 605.
- [50] Orian, L; Stralen, J.N.P; Bickelhaupt, F.M. *Organometallics.* **2007**, *26*, 3816.
- [51] Varela, J.A.; Rubín, S.G.; Castedo, L.; Saá, C. *J. Org. Chem.* **2008**, *73*, 1320.
- [52] (a) Morokuma, K.; Musaev, D. G. *Computational Modeling for Homogeneous and Enzymatic Catalysis: A Knowledge Base for Designing Efficient Catalysts*; Wiley-VCH, Weinheim, 2008 (b) Maseras, F.; Lledós, A. *Computational Modeling of Homogeneous Catalysis*; Kluwer Academic Publishers, Netherlands, 2002. (c) Cundari, T.R. *Computational Organometallic Chemistry*; Marcel Dekker, Inc., Basel, 2001 (d)
- [53] Torrent, M.; Solà, M.; Frenking, G. *Chem. Rev.* **2000**, *100*, 439.
- [54] Szabo, A.; Ostlund, N. S. *Modern Quantum Chemistry: Introduction to Advanced Electronic Structure Theory*; Dover Publications: Mineola NY, 1996.
- [55] Jensen, F. *Introduction to Computational Chemistry*; John Wiley and Sons Ltd: New York, 1999.

Bibliography

- [56] Nebot, I.; Ugalde, J. M.; Caballol, R.; Solà, M.; Novoa, J.; Largo, A.; Illas, F.; Ricart, J. M.; Alvaríño, J. M.; Borondo, F.; Merchan, M.; Frau, J.; Sánchez, E.; Andrés, J. *Química Teórica y Computacional*; Universitat Jaume I, Castelló de la Plana, 2000.
- [57] The Pauli Exclusion Principle is a quantum mechanical principle formulated by the Austrian physicist Wolfgang Pauli in 1925. In its simplest form for electrons in a single atom, it states that no two electrons can have the same four quantum numbers; that is, if n (energy), l (angular moment magnitude), and m_l (angular moment orientation) are the same, m_s (orientation of intrinsic spin) must be different such that the electrons have opposite spins.
- [58] (a) Jensen, F. *Introduction to Computational Chemistry*, John Wiley and Sons, **1999**, 65 - 69, New York (b) Roothaan, C. C. J. *Rev. Mod. Phys.* **1951**, 69, 23. (c) Hall, G. G. *Proc. Roy. Soc. London*, **1951**, 541, A205.
- [59] Koch, W.; Holthausen, M. C. *A Chemist's Guide to Density Functional Theory*. Second Edition. Wiley-VCH and John Wiley & Sons, Berlin, **2001**.
- [60] Hohenberg, P.; Kohn, W. *Phys. Rev.* **1964**, 136, B864.
- [61] Kohn, W.; Sham, L. *Phys. Rev.* **1965**, 140, A1133.
- [62] Slater, J. C. *Phys. Rev.* **1951**, 81, 385.
- [63] Vosko, S. H., Wilk, L., and Nusair, M. *Can. J. Phys.* **1980**, 58, 1200.
- [64] Andrés, J.; Bertran, J. *Theoretical and Computational Chemistry: Foundation, methods and techniques*; Eds., Universitat Jaume I, Castelló, 2007.
- [65] Perdew, J. and Wang, W. *Phys. Rev. B* **1986**, 33, 8800.
- [66] Becke, A. D. *Phys. Rev. A.* **1988**, 38, 3098.
- [67] Lee, C., Yang, W., and Parr, R. *Phys. Rev. B.* **1988**, 37, 785.

- [68] Perdew, J. P. *Phys. Rev. B.* **1986**, *33*, 8822.
- [69] Becke, A. *Int. J. Quantum Chem.* **1983**, *23*, 1915.
- [70] Miehlich, B.; Savin, A.; Stoll, H.; Preuss, H. *Chem. Phys. Lett.* **1989**, *157*, 200.
- [71] Simón, L.; Goodman, J. M. *Org. Biomol. Chem.* **2011**, *9*, 689.
- [72] Gaussian 03, Revision C.01 ed., Frisch, M. J.; Trucks, G. W.; Schlegel, H. B.; Scuseria, G. E.; Robb, M. A.; Cheeseman, J. R.; Montgomery Jr., J. A.; Vreven, T.; Kudin, K. N.; Burant, J. C.; Millam, J. M.; Iyengar, S. S.; Tomasi, J.; Barone, V.; Mennucci, B.; Cossi, M.; Scalmani, G.; Rega, N.; Petersson, G. A.; Nakatsuji, H.; Hada, M.; Ehara, M.; Toyota, K.; Fukuda, R.; Hasegawa, J.; Ishida, M.; Nakajima, T.; Honda, Y.; Kitao, O.; Nakai, H.; Klene, M.; Li, X.; Knox, J. E.; Hratchian, H. P.; Cross, J. B.; Bakken, V.; Adamo, C.; Jaramillo, J.; Gomperts, R.; Stratmann, R. E.; Yazyev, O.; Austin, A. J.; Cammi, R.; Pomelli, C.; Ochterski, J. W.; Ayala, P. Y.; Morokuma, K.; Voth, G. A.; Salvador, P.; Dannenberg, J. J.; Zakrzewski, G.; Dapprich, S.; Daniels, A. D.; Strain, M. C.; Farkas, O.; Malick, D. K.; Rabuck, A. D.; Raghavachari, K.; Foresman, J. B.; Ortiz, J. V.; Cui, Q.; Baboul, A. G.; Clifford, S.; Cioslowski, J.; Stefanov, B. B.; Liu, G.; Liashenko, A.; Piskorz, P.; Komaromi, I.; Martin, R. L.; Fox, D. J.; Keith, T.; Al-Laham, M. A.; Peng, C. Y.; Nanayakkara, A.; Challacombe, M.; Gill, P. M. W.; Johnson, B.; Chen, W.; Wong, M. W.; Gonzalez, C.; Pople, J. A. Gaussian, Inc. Pittsburgh, PA, **2003**.
- [73] (a) Poater, J.; Solà, M.; Duran, M.; Robles, J. *Phys. Chem. Chem. Phys.* **2002**, *4*, 722. (b) Simón, L.; Goodman, J.M. *Org. Biomol. Chem.* **2011**, *9*, 689.
- [74] Cases, M.; Duran, M.; Mestres, J.; Martin, N.; Solà, M. *J. Org. Chem.* **2001**, *66*, 433.
- [75] (a) Freccero, M.; Gandolfi, R.; Sarziamade, M.; Rastelli, A. *J. Chem. Soc. Perkin Trans. 2*, **1998**, 2413. (b) Wiest, O.; Houk, K. N.; Black, K. A.; Thomas, B. *J. Am. Chem. Soc.* **1995**, *117*, 8594. (c) Wiest, O.; Houk, K. N. *Top. Curr. Chem.* **1996**, *183*, 1. (d) Goldstein, E.; Beno, B.; Houk, K. N. *J. Am. Chem. Soc.* **1996**, *118*, 6036. (e) Dinadayalane, T. C.; Vijaya, R.; Smitha, A.; Sastry, G. N. *J. Phys. Chem. A* **2002**,

Bibliography

- 106, 1627. (f) Isobe, H.; Yamanaka, S.; Yamaguchi, K. *Int. J. Quantum Chem.* **2003**, *95*, 532. (g) Di Valentin, C.; Freccero, M.; Gandolfi, R.; Rastelli, A. *J. Org. Chem.* **2000**, *65*, 6112.
- [76] (a) Fukui, K. *Acc Chem Res.* **1981**, *14*, 363. (b) González, C.; Schlegel, H. B. *J Chem Phys.* **1991**, *95*, 5853.
- [77] (a) Woon, D. E.; Dunning Jr., T. H. *J. Chem. Phys.* **1993**, *98*, 1358. (b) Kendall, R. A.; Dunning Jr., T. H.; Harrison, R. J. *J. Chem. Phys.* **1992**, *96*, 6796. (c) Dunning Jr., T. H. *J. Chem. Phys.* **1989**, *90*, 1007. (d) Peterson, K. A.; Woon, D. E.; Dunning Jr., T. H. *J. Chem. Phys.* **1994**, *100*, 7410. (e) Wilson, A.; Van Mourik, T.; Dunning Jr., T. H. *J. Mol. Struct. (Theochem)* **1997**, *388*, 339.
- [78] Hellmann, H. *J. Chem. Phys.* **1930**, *3*, 61.
- [79] Bofill, J. *J. Comput. Chem.* **1994**, *15*, 1.
- [80] Swart, M.; Bickelhaupt, F.M. *Int. J. Quant. Chem.* **2006**, *106*, 2536.
- [81] (a) Bickelhaupt, F. M.; Nibbering, N. M. M.; van Wezenbeek, E. M.; Baerends, E. J. *J. Phys. Chem.* **1992**, *96*, 4864. (b) Bickelhaupt, F. M.; Diefenbach, A.; de Visser, S. P.; de Koning, L. J.; Nibbering, N. M. M. *J. Phys. Chem. A* **1998**, *102*, 9549. (c) Ziegler, T.; Rauk, A. *Theor. Chim. Acta* **1977**, *46*, 1. (d) Ziegler, T.; Rauk, A. *Inorg. Chem.* **1979**, *18*, 1558. (e) Ziegler, T.; Rauk, A. *Inorg. Chem.* **1979**, *18*, 1755.
- [82] Baerends, E. J.; Gritsenko, O. V. *J. Phys. Chem. A.* **1997**, *101*, 5383.
- [83] Bickelhaupt, F. M.; Baerends E. J. In *Reviews in Computational Chemistry*; Lipkowitz, K. B., Boyd, D. B., Eds.; Wiley-VCH: New York, 2000; Vol. 15, pp. 1-86.
- [84] Goodman, J. Grushin, V.V.; Larichev, R.; Macgregor, S.A.; Marshall, W.J.; Roe, D.C. *J. Am. Chem. Soc.* **2010**, *132*, 12013.

- [85] The experimental part belongs to the thesis carried out by Anna Torrent in the research group of Anna Roglans: *Síntesi de nous macrocycles nitrogenats poliinsaturats. Estudis de coordinació i reactivitat*, 2007.
- [86] The experimental part belongs to the thesis carried out by Iván González in the research group of Anna Roglans: *Síntesi i reactivitat de nous macrocycles nitrogenats poliinsaturats*, 2008.
- [87] (a) Robinson, J. M.; Sakai, T.; Okano, K.; Kitawaki, T.; Danheiser, R. L. *J. Am. Chem. Soc.* **2010**, *132*, 11039. (b) Sakai, T.; Danheiser, R. L. *J. Am. Chem. Soc.* **2010**, *132*, 13203.

